Stochastic reverberation model for uniform and non-diffuse acoustic fields

Modèle stochastique de réverbération pour les champs acoustiques uniformes et non diffus

Roland Badeau

2019D003

avril 2019

Département Image, Données, Signal
Groupe S^2A : Signal, Statistiques et Apprentissage

Stochastic reverberation model for uniform and non-diffuse acoustic fields

Modèle stochastique de réverbération pour les champs acoustiques uniformes et non diffus

Roland Badeau
Image, Data, Signal department (IDS)
LTCI, Télécom ParisTech, Université Paris-Saclay, Paris, France
roland.badeau@telecom-paristech.fr

***Abstract*—In a recent research report, we introduced a general stochastic reverberation model that aims to represent the statistical properties of reverberation in a broad variety of acoustic environments. A simplified version of this model, dedicated to the particular case of diffuse (i.e. uniform and isotropic) acoustic fields, omnidirectional sources and microphones, and constant attenuation w.r.t frequency, has been investigated both mathematically and experimentally in a recent research paper. We showed that this model provides a common mathematical framework that unifies several well-known results regarding the statistical properties of reverberation in the space, time and frequency domains.**

In this research report, we aim to extend this mathematical analysis to uniform and non-diffuse acoustic fields, and directive sources and microphones. We show that the predictions of the general stochastic model experimentally match the observations, based on both synthetic and real room impulse responses, measured in various acoustic environments.

***Index Terms*—Reverberation; Diffusion; Room impulse response; Stochastic models.**

***Résumé*—Dans un récent rapport de recherche, nous avons introduit un modèle stochastique général de réverbération qui vise à représenter les propriétés statistiques de la réverbération dans une grande variété d'environnements acoustiques. Une version simplifiée de ce modèle, dédiée au cas particulier de champs acoustiques diffus (c'est-à-dire uniformes et isotropes), de sources et microphones omnidirectionnels, et d'une atténuation indépendante de la fréquence, a été étudiée mathématiquement et expérimentalement dans un récent article de recherche. Nous avons montré que ce modèle fournit un cadre mathématique commun qui unifie plusieurs résultats bien connus concernant les propriétés statistiques de la réverbération dans les domaines spatial, temporel et fréquentiel.**

Dans ce rapport de recherche, nous visons à étendre cette analyse mathématique à des champs acoustiques uniformes et non diffus, et à des sources et des microphones directifs. Nous montrons que les prédictions du modèle stochastique général correspondent aux observations expérimentales, à partir de réponses impulsionnelles de salles synthétiques et réelles, mesurées dans divers environnements acoustiques.

***Mots clés*—Réverbération; Diffusion; Réponse impulsionnelle de salle; Modèles stochastiques.**

I. Introduction

In [1], [2], we introduced a common mathematical framework for stochastic reverberation models, that aimed to unify several well-known results regarding the statistical properties of reverberation, in the spatial, temporal and spectral domains [3]–[10]. This framework was based on the source image principle [11], [12], which represents the sound wave reflected by a flat surface as if it was emitted by a so-called source image. In [1], [2], the positions of the source images were modeled as random, and uniformly distributed according to a Poisson point process.

However, the stochastic reverberation model introduced in [1], [2] was limited to diffuse (*i.e.* uniform and isotropic[1]) acoustic fields, omnidirectional sources and microphones, and constant attenuation w.r.t. frequency. In [13], we proposed several extensions of this model, that aim to represent reverberation more realistically, by considering anisotropic and non-uniform acoustic fields, directive sources and microphones, and frequency-varying attenuation coefficients.

In this research report, we aim to investigate the statistical properties of this generalized model. In order to keep the mathematical analysis as simple as possible, we chose to restrict the study to uniform acoustic fields and constant attenuation w.r.t. frequency as in [1], [2], but we address the generalization to anisotropic acoustic fields and directive sources and microphones as introduced in [13]. We will first provide a mathematical analysis of the statistical properties of the model, regarding its first and second order moments in the spatial, temporal, spectral and time-frequency domains, and its asymptotic Gaussianity. Then we will show that the predicted statistical properties experimentally match the observations, based on both synthetic and real room impulse responses (RIRs), measured in various acoustic environments.

This research report is organized as follows: the uniform stochastic reverberation model will be formally defined in

[1] *Uniform* means invariant under any translation, and *isotropic* means invariant under any rotation in the three-dimensional (3D) space.

Section II, then its statistical properties will be analyzed mathematically in Section III and experimentally in Section IV. Conclusions will be drawn in Section V, and the proofs of the mathematical results will be presented in Appendices A to G. Throughout the report, we will use the following mathematical notation:

- $\mathbb{N}$: set of whole numbers;
- $\mathbb{R}$, $\mathbb{C}$: sets of real and complex numbers, respectively;
- $\mathbb{R}_+$: set of nonnegative real numbers;
- $\imath = \sqrt{-1}$: imaginary unit;
- $\triangleq$: equal by definition to;
- $\overset{c}{=}$: equal up to an additive constant to;
- $\propto$: proportional to;
- $\boldsymbol{x}$ (bold font), z (regular): vector and scalar, respectively;
- $\overline{z}$: complex conjugate of $z \in \mathbb{C}$;
- $|.|$: absolute value of a scalar or a vector (entrywise);
- x_m: m-th entry of vector $\boldsymbol{x}$;
- $\boldsymbol{x}^\top$: transpose of vector $\boldsymbol{x}$;
- $\mathcal{S}^2$: unit sphere in $\mathbb{R}^3$ ($\mathcal{S}^2 = \{\boldsymbol{x} \in \mathbb{R}^3; \|\boldsymbol{x}\|_2 = 1\}$);
- $\boldsymbol{I}$: identity matrix;
- $\mathrm{span}(\boldsymbol{A})$: column (or *range*) space of matrix $\boldsymbol{A}$;
- $[a, b]$: closed interval, including a and $b \in \mathbb{R}$;
- $]a, b[$: open interval, excluding a and $b \in \mathbb{R}$;
- $\{a, \ldots, b\}$: set including all elements listed from a to b;
- $L^\infty(V)$, where V is a Borel set: Lebesgue space of essentially bounded functions f of support V (i.e. such that $\|f\|_\infty = \mathrm{ess\,sup}_V |f| < +\infty$);
- $L^p(V)$, where V is a Borel set and $p \in \mathbb{N}\backslash\{0\}$: Lebesgue space of measurable functions f of support V, such that $\|f\|_p = (\int_V |f(\boldsymbol{x})|^p d\boldsymbol{x})^{\frac{1}{p}} < +\infty$;
- $\|.\|_2$: Euclidean/Hermitian norm of a vector or a function;
- $\mathbf{J}_{\boldsymbol{q}}(.)$: Jacobian matrix of the multivariate function $\boldsymbol{q}(.)$;
- $O(.)$: asymptotically bounded by;
- $o(.)$: asymptotically dominated by;
- $\sim$: has distribution *or* is asymptotically equivalent to;
- δ: Dirac delta function;
- $\mathbb{E}[X]$: expected value of a complex random variable X;
- $\phi_X(\theta) = \mathbb{E}[e^{\imath Re(\overline{\theta} X)}]$: characteristic function of X;
- Covariance of two complex random variables X and Y:

$$\mathrm{cov}[X, Y] = \mathbb{E}[(X - \mathbb{E}[X])\overline{(Y - \mathbb{E}[Y])}];$$

- $\mathrm{var}[X] = \mathrm{cov}[X, X]$: variance of a random variable X;
- Correlation of two complex random variables X and Y:

$$\mathrm{corr}[X, Y] = \frac{\mathrm{cov}[X, Y]}{\sqrt{\mathrm{var}[X]\,\mathrm{var}[Y]}};$$

- $\mathcal{P}(\lambda)$: Poisson distribution of parameter $\lambda > 0$:

$$N \sim \mathcal{P}(\lambda) \Leftrightarrow P(N{=}n) = e^{-\lambda}\frac{\lambda^n}{n!} \Leftrightarrow \phi_N(\theta) = e^{\lambda(e^{\imath\theta}-1)};$$

- $\mathrm{sinc}(x) = \frac{\sin(x)}{x}$: cardinal sine function;
- $\mathbf{1}_A$: indicator function of a set A ($\mathbf{1}_A(x)$ is 1 if $x \in A$ or 0 if $x \notin A$);
- $\widetilde{\psi}(t) = \overline{\psi(-t)}$: conjugate and time-reverse of $\psi : \mathbb{R} \to \mathbb{C}$;
- Convolution of two functions ψ_1 and $\psi_2 : \mathbb{R} \to \mathbb{C}$:

$$(\psi_1 * \psi_2)(t) = \textstyle\int_{u\in\mathbb{R}} \psi_1(u)\psi_2(t-u)du;$$

- Fourier transform of a function $\psi : \mathbb{R} \to \mathbb{C}$:

$$\widehat{\psi}(f) = \textstyle\int_{t\in\mathbb{R}} \psi(t)e^{-2\imath\pi f t}dt \quad (f \in \mathbb{R});$$

- $\otimes$: outer product ($(\psi_1 \otimes \psi_2)(t_1, t_2) = \psi_1(t_1)\psi_2(t_2)$);
- Wigner distribution (*a.k.a.* Wigner-Ville distribution) of a function $\gamma : \mathbb{R}^2 \to \mathbb{R}$:

$$\mathcal{W}_\gamma(t, f) = \int_{\tau\in\mathbb{R}} \gamma(t + \tfrac{\tau}{2}, t - \tfrac{\tau}{2})e^{-2\imath\pi f\tau}d\tau. \quad (1)$$

Note that the Wigner distribution satisfies several important properties [14]:

- *even symmetry*: $\forall t, f \in \mathbb{R}$, $\mathcal{W}_\gamma(t, -f) = \overline{\mathcal{W}_\gamma(t, f)}$;
- *real property*: if γ is symmetric ($\forall t_1, t_2 \in \mathbb{R}$, $\gamma(t_1, t_2) = \gamma(t_2, t_1)$), then $\forall t, f \in \mathbb{R}$, $\mathcal{W}_\gamma(t, f) \in \mathbb{R}$;
- *projection property*: for any functions ψ_1, $\psi_2 : \mathbb{R} \to \mathbb{R}$,

$$\int_{t\in\mathbb{R}} \mathcal{W}_{\psi_1\otimes\psi_2}(t, f)dt = \widehat{\psi_1}(f)\overline{\widehat{\psi_2}(f)}, \quad (2)$$

$$\int_{f\in\mathbb{R}} \mathcal{W}_\gamma(t, f)df = \gamma(t, t); \quad (3)$$

- *convolution property*: if $\gamma(t_1, t_2) = (\gamma_1 \overset{t_1}{*} \overset{t_2}{*}\gamma_2)(t_1, t_2)$,

$$\mathcal{W}_\gamma(t, f) = (\mathcal{W}_{\gamma_1} \overset{t}{*} \mathcal{W}_{\gamma_2})(t, f), \quad (4)$$

  where $\overset{t}{*}$ denotes convolution over variable t;
- *temporal support property*: if the support of function $\gamma : \mathbb{R}^2 \to \mathbb{R}$ is compact, then the temporal support of $\mathcal{W}_\gamma(t, f)$ is also compact.

Finally, in order to model the spatial distribution of the source images, we will use the concept of *Poisson random measure* with independent increments (also refered to as *Poisson point process*), as we did in [1], [2]: given a Borel set $V \subset \mathbb{R}^3$ of finite volume $|V|$, we assumed that the number $N(V)$ of source images contained in V follows a Poisson distribution of rate parameter $\lambda|V|$: $N(V) \sim \mathcal{P}(\lambda|V|)$ with $\lambda > 0$. Formally, given a non-negative, locally integrable function $\Lambda(\boldsymbol{x})$ on $\mathbb{R}^p$, the Poisson random increment $dN(\boldsymbol{x}) \sim \mathcal{P}(\Lambda(\boldsymbol{x})d\boldsymbol{x})$ corresponds to an infinitesimal volume $|V| = d\boldsymbol{x}$. Then for any Borel set $V \subset \mathbb{R}^p$ of finite Lebesgue measure, the number $N(V) = \int_V dN(\boldsymbol{x})$ of points contained in V follows a Poisson distribution of rate parameter $\int_V \Lambda(\boldsymbol{x})d\boldsymbol{x}$: $N(V) \sim \mathcal{P}(\int_V \Lambda(\boldsymbol{x})d\boldsymbol{x})$, and for any disjoint Borel sets V_1 and V_2, $N(V_1)$ and $N(V_2)$ are independent. Note that in the stochastic reverberation model proposed in [1], [2], we considered a spatially uniform distribution of the source images in the 3D-space, so that $p = 3$ and $\Lambda(\boldsymbol{x}) = \lambda > 0$ is constant.

II. Uniform stochastic reverberation model

In this research report, we consider the following stochastic reverberation model (see [13] for a description of the basic geometric principles that underlie this model):

Definition 1 (Uniform stochastic reverberation model)**.** *For any sensor $i \in \{1 \ldots I\}$, time $t \in \mathbb{R}$, and frequency $f \in \mathbb{R}$, let*

$$h_i(t) = \int_{\boldsymbol{x}\in\mathbb{R}^3}\int_{\boldsymbol{y}\in\mathbb{R}^M} V_i(\boldsymbol{x},\boldsymbol{y};\boldsymbol{y}\text{-}\boldsymbol{q}(\boldsymbol{x}\text{-}\boldsymbol{x}_i))\, g_i\left(\frac{\boldsymbol{x}-\boldsymbol{x}_i}{\|\boldsymbol{x}-\boldsymbol{x}_i\|_2},.\right) \overset{t}{*} \frac{s\left(\Theta(\boldsymbol{x},\boldsymbol{y})\frac{\boldsymbol{x}-\boldsymbol{x}_i}{\|\boldsymbol{x}-\boldsymbol{x}_i\|_2},t-\frac{\|\boldsymbol{x}-\boldsymbol{x}_i\|_2}{c}\right)e^{-\frac{\boldsymbol{y}^\top\widehat{\boldsymbol{\alpha}}}{c}}}{\|\boldsymbol{x}-\boldsymbol{x}_i\|_2} dN(\boldsymbol{x},\boldsymbol{y}), \tag{5}$$

$$\widehat{h}_i(f) = \int_{\boldsymbol{x}\in\mathbb{R}^3}\int_{\boldsymbol{y}\in\mathbb{R}^M} V_i(\boldsymbol{x},\boldsymbol{y};\boldsymbol{y}\text{-}\boldsymbol{q}(\boldsymbol{x}\text{-}\boldsymbol{x}_i))\, \widehat{g}_i\left(\frac{\boldsymbol{x}-\boldsymbol{x}_i}{\|\boldsymbol{x}-\boldsymbol{x}_i\|_2},f\right) \frac{\widehat{s}\left(\Theta(\boldsymbol{x},\boldsymbol{y})\frac{\boldsymbol{x}-\boldsymbol{x}_i}{\|\boldsymbol{x}-\boldsymbol{x}_i\|_2},f\right)e^{-\frac{\boldsymbol{y}^\top\widehat{\boldsymbol{\alpha}}+2\imath\pi f\|\boldsymbol{x}-\boldsymbol{x}_i\|_2}{c}}}{\|\boldsymbol{x}-\boldsymbol{x}_i\|_2} dN(\boldsymbol{x},\boldsymbol{y}), \tag{6}$$

where

- $h_i(t) \in \mathbb{R}$ *(resp.* $\widehat{h}_i(f) \in \mathbb{C}$*) is the room impulse response (resp. room frequency response) at sensor* i*;*
- $g_i(\boldsymbol{u},t) \in \mathbb{R}$ *(resp.* $\widehat{g}_i(\boldsymbol{u},f) \in \mathbb{C}$*) is the response of sensor* i *at direction* $\boldsymbol{u} \in \mathcal{S}^2$ *(taking into account both its directivity and orientation) and time* t *(resp. frequency* f*);*
- $s(\boldsymbol{u},t) \in \mathbb{R}$ *(resp.* $\widehat{s}(\boldsymbol{u},f) \in \mathbb{C}$*) is the response of the source at direction* $\boldsymbol{u} \in \mathcal{S}^2$ *(taking into account its directivity) and time* t *(resp. frequency* f*);*
- *vector* $\boldsymbol{x}_i \in \mathbb{R}^3$ *(in meters) is the position of sensor* i*;*
- *vector* $\boldsymbol{x} \in \mathbb{R}^3$ *(in meters) represents the possible positions of the source images;*
- $c > 0$ *is the speed of sound (in meters.hertz);*
- *the term* $\frac{e^{-\frac{2\imath\pi f\|\boldsymbol{x}-\boldsymbol{x}_i\|_2}{c}}}{\|\boldsymbol{x}-\boldsymbol{x}_i\|_2}$ *corresponds to the propagation of a monochromatic spherical wave from* $\boldsymbol{x}$ *to* $\boldsymbol{x}_i$*;*
- $\widehat{\boldsymbol{\alpha}} \in \mathbb{R}^M_+$ *is a vector of attenuation coefficients (in hertz);*
- *the term* $e^{-\frac{\boldsymbol{y}^\top\widehat{\boldsymbol{\alpha}}}{c}}$ *corresponds to the total attenuation of the sound wave during its propagation from* $\boldsymbol{x}$ *to* $\boldsymbol{x}_i$*;*
- $\boldsymbol{r} \in \mathbb{R}^3 \mapsto \boldsymbol{q}(\boldsymbol{r}) \in \mathbb{R}^M_+$ *(in meters) is a 1-homogeneous function (*i.e. $\forall \boldsymbol{r} \in \mathbb{R}^3$, $\forall \nu \in \mathbb{R}_+$, $\boldsymbol{q}(\nu\boldsymbol{r}) = \nu\boldsymbol{q}(\boldsymbol{r})$*);*
- *the coordinates* $(\boldsymbol{x},\boldsymbol{y}) \in \mathbb{R}^3 \times \mathbb{R}^M$ *(in meters) are distributed according to a uniform Poisson point process* $dN(\boldsymbol{x},\boldsymbol{y}) \sim \mathcal{P}(\lambda d\boldsymbol{x}d\boldsymbol{y})$ *with* $\lambda > 0$ *(in meters*$^{-(3+M)}$*);*
- $\Theta(\boldsymbol{x},\boldsymbol{y}) \in SO(3)$ *is a random rotation matrix that represents the orientation of the source image of coordinates* $(\boldsymbol{x},\boldsymbol{y})$*. Its distribution is i.i.d. w.r.t.* $(\boldsymbol{x},\boldsymbol{y})$ *and not necessarily uniform on the rotation group* $SO(3)$*;*
- $V_i(\boldsymbol{x},\boldsymbol{y};\boldsymbol{z}_i) \in \{0,1\}$ *is a Boolean that indicates whether the source image of coordinates* $(\boldsymbol{x},\boldsymbol{y})$ *is visible from sensor* i *or not. Formally,* $V_i(\boldsymbol{x},\boldsymbol{y};\boldsymbol{z}_i)$ *is a random field on* $\mathbb{R}^3 \times \mathbb{R}^M$*, whose probability distribution is parameterized by the vector* $\boldsymbol{z}_i \in \mathbb{R}^M$*. The joint distribution for all sensors* i *of the random vector*

  $$\boldsymbol{V}(\boldsymbol{x},\boldsymbol{y};\boldsymbol{z}_1\dots\boldsymbol{z}_I) \triangleq [V_1(\boldsymbol{x},\boldsymbol{y};\boldsymbol{z}_1)\dots V_I(\boldsymbol{x},\boldsymbol{y};\boldsymbol{z}_I)]_{i\in\{1\dots I\}}$$

  is i.i.d. w.r.t. $(\boldsymbol{x},\boldsymbol{y})$*, and it is denoted* $p(b_1\dots b_I;\boldsymbol{z}_1\dots\boldsymbol{z}_I) \in [0,1]$ *where* $b_i \in \{0,1\}$ *and* $\boldsymbol{z}_i \in \mathbb{R}^M$*. The marginals for every sensor* i *are denoted* $p(b;\boldsymbol{z}) \in [0,1]$ *(they are such that the closer* $\boldsymbol{z}$ *is to zero, the higher* $p(1;\boldsymbol{z})$*), and the marginals for every pair of sensors* (i,j) *are denoted* $p(b_i,b_j;\boldsymbol{z}_i,\boldsymbol{z}_j) \in [0,1]$*;*
- *the three random fields* dN*,* Θ *and* $\boldsymbol{V}$ *on* $\mathbb{R}^3 \times \mathbb{R}^M$ *are independent.*

Then let the attenuation function *be defined as*

$$\forall \boldsymbol{r} \in \mathbb{R}^3, \quad \widehat{\alpha}(\boldsymbol{r}) = \boldsymbol{q}(\boldsymbol{r})^\top\widehat{\boldsymbol{\alpha}} \geq 0. \tag{7}$$

Based on (7)*, we define the following prime notation for functions:*

- *for any function* $\psi(\boldsymbol{u},t)$ *defined on* $\mathcal{S}^2\times\mathbb{R}$*, let* $\psi'(\boldsymbol{u},t) = \psi(\boldsymbol{u},t)\, e^{\widehat{\alpha}(\boldsymbol{u})t}$*;*
- *if function* $\widehat{\alpha}(.)$ *is constant on* $\mathcal{S}^2$ (i.e. $\forall \boldsymbol{u} \in \mathcal{S}^2, \widehat{\alpha}(\boldsymbol{u}) = \widehat{\alpha}^{\inf}$*), then for any function* $\psi(t)$ *defined on* $\mathbb{R}$*, let* $\psi'(t) = \psi(t)\, e^{\widehat{\alpha}^{\inf}t}$*.*

In addition, we assume that:

- *all functions defined above are not identically zero;*
- $\boldsymbol{r} \mapsto \boldsymbol{q}(\boldsymbol{r})$ *is four times continuously differentiable;*
- $\widehat{\alpha}^{\inf} \triangleq \inf_{\boldsymbol{u}\in\mathcal{S}^2}\widehat{\alpha}(\boldsymbol{u}) > 0$*;*
- $\forall i \in \{1\dots I\}$*, function* $g_i(\boldsymbol{u},t)$ *is continuous w.r.t.* $t \in \mathbb{R}$ *and twice continuously differentiable w.r.t.* $\boldsymbol{u} \in \mathcal{S}^2$*. Moreover,* $\forall \boldsymbol{u} \in \mathcal{S}^2$*, the temporal support of function* $t \mapsto g_i(\boldsymbol{u},t)$ *is included in* $[0,T_g]$ *with* $T_g > 0$*;*
- *function* $s(\boldsymbol{u},t)$ *is continuous w.r.t.* $t \in \mathbb{R}$ *and twice continuously differentiable w.r.t.* $\boldsymbol{u} \in \mathcal{S}^2$*. Moreover,* $\forall \boldsymbol{u} \in \mathcal{S}^2$*, the temporal support of function* $t \mapsto s(\boldsymbol{u},t)$ *is included* $[0,T_s]$ *with* $T_s > 0$*;*
- *at least one of the three following properties holds* $\forall \boldsymbol{u} \in \mathcal{S}^2$ *at* $f = 0$*:*
  - $\forall i \in \{1\dots I\}$*,* $\widehat{g_i'}(\boldsymbol{u},0) = 0$ *and* $m_{\widehat{s'}}(\boldsymbol{u},0) = 0$*;*
  - $\forall i \in \{1\dots I\}$*,* $\widehat{g_i'}(\boldsymbol{u},0) = 0$ *and* $\frac{\partial\widehat{g_i'}}{\partial f}(\boldsymbol{u},0) = 0$*;*
  - $m_{\widehat{s'}}(\boldsymbol{u},0) = 0$ *and* $\frac{\partial m_{\widehat{s'}}}{\partial f}(\boldsymbol{u},0) = 0$*;*

  where $\forall \boldsymbol{u} \in \mathcal{S}^2$*,* $\forall f \in \mathbb{R}$*,* $\forall (\boldsymbol{x},\boldsymbol{y}) \in \mathbb{R}^3 \times \mathbb{R}^M$*,*

  $$m_{\widehat{s'}}(\boldsymbol{u},f) = \mathbb{E}\left[\widehat{s'}(\Theta(\boldsymbol{x},\boldsymbol{y})\boldsymbol{u},f)\right]; \tag{8}$$

- *function* $\boldsymbol{z} \mapsto p(1;\boldsymbol{z})$ *is continuously differentiable and it is not constant;*
- *the support of function* $\boldsymbol{z} \mapsto p(1;\boldsymbol{z})$ *is left-bounded,* i.e. $\exists \boldsymbol{z}^{\inf} \in \mathbb{R}^M$ *such that* $\forall m \in \{1\dots M\}$*,* $z_m^{\inf} < 0$*, and* $\forall \boldsymbol{z} \in \mathbb{R}^M$*, if* $\exists m \in \{1\dots M\}$ *such that* $z_m < z_m^{\inf}$*, then* $p(1;\boldsymbol{z}) = 0$*;*
- *function* $(\boldsymbol{z}_1,\boldsymbol{z}_2) \mapsto p(1,1;\boldsymbol{z}_1,\boldsymbol{z}_2)$ *is continuous and differentiable almost everywhere in* $\mathbb{R}^M \times \mathbb{R}^M$*, and all its partial derivatives belong to* $L^\infty(\mathbb{R}^M \times \mathbb{R}^M)$*;*
- $(\boldsymbol{z}_1,\boldsymbol{z}_2) \mapsto p(1,1;\boldsymbol{z}_1,\boldsymbol{z}_2)$ *is such that* $\forall \boldsymbol{z} \in \mathbb{R}^M$*,*

$$p(1,1;\boldsymbol{z},\boldsymbol{z}) = p(1;\boldsymbol{z}). \tag{9}$$

Note that (9) is derived from geometrical considerations: when $\boldsymbol{x}_j \to \boldsymbol{x}_i$, a source image of coordinates $(\boldsymbol{x},\boldsymbol{y})$ is visible from both sensors i and j if and only if it is visible from sensor i. This can be expressed as $\forall \boldsymbol{x} \in \mathbb{R}^3$, $\forall \boldsymbol{y} \in \mathbb{R}^M$,

$$\lim_{\boldsymbol{x}_j\to\boldsymbol{x}_i} p(1,1;\boldsymbol{y}-\boldsymbol{q}(\boldsymbol{x}\text{-}\boldsymbol{x}_i),\boldsymbol{y}-\boldsymbol{q}(\boldsymbol{x}\text{-}\boldsymbol{x}_j)) = p(1;\boldsymbol{y}-\boldsymbol{q}(\boldsymbol{x}\text{-}\boldsymbol{x}_i)),$$

which implies (9). Moreover, because of (9), function $(\boldsymbol{z}_1,\boldsymbol{z}_2) \mapsto p(1,1;\boldsymbol{z}_1,\boldsymbol{z}_2)$ cannot be smoother than what we assumed in Definition 1 (*cf.* Lemma 5 in Appendix D) [2].

Also note that since functions $g_i(\boldsymbol{u},t)$ and $s(\boldsymbol{u},t)$ are causal $\forall \boldsymbol{u} \in \mathcal{S}^2$, the RIR $h_i(t)$ defined in (5) is also

[2]This remark is very important, because the fact that this function is not twice continuously differentiable is the reason for the slower speed of convergence $O(\frac{1}{\sqrt{t}})$ in late asymptotic state (see the discussion in Section III-E).

causal. Besides, all functions $g_i(\boldsymbol{u},t)$, $g_i'(\boldsymbol{u},t)$, $s(\boldsymbol{u},t)$ and $s'(\boldsymbol{u},t)$ are continuous w.r.t. $t \in \mathbb{R}$ and twice continuously differentiable w.r.t. $\boldsymbol{u} \in \mathcal{S}^2$, and since they all have finite temporal support, all functions $\widehat{g_i}(\boldsymbol{u},f)$, $\widehat{g_i'}(\boldsymbol{u},f)$, $\widehat{s}(\boldsymbol{u},f)$ and $\widehat{s'}(\boldsymbol{u},f)$ are smooth w.r.t. $f \in \mathbb{R}$ and twice continuously differentiable w.r.t. $\boldsymbol{u} \in \mathcal{S}^2$. Moreover, since $\boldsymbol{r} \mapsto \boldsymbol{q}(\boldsymbol{r})$ is four times continuously differentiable, function $\boldsymbol{r} \mapsto \widehat{\alpha}(\boldsymbol{r})$ is also four times continuously differentiable.

The stochastic model in Definition 1 is a particular case of the general stochastic reverberation model presented in [13], from which we introduced two simplifications[3]:

- the attenuation coefficients in vector $\widehat{\boldsymbol{\alpha}}$ are constant and do not depend on frequency f;
- the acoustic field is uniform: function $\boldsymbol{r} \mapsto \boldsymbol{q}(\boldsymbol{r})$ does not depend on sensor i.

In this report, we will address several particular cases of interest:

Definition 2 (Diffuse acoustic field)**.** *Considering the uniform stochastic reverberation model in Definition 1, the acoustic field is* diffuse *when the two following conditions hold:*

- $\forall \boldsymbol{r} \in \mathbb{R}^3$, $\boldsymbol{q}(\boldsymbol{r}) = \boldsymbol{q}\|\boldsymbol{r}\|_2$ *where* $\boldsymbol{q} \in \mathbb{R}_+^M$ *is a constant (dimensionless) vector, therefore function* $\widehat{\alpha}(.)$ *defined in* (7) *is constant on* $\mathcal{S}^2$*:* $\forall \boldsymbol{u} \in \mathcal{S}^2$, $\widehat{\alpha}(\boldsymbol{u}) = \widehat{\alpha}^{\text{inf}}$*, where* $\widehat{\alpha}^{\text{inf}} = \boldsymbol{q}^\top \widehat{\boldsymbol{\alpha}}$*;*
- *the random rotation matrices* $\Theta(\boldsymbol{x},\boldsymbol{y})$ *are uniformly distributed on SO(3).*

Definition 3 (Omnidirectional sensor)**.** *Considering the stochastic reverberation model in Definition 1, sensor* i *is* omnidirectional *when* $g_i(\boldsymbol{u},t) = g_i(t)\ \forall t \in \mathbb{R}$ *and* $\widehat{g_i}(\boldsymbol{u},f) = \widehat{g_i}(f)\ \forall f \in \mathbb{R}$ *do not depend on* $\boldsymbol{u} \in \mathcal{S}^2$*.*

Definition 4 (Omnidirectional source)**.** *Considering the stochastic reverberation model in Definition 1, the source is* omnidirectional *when* $s(\boldsymbol{u},t) = s(t)\ \forall t \in \mathbb{R}$ *and* $\widehat{s}(\boldsymbol{u},f) = \widehat{s}(f)\ \forall f \in \mathbb{R}$ *do no not depend on* $\boldsymbol{u} \in \mathcal{S}^2$*.*

Note that in the case of an omnidirectional source, the random rotation matrices $\Theta(\boldsymbol{x},\boldsymbol{y})$ disappear from Definition 1.

Finally, in order to characterize the correlations between sensors in the time-frequency domain, we will use two kinds of indicators that will be illustrated in the experiments presented in Section IV:

Definition 5 (Time-frequency correlation)**.** *Considering the stochastic reverberation model in Definition 1, the* time-frequency correlation *between two sensors* $i,j \in \{1 \dots I\}$ *is defined* $\forall t,f \in \mathbb{R}$ *as*

$$\rho_{i,j}(t,f,\boldsymbol{x}_j - \boldsymbol{x}_i) \frac{\mathcal{W}_{\gamma_{i,j}}(t,f)}{\sqrt{\mathcal{W}_{\gamma_{i,i}}(t,f)\mathcal{W}_{\gamma_{j,j}}(t,f)}} \tag{10}$$

[3]Moreover, compared to [13], we simplified the mathematical expressions (without loss of generality), by removing the rotation matrix Θ_i in $g_i\left(\Theta_i \frac{\boldsymbol{x}-\boldsymbol{x}_i}{\|\boldsymbol{x}-\boldsymbol{x}_i\|_2}, t\right)$ and $\widehat{g_i}\left(\Theta_i \frac{\boldsymbol{x}-\boldsymbol{x}_i}{\|\boldsymbol{x}-\boldsymbol{x}_i\|_2}, f\right)$, and by changing the sign of the rotation matrices $\Theta(\boldsymbol{x},\boldsymbol{y})$ in $s\left(\Theta(\boldsymbol{x},\boldsymbol{y})\frac{\boldsymbol{x}_i-\boldsymbol{x}}{\|\boldsymbol{x}_i-\boldsymbol{x}\|_2}, t\right)$ and $\widehat{s}\left(\Theta(\boldsymbol{x},\boldsymbol{y})\frac{\boldsymbol{x}_i-\boldsymbol{x}}{\|\boldsymbol{x}_i-\boldsymbol{x}\|_2}, f\right)$.

whenever the denominator is positive, where $\mathcal{W}$ *denotes the Wigner distribution defined in* (1)*, and*

$$\gamma_{i,j}(t_1,t_2) = \text{cov}[h_i(t_1), h_j(t_2)]. \tag{11}$$

In (10), we introduced the redundant notation $\rho_{i,j}(t,f,\boldsymbol{x}_j - \boldsymbol{x}_i)$ (which makes a double use of indexes i and j) in order to insist on the fact that $\rho_{i,j}$ will depend on $\boldsymbol{x}_i$ and $\boldsymbol{x}_j$, only via their difference $\boldsymbol{x}_j - \boldsymbol{x}_i$, since the acoustic field is uniform (*i.e.* invariant under any translation). Also note that, since function $f \mapsto \mathcal{W}_{\gamma_{i,j}}(t,f)$ is even symmetric, function $f \mapsto \rho_{i,j}(t,f,\boldsymbol{x}_j - \boldsymbol{x}_i)$ is also even symmetric.

If the time-frequency correlation converges when $t \to +\infty$, we also define the following indicator:

Definition 6 (Asymptotic correlation function)**.** *Considering the stochastic reverberation model in Definition 1, the* asymptotic correlation function *between two sensors* $i,j \in \{1 \dots I\}$ *is defined* $\forall \tau \in \mathbb{R}$ *as*

$$\sigma_{i,j}(\tau, \boldsymbol{x}_j - \boldsymbol{x}_i) = \int_{f \in \mathbb{R}} \lim_{t \to +\infty} \rho_{i,j}(t,f,\boldsymbol{x}_j - \boldsymbol{x}_i) e^{+2\imath\pi f \tau} df, \tag{12}$$

whenever the limit exists and the integral converges, where $\rho_{i,j}$ *was defined in* (10)*.*

Note that, since function $f \mapsto \rho_{i,j}(t,f,\boldsymbol{x}_j - \boldsymbol{x}_i)$ is even symmetric, $\sigma_{i,j}(\tau, \boldsymbol{x}_j - \boldsymbol{x}_i) \in \mathbb{R}\ \forall \tau \in \mathbb{R}$.

III. Mathematical analysis

In this section, we analyze the statistical properties of the stochastic model introduced in Definition 1, in terms of first order (Section III-A) and second order moments (Section III-B). Then we will be able to relax some restricting assumptions regarding the acoustic field, the source and the microphones, by focusing on late reverberation only, *i.e.* by assuming that $t \to +\infty$. Actually, the mathematical analysis in Section III, as well as the observations in Section IV based on both synthetic and real RIRs, will show that two different asymptotic states can be distinguished: at first, the variations of the attenuation $\widehat{\alpha}(.)$ defined in (7) over the direction $\boldsymbol{u} \in \mathcal{S}^2$ can be neglected; this period of time will be called *early asymptotic state* (Section III-C). Then after a while, the directions $\boldsymbol{u}$ that are less attenuated (*i.e.* such that $\widehat{\alpha}(\boldsymbol{u}) > 0$ is the lowest) start to dominate the other directions; this period of time will be called *late asymptotic state* (Section III-D). In both asymptotic states, we will prove that the RIR $h_i(t)$ is asymptotically normally distributed.

A. First order moments

Before analyzing the first order moments, we need to define some coefficients that are related to the discrete probability distribution p introduced in Definition 1, and that will play an important role throughout this research report:

Lemma 1. *Let* $p(b,\boldsymbol{z})$ *(where* $b \in \{0,1\}$ *and* $\boldsymbol{z} \in \mathbb{R}^M$*) be the probability distribution introduced in Definition 1. Let* $\forall n \in \mathbb{N}\backslash\{0\}$*,*

$$\beta_n = \int_{\boldsymbol{z} \in \mathbb{R}^M} p(1;\boldsymbol{z}) e^{-n\frac{\boldsymbol{z}^\top \widehat{\boldsymbol{\alpha}}}{c}} d\boldsymbol{z} > 0. \tag{13}$$

Then we have the following majoration: $\forall n \in \mathbb{N}\backslash\{0\}$,

$$\beta_n = O\left(\frac{e^{n\frac{|\boldsymbol{z}^{\inf}|^\top \widehat{\boldsymbol{\alpha}}}{c}}}{n^M}\right). \tag{14}$$

Lemma 1 is proved in Appendix D. We are now ready to investigate the first order moments of the stochastic reverberation model:

Proposition 1 (First order moments)**.** *Given the stochastic reverberation model in Definition 1, the room response has the following first order moments: for any sensor* $i \in \{1 \dots I\}$,

- *Temporal domain:* $\forall t \geq T \triangleq T_g + T_s$, $\mathbb{E}[h_i(t)] = 0$.
- *Spectral domain: let* $\forall \boldsymbol{u} \in \mathcal{S}^2$, $\forall f \in \mathbb{R}$,

$$m_{\widehat{s}}(\boldsymbol{u}, f) = \mathbb{E}\left[\widehat{s}\left(\Theta(\boldsymbol{x}, \boldsymbol{y})\boldsymbol{u}, f\right)\right] \tag{15}$$

$\forall (\boldsymbol{x}, \boldsymbol{y}) \in \mathbb{R}^3 \times \mathbb{R}^M$. *Then function* $m_{\widehat{s}}$ *is twice continuously differentiable w.r.t.* $\boldsymbol{u} \in \mathcal{S}^2$ *and smooth w.r.t.* $f \in \mathbb{R}$. *Moreover,* $\forall f \in \mathbb{R}$,

$$\mathbb{E}[\widehat{h_i}(f)] = \lambda c^2 \beta_1 \int_{\boldsymbol{u} \in \mathcal{S}^2} \frac{\widehat{g_i}(\boldsymbol{u}, f)\, m_{\widehat{s}}(\boldsymbol{u}, f)}{\left(\widehat{\alpha}(\boldsymbol{u}) + 2\imath\pi f\right)^2} d\boldsymbol{u} \tag{16}$$

where β_1 *is defined in* (13) *for* $n = 1$, *and function* $f \mapsto \mathbb{E}[\widehat{h_i}(f)]$ *is smooth.*

Proposition 1 is proved in Appendix E. Note that this proposition generalizes the results already established in [2]. In particular, $h_i(t)$ is centered for $t \geq T$ (the fact that it is *not* centered for $t \in [0, T]$ explains why the expected value of the frequency response $\mathbb{E}[\widehat{h_i}(f)]$ in (16) is not zero).

B. Second order moments

Before analyzing the second order moments, we need to further investigate the properties of the discrete probability distribution p introduced in Definition 1.

Lemma 2. *Let* $p(b_i, b_j, \boldsymbol{z}_i, \boldsymbol{z}_j)$ *(where* $b_i, b_j \in \{0, 1\}$ *and* $\boldsymbol{z}_i, \boldsymbol{z}_j \in \mathbb{R}^M$*) be the joint probability distribution introduced in Definition 1. Let* $\forall \boldsymbol{e} \in \mathbb{R}^M$,

$$\beta(\boldsymbol{e}) = \int_{\boldsymbol{z} \in \mathbb{R}^M} p(1, 1; \boldsymbol{z} - \tfrac{\boldsymbol{e}}{2}, \boldsymbol{z} + \tfrac{\boldsymbol{e}}{2}) e^{-\frac{2\boldsymbol{z}^\top \widehat{\boldsymbol{\alpha}}}{c}} d\boldsymbol{z} \geq 0. \tag{17}$$

Then function $\boldsymbol{e} \mapsto \beta(\boldsymbol{e})$ *is even. Moreover, it is continuous and differentiable almost everywhere in* $\mathbb{R}^M$*, and all its partial derivatives belong to* $L^\infty(\mathbb{R}^M)$.

At $\boldsymbol{e} = \boldsymbol{0}$, $\beta(\boldsymbol{0}) = \beta_2$, *where* β_2 *is defined in* (13) *for* $n = 2$. *Besides,* $\forall \boldsymbol{e} \in \mathbb{R}^M$,

$$\beta(\boldsymbol{e}) \leq \beta_2\, e^{-\frac{|\boldsymbol{e}^\top \widehat{\boldsymbol{\alpha}}|}{c}}. \tag{18}$$

In particular, function $\boldsymbol{e} \mapsto \beta(\boldsymbol{e})$ *reaches its maximum at* $\boldsymbol{e} = 0$, *and it is not differentiable at* $\boldsymbol{e} = 0$.

Lemma 2 is proved in Appendix D. Note that, in connection with the remark in Footnote 2, the fact that function $\beta(.)$ is not twice continuously differentiable is the reason for the slower speed of convergence $O(\frac{1}{\sqrt{t}})$ in late asymptotic state (see the discussion in Section III-E).

In the following lemma, we introduce a function that will play a prominent role to characterize the second order moments of the RIR in the spatial, temporal, spectral and time-frequency domains.

Lemma 3. *Given the stochastic reverberation model in Definition 1, let* $\beta(.)$ *be the function introduced in Lemma 2 in* (17)*, let* β_2 *be defined in* (13) *for* $n = 2$, *and let* $D \geq 0$ *denote the distance between two sensors. We also assume that* $\forall \boldsymbol{r} \in \mathbb{R}^3$, $\boldsymbol{q}(\boldsymbol{r}) = \boldsymbol{q}\|\boldsymbol{r}\|_2$ *where* $\boldsymbol{q} \in \mathbb{R}_+^M$ *is a constant vector, therefore function* $\widehat{\alpha}(.)$ *defined in* (7) *is constant on* $\mathcal{S}^2$*:* $\forall \boldsymbol{u} \in \mathcal{S}^2$, $\widehat{\alpha}(\boldsymbol{u}) = \widehat{\alpha}^{\inf}$, *where* $\widehat{\alpha}^{\inf} = \boldsymbol{q}^\top \widehat{\boldsymbol{\alpha}}$. *If* $D > 0$, *let*

$$b(\tau, D) = \tfrac{c}{2D}\beta\left(\boldsymbol{q}c\tau\right) \mathbf{1}_{\left[-\frac{D}{c}, +\frac{D}{c}\right]}(\tau) \geq 0 \quad \forall \tau \in \mathbb{R}, \tag{19}$$

otherwise if $D = 0$, *let* $b(\tau, 0) = \beta_2 \delta(\tau)$ *and* $\widehat{b}(f, 0) = \beta_2$ $\forall f \in \mathbb{R}$. *Then function* $\tau \mapsto b(\tau, D)$ *is even. Moreover, it is continuous w.r.t.* τ *and differentiable almost everywhere in the interior of its support, and* $\frac{\partial b}{\partial \tau}(\tau, D) \in L^\infty(]-\frac{D}{c}, +\frac{D}{c}[)$. *Function* $f \mapsto \widehat{b}(f, D)$ *is smooth and real-valued. Moreover, we have the two majorations:* $\forall \tau \in \mathbb{R}$,

$$b(\tau, D) \leq \tfrac{c\beta_2}{2D} e^{-\widehat{\alpha}^{\inf}|\tau|} \mathbf{1}_{\left[-\frac{D}{c}, +\frac{D}{c}\right]}(\tau), \tag{20}$$

and $\forall f \in \mathbb{R}$,

$$|\widehat{b}(f, D)| \leq \beta_2. \tag{21}$$

In particular, function $\tau \mapsto b(\tau, D)$ *reaches its maximum at* $\tau = 0$, *and it is not differentiable at* $\tau = 0$.

Besides, when $D \to 0$, *we get*

$$b(\tau, D) = \left(\tfrac{c\beta_2}{2D} + O(1)\right) \mathbf{1}_{\left[-\frac{D}{c}, +\frac{D}{c}\right]}(\tau) \tag{22}$$

and

$$\widehat{b}(f, D) = \beta_2 \operatorname{sinc}\left(\tfrac{2\pi f D}{c}\right) + O(D). \tag{23}$$

Lemma 3 is proved in Appendix F. We are now ready to investigate the second order moments of the stochastic reverberation model in the case of diffuse acoustic fields:

Proposition 2 (Second order moments in diffuse acoustic fields)**.** *Considering the stochastic reverberation model in Definition 1, suppose that the acoustic field is diffuse (*cf. *Definition 2) and that the source and microphones are omnidirectional (*cf. *Definitions 3 and 4). For any sensors* $i, j \in \{1 \dots I\}$, *let* $D = \|\boldsymbol{x}_i - \boldsymbol{x}_j\|_2$ *denote the distance between the two sensors, and let* $\gamma_{i,j}(t_1, t_2)$ *be the function defined in* (11). *Finally, let* $b(\tau, D)$ *be the function introduced in Lemma 3. Then the room response has the following second order moments:*

- *Temporal domain:* $\forall t_1 + t_2 \geq 2T + \frac{D}{c}$ *with* $T \triangleq T_g + T_s$,

$$\gamma_{i,j}(t_1, t_2) = 4\pi\lambda c\, e^{-\widehat{\alpha}^{\inf}(t_1 + t_2)} \left(b(., D) * g_i' * \widetilde{g_j'} * s' * \widetilde{s'}\right)(t_1 - t_2), \tag{24}$$

and function $(t_1, t_2) \mapsto \gamma_{i,j}(t_1, t_2)$ *is continuous. In particular, if* $i = j$, $\forall t \geq T$,

$$\operatorname{var}[h_i(t)] = 4\pi\lambda c\, \beta_2 e^{-2\widehat{\alpha}^{\inf} t} \left(g_i' * \widetilde{g_i'} * s' * \widetilde{s'}\right)(0) \tag{25}$$

and $\forall t_1+t_2 \geq 2T+\frac{D}{c}$*, the temporal correlation*

$$\operatorname{corr}[h_i(t_1),h_j(t_2)]=\frac{\left(b(.,D)*g_i'*\widetilde{g_j'}*s'*\widetilde{s'}\right)(t_1-t_2)}{\beta_2\sqrt{\left(\left(g_i'*\widetilde{g_i'}*s'*\widetilde{s'}\right)(0)\right)\left(\left(g_j'*\widetilde{g_j'}*s'*\widetilde{s'}\right)(0)\right)}} \tag{26}$$

only depends on t_1-t_2*.*

- *Spectral domain:* $\forall f_1,f_2\in\mathbb{R}$*,*

$$\begin{aligned}&\operatorname{cov}[\widehat{h_i}(f_1),\widehat{h_j}(f_2)]\\ =\;&\frac{2\pi\lambda c\,\widehat{b}(\frac{f_1+f_2}{2},D)\widehat{g_i}(f_1)\overline{\widehat{g_j}(f_2)}\widehat{s}(f_1)\overline{\widehat{s}(f_2)}e^{-\frac{(\widehat{\alpha}^{\inf}+\imath\pi(f_1-f_2))D}{c}}}{\widehat{\alpha}^{\inf}+\imath\pi(f_1-f_2)},\end{aligned} \tag{27}$$

and function $(f_1,f_2)\mapsto\operatorname{cov}[\widehat{h_i}(f_1),\widehat{h_j}(f_2)]$ *is smooth. In particular, if* $i=j$*,* $\forall f\in\mathbb{R}$*,*

$$\operatorname{var}[\widehat{h_i}(f)]=\frac{2\pi\lambda c\beta_2\,|\widehat{g_i}(f)|^2|\widehat{s}(f)|^2}{\widehat{\alpha}^{\inf}} \tag{28}$$

and $\forall f_1,f_2\in\mathbb{R}$*,*

$$\begin{aligned}\operatorname{corr}[\widehat{h_i}(f_1),\widehat{h_j}(f_2)]=\;&e^{\imath(\angle\widehat{g_i}(f_1)-\angle\widehat{g_j}(f_2)+\angle\widehat{s}(f_1)-\angle\widehat{s}(f_2))}\\ &\frac{\widehat{b}(\frac{f_1+f_2}{2},D)e^{-\frac{(\widehat{\alpha}^{\inf}+\imath\pi(f_1-f_2))D}{c}}}{\beta_2\left(1+\frac{\imath\pi(f_1-f_2)}{\widehat{\alpha}^{\inf}}\right)}.\end{aligned} \tag{29}$$

- *Time-frequency domain:* $\forall t\geq T+\frac{D}{2c}$*,* $\forall f\in\mathbb{R}$*,*

$$\mathcal{W}_{\gamma_{i,j}}(t,f)=e^{-2\widehat{\alpha}^{\inf}t}B_{i,j}(f,D) \tag{30}$$

where

$$B_{i,j}(f,D)=4\pi\lambda c\,\widehat{b}(f,D)\widehat{g_i'}(f)\overline{\widehat{g_j'}(f)}|\widehat{s'}(f)|^2, \tag{31}$$

and function $f\mapsto B_{i,j}(f,D)$ *is smooth.*
In particular, if $i=j$*,*

$$\mathcal{W}_{\gamma_{i,i}}(t,f)=4\pi\lambda c\,\beta_2 e^{-2\widehat{\alpha}^{\inf}t}|\widehat{g_i'}(f)|^2|\widehat{s'}(f)|^2\geq 0 \tag{32}$$

and the time-frequency correlation introduced in Definition 5 only depends on f*:*

$$\rho_{i,j}(t,f,\boldsymbol{x}_j-\boldsymbol{x}_i)=e^{\imath(\angle\widehat{g_i'}(f)-\angle\widehat{g_j'}(f))}\frac{\widehat{b}(f,D)}{\beta_2}. \tag{33}$$

Finally, if $\forall f\in\mathbb{R}$*,* $\angle\widehat{g_i'}(f)=\angle\widehat{g_j'}(f)$*, the asymptotic correlation function introduced in Definition 6 is*

$$\sigma_{i,j}(\tau,\boldsymbol{x}_j-\boldsymbol{x}_i)=\frac{b(\tau,D)}{\beta_2}\in[0,\tfrac{c}{2D}], \tag{34}$$

and function $\tau\mapsto\sigma_{i,j}(\tau,\boldsymbol{x}_j-\boldsymbol{x}_i)$ *is continuous in the interior of its support* $[-\frac{D}{c},\frac{D}{c}]$*, it reaches its maximum at* $\tau=0$*, and it is not differentiable at* $\tau=0$*.*

Proposition 2 is proved in Appendix F. Note that Lemma 3 shows that when $D\to 0$, the results in Proposition 2 come down to those already established in [2].

C. Early asymptotic state

Proposition 2 holds only in the case of diffuse acoustic fields and omnidirectional source and microphones. If we now focus on late reverberation (i.e. $t\to+\infty$), these assumptions can be relaxed:

Proposition 3 (Early asymptotic state)**.** *Considering the stochastic reverberation model in Definition 1, suppose that* $\forall\boldsymbol{r}\in\mathbb{R}^3$*,* $\boldsymbol{q}(\boldsymbol{r})=\boldsymbol{q}\|\boldsymbol{r}\|_2$ *where* $\boldsymbol{q}\in\mathbb{R}_+^M$ *is a constant vector, therefore function* $\widehat{\alpha}(.)$ *defined in* (7) *is constant on* $\mathcal{S}^2$*:* $\forall\boldsymbol{u}\in\mathcal{S}^2$*,* $\widehat{\alpha}(\boldsymbol{u})=\widehat{\alpha}^{\inf}$*, where* $\widehat{\alpha}^{\inf}=\boldsymbol{q}^\top\widehat{\boldsymbol{\alpha}}$*. For any sensors* $i,j\in\{1\dots I\}$*, let* $\gamma_{i,j}(t_1,t_2)$ *be the function defined in* (11)*. Then the room response has the following statistical properties:*

- *Temporal domain: let* $\forall\boldsymbol{u}\in\mathcal{S}^2$*,* $\forall t\in\mathbb{R}$*,*

$$m_{s'*\widetilde{s'}}(\boldsymbol{u},t)=\mathbb{E}\left[s'\left(\Theta(\boldsymbol{x},\boldsymbol{y})\boldsymbol{u},.\right)\overset{t}{*}\widetilde{s'}\left(\Theta(\boldsymbol{x},\boldsymbol{y})\boldsymbol{u},.\right)\right] \tag{35}$$

$\forall(\boldsymbol{x},\boldsymbol{y})\in\mathbb{R}^3\times\mathbb{R}^M$*. Then function* $m_{s'*\widetilde{s'}}(\boldsymbol{u},t)$ *is continuous w.r.t.* $t\in\mathbb{R}$ *and twice continuously differentiable w.r.t.* $\boldsymbol{u}\in\mathcal{S}^2$*. Moreover,* $\forall t\geq T\triangleq T_g+T_s$*,*

$$\begin{aligned}&\operatorname{var}[h_i(t)]=\lambda c\beta_2\,e^{-2\widehat{\alpha}^{\inf}t}\Big(\int_{\boldsymbol{u}\in\mathcal{S}^2}\\ &\left(g_i'(\boldsymbol{u},.)*\widetilde{g_i'}(\boldsymbol{u},.)*m_{s'*\widetilde{s'}}(\boldsymbol{u},.)\right)(0)d\boldsymbol{u}\Big).\end{aligned} \tag{36}$$

- *Time-frequency domain: let* $\forall\boldsymbol{u}\in\mathcal{S}^2$*,* $\forall f\in\mathbb{R}$*,*

$$m_{|\widehat{s'}|^2}(\boldsymbol{u},f)=\mathbb{E}\Big[\left|\widehat{s'}\left(\Theta(\boldsymbol{x},\boldsymbol{y})\boldsymbol{u},f\right)\right|^2\Big] \tag{37}$$

$\forall(\boldsymbol{x},\boldsymbol{y})\in\mathbb{R}^3\times\mathbb{R}^M$*. Then function* $m_{|\widehat{s'}|^2}$ *is smooth w.r.t.* $f\in\mathbb{R}$ *and twice continuously differentiable w.r.t.* $\boldsymbol{u}\in\mathcal{S}^2$*. Moreover,* $\forall f\in\mathbb{R}$*, when* $t\to+\infty$*,*

$$\mathcal{W}_{\gamma_{i,j}}(t,f)=e^{-2\widehat{\alpha}^{\inf}t}\left(B_{i,j}(f,\boldsymbol{x}_j-\boldsymbol{x}_i)+O\left(\tfrac{1}{t}\right)\right) \tag{38}$$

where $\forall f\in\mathbb{R}$*,* $\forall\boldsymbol{r}\in\mathbb{R}^3$*,*

$$\begin{aligned}&B_{i,j}(f,\boldsymbol{r})=\lambda c\int_{\boldsymbol{u}\in\mathcal{S}^2}\beta\left(\boldsymbol{q}\boldsymbol{u}^\top\boldsymbol{r}\right)\\ &\widehat{g_i'}(\boldsymbol{u},f)\overline{\widehat{g_j'}(\boldsymbol{u},f)}m_{|\widehat{s'}|^2}(\boldsymbol{u},f)e^{-2\imath\pi f\frac{\boldsymbol{u}^\top\boldsymbol{r}}{c}}d\boldsymbol{u},\end{aligned} \tag{39}$$

and function $f\mapsto B_{i,j}(f,\boldsymbol{r})$ *is smooth and even symmetric. In particular, if* $i=j$*, then* $\forall t\geq T$*,*

$$\begin{aligned}\mathcal{W}_{\gamma_{i,i}}(t,f)=\;&\lambda c\beta_2\,e^{-2\widehat{\alpha}^{\inf}t}\\ &\left(\int_{\boldsymbol{u}\in\mathcal{S}^2}|\widehat{g_i'}(\boldsymbol{u},f)|^2m_{|\widehat{s'}|^2}(\boldsymbol{u},f)d\boldsymbol{u}\right)\geq 0\end{aligned} \tag{40}$$

and the time-frequency correlation in Definition 5,

$$\rho_{i,j}(t,f,\boldsymbol{x}_j-\boldsymbol{x}_i)=\frac{B_{i,j}(f,\boldsymbol{x}_j-\boldsymbol{x}_i)}{\sqrt{B_{i,i}(f,\boldsymbol{0})B_{j,j}(f,\boldsymbol{0})}}+O\left(\tfrac{1}{t}\right) \tag{41}$$

only depends on f *when* $t\to+\infty$*, and it is asymptotically smooth and even symmetric w.r.t.* f*.*

- *Asymptotic Gaussianity: when* $t\to+\infty$*, the sequence of random variables* $\frac{h_i(t)}{\sqrt{\operatorname{var}[h_i(t)]}}$ *converges in law to the standard Gaussian distribution.*

Proposition 3 is proved in Appendix G. By introducing an additional assumption that holds in various experimental setups (*cf.* Section IV), the results in Proposition 3 can be simplified:

Corollary 1 (Early asymptotic state)**.** *Considering the stochastic reverberation model in Definition 1, suppose that* $\forall\boldsymbol{r}\in\mathbb{R}^3$*,* $\boldsymbol{q}(\boldsymbol{r})=\boldsymbol{q}\|\boldsymbol{r}\|_2$ *where* $\boldsymbol{q}\in\mathbb{R}_+^M$ *is a constant vector, therefore function* $\widehat{\alpha}(.)$ *defined in* (7) *is constant on* $\mathcal{S}^2$*:* $\forall\boldsymbol{u}\in\mathcal{S}^2$*,* $\widehat{\alpha}(\boldsymbol{u})=\widehat{\alpha}^{\inf}$*, where* $\widehat{\alpha}^{\inf}=\boldsymbol{q}^\top\widehat{\boldsymbol{\alpha}}$*. Also suppose that*

the product $\widehat{g_i'}(\boldsymbol{u},f)\overline{\widehat{g_j'}(\boldsymbol{u},f)}m_{|\widehat{s'}|^2}(\boldsymbol{u},f)$ *with* $m_{|\widehat{s'}|^2}$ *defined in* (37) *can be factorized as*

$$\widehat{g_i'}(\boldsymbol{u},f)\overline{\widehat{g_j'}(\boldsymbol{u},f)}m_{|\widehat{s'}|^2}(\boldsymbol{u},f)=\xi_{i,j}(\boldsymbol{u})\,\chi(f), \tag{42}$$

where function $\boldsymbol{u}\mapsto\xi_{i,j}(\boldsymbol{u})\geq 0$ *is twice continuously differentiable, and function* $f\mapsto\chi(f)\geq 0$ *is smooth. For any sensors* $i,j\in\{1\dots I\}$*, let* $D=\|\boldsymbol{x}_i-\boldsymbol{x}_j\|_2$ *denote the distance between the two sensors and let* $\gamma_{i,j}(t_1,t_2)$ *be the function defined in* (11)*. Then* $\forall f\in\mathbb{R}$*,* $\forall t\geq T\triangleq T_g+T_s$*,*

$$\mathcal{W}_{\gamma_{i,i}}(t,f)=\lambda c\beta_2 e^{-2\widehat{\alpha}^{\inf}t}\chi(f)\int_{\boldsymbol{u}\in\mathcal{S}^2}\xi_{i,i}(\boldsymbol{u})d\boldsymbol{u}. \tag{43}$$

Besides, the asymptotic correlation function $\sigma_{i,j}(\tau,\boldsymbol{x}_j-\boldsymbol{x}_i)$ *introduced in Definition 6 is nonnegative and it is continuous w.r.t.* τ *in the interior of its support* $[-\frac{D}{c},\frac{D}{c}]$*.*

If moreover function $\xi_{i,j}(.)$ *is even on* $\mathcal{S}^2$ *(*symmetric case*), then function* $\tau\mapsto\sigma_{i,j}(\tau,\boldsymbol{x}_j-\boldsymbol{x}_i)$ *is also even, and its Fourier transform* $\lim_{t\to+\infty}\rho_{i,j}(t,f,\boldsymbol{x}_j-\boldsymbol{x}_i)$ *is real-valued.*

If moreover function $\xi_{i,j}(.)$ *is constant on* $\mathcal{S}^2$ *(*isotropic case*), then when* $t\to+\infty$*,*

$$\rho_{i,j}(t,f,\boldsymbol{x}_j-\boldsymbol{x}_i)=\tfrac{\widehat{b}(f,D)}{\beta_2}+O(\tfrac{1}{t}) \tag{44}$$

and

$$\sigma_{i,j}(\tau,\boldsymbol{x}_j-\boldsymbol{x}_i)=\tfrac{b(\tau,D)}{\beta_2}\in[0,\tfrac{c}{2D}], \tag{45}$$

and function $\tau\mapsto\sigma_{i,j}(\tau,\boldsymbol{x}_j-\boldsymbol{x}_i)$ *reaches its maximum at* $\tau=0$*, and it is not differentiable at* $\tau=0$*.*

If in addition $D\to 0$*, we get*

$$\lim_{t\to+\infty}\rho_{i,j}(t,f,\boldsymbol{x}_j-\boldsymbol{x}_i)=\operatorname{sinc}\left(\tfrac{2\pi fD}{c}\right)+O(D) \tag{46}$$

and

$$\sigma_{i,j}(\tau,\boldsymbol{x}_j-\boldsymbol{x}_i)=\left(\tfrac{c}{2D}+O(1)\right)\mathbf{1}_{[-\frac{D}{c},\frac{D}{c}]}(\tau). \tag{47}$$

Corollary 1 is proved in Appendix G.5. Note that the additional assumption in Corollary 1 is necessary to conclude that the asymptotic correlation function $\sigma_{i,j}(\tau,\boldsymbol{x}_j-\boldsymbol{x}_i)$ is nonnegative and that its temporal support lies in $[-\frac{D}{c},\frac{D}{c}]$. Under the more general assumptions of Proposition 3, these properties may not hold.

D. Late asymptotic state

In Section III-C we assumed that the attenuation function $\widehat{\alpha}(.)$ in (7) is constant on $\mathcal{S}^2$. Now we aim to relax this assumption:

Definition 7 (Regular attenuation function)**.** *Let* $\widehat{\alpha}:\mathcal{S}^2\to\mathbb{R}_+$ *denote the restriction to* $\mathcal{S}^2$ *of the function introduced in Definition 1 in* (7)*. Let* $\widehat{\alpha}^{\inf}=\inf_{\boldsymbol{u}\in\mathcal{S}^2}\widehat{\alpha}(\boldsymbol{u})>0$*, and suppose that function* $\boldsymbol{u}\mapsto\widehat{\alpha}(\boldsymbol{u})$ *reaches its global minimum* $\widehat{\alpha}^{\inf}$ *at a finite set* $\mathcal{U}=\{\boldsymbol{u}_k\}_{k\in\mathcal{K}}$ *of distinct points* $\boldsymbol{u}_k\in\mathcal{S}^2$*. We further assume that the Hessian* $\ddot{\widehat{\alpha}}_k\in\mathbb{R}$ *of function* $\widehat{\alpha}$ *at every minimum point* $\boldsymbol{u}_k$ *on the Riemannian manifold* $\mathcal{S}^2$ *is positive.*

Proposition 4 (Late asymptotic state)**.** *Considering the stochastic reverberation model in Definition 1, suppose that the attenuation function is regular (Definition 7). Let* $\forall\boldsymbol{u}\in\mathcal{S}^2$*,*

$$\mathring{\mathbf{J}}_{\boldsymbol{q}}(\boldsymbol{u})=\mathbf{J}_{\boldsymbol{q}}(\boldsymbol{u})\left(\boldsymbol{I}-\boldsymbol{u}\boldsymbol{u}^T\right) \tag{48}$$

where $\mathbf{J}_{\boldsymbol{q}}(\boldsymbol{x})$ *denotes the Jacobian matrix of function* $\boldsymbol{q}(.)$ *at* $\boldsymbol{x}\in\mathbb{R}^3$*. For any sensors* $i,j\in\{1\dots I\}$*, let* $\gamma_{i,j}(t_1,t_2)$ *be the function defined in* (11)*. Then the room response has the following statistical properties when* $t\to+\infty$*:*

- *Temporal domain:*

$$\begin{aligned}&\operatorname{var}[h_i(t)]=\tfrac{\pi\lambda c\beta_2\,e^{-2\widehat{\alpha}^{\inf}t}}{t}\\&\left(\sum_{k\in\mathcal{K}}\tfrac{(g_i'(\boldsymbol{u}_k,.)*\widetilde{g_i'}(\boldsymbol{u}_k,.)*m_{s'*\widetilde{s'}}(\boldsymbol{u}_k,.))(0)}{\sqrt{\ddot{\widehat{\alpha}}_k}}+O(\tfrac{1}{t})\right)\end{aligned} \tag{49}$$

  where $\forall\boldsymbol{u}_k\in\mathcal{U}$*,* $t\mapsto m_{s'*\widetilde{s'}}(\boldsymbol{u}_k,t)$ *is the continuous function defined in* (35)*.*

- *Time-frequency domain: let* $\forall f\in\mathbb{R}$*,* $\forall\boldsymbol{r}\in\mathbb{R}^3$*,*

$$B_{i,j}(f,\boldsymbol{r})=\tfrac{\pi\lambda c\sum_{k\in\mathcal{K}}\beta_k(\boldsymbol{r})\,\widehat{g_i'}(\boldsymbol{u}_k,f)\overline{\widehat{g_j'}(\boldsymbol{u}_k,f)}m_{|\widehat{s'}|^2}(\boldsymbol{u}_k,f)e^{-2\imath\pi f\frac{\boldsymbol{u}_k^\top\boldsymbol{r}}{c}}}{\sqrt{\ddot{\widehat{\alpha}}_k}} \tag{50}$$

  where $\forall k\in\mathcal{K}$*,* $\forall\boldsymbol{r}\in\mathbb{R}^3$*,*

$$\beta_k(\boldsymbol{r})=\beta\left(\left(\boldsymbol{q}\left(\boldsymbol{u}_k\right)\boldsymbol{u}_k^T+\mathring{\mathbf{J}}_{\boldsymbol{q}}(\boldsymbol{u}_k)\right)\boldsymbol{r}\right) \tag{51}$$

  and $\forall\boldsymbol{u}_k\in\mathcal{U}$*,* $f\mapsto m_{|\widehat{s'}|^2}(\boldsymbol{u}_k,f)$ *is the smooth function defined in* (37)*. Then function* $f\mapsto B_{i,j}(f,\boldsymbol{r})$ *is smooth and even symmetric. Moreover,* $\forall f\in\mathbb{R}$*,*

$$\mathcal{W}_{\gamma_{i,j}}(t,f)=\tfrac{e^{-2\widehat{\alpha}^{\inf}t}}{t}\left(B_{i,j}(f,\boldsymbol{x}_j-\boldsymbol{x}_i)+O\left(\tfrac{1}{\sqrt{t}}\right)\right). \tag{52}$$

  In particular, if $i=j$*,*

$$\begin{aligned}&\mathcal{W}_{\gamma_{i,i}}(t,f)=\tfrac{\pi\lambda c\beta_2 e^{-2\widehat{\alpha}^{\inf}t}}{t}\\&\left(\sum_{k\in\mathcal{K}}\tfrac{|\widehat{g_i'}(\boldsymbol{u}_k,f)|^2m_{|\widehat{s'}|^2}(\boldsymbol{u}_k,f)}{\sqrt{\ddot{\widehat{\alpha}}_k}}+O(\tfrac{1}{t})\right)\geq 0\end{aligned} \tag{53}$$

  and the time-frequency correlation in Definition 5,

$$\rho_{i,j}(t,f,\boldsymbol{x}_j-\boldsymbol{x}_i)=\tfrac{B_{i,j}(f,\boldsymbol{x}_j-\boldsymbol{x}_i)}{\sqrt{B_{i,i}(f,\mathbf{0})B_{j,j}(f,\mathbf{0})}}+O\left(\tfrac{1}{\sqrt{t}}\right) \tag{54}$$

  only depends on f *when* $t\to+\infty$*, and it is asymptotically smooth and even symmetric w.r.t.* f*.*

- *Asymptotic Gaussianity: the sequence of random variables* $\frac{h_i(t)}{\sqrt{\operatorname{var}[h_i(t)]}}$ *converges in law to the standard Gaussian distribution.*

Proposition 4 is proved in Appendix G. By introducing the same additional assumption as in Corollary 1 that holds in various experimental setups (*cf.* Section IV), the results in Proposition 4 can be simplified:

Corollary 2 (Late asymptotic state)**.** *Considering the stochastic reverberation model in Definition 1, suppose that the attenuation function is regular (*cf. *Definition 7). Also suppose that the product* $\widehat{g_i'}(\boldsymbol{u},f)\overline{\widehat{g_j'}(\boldsymbol{u},f)}m_{|\widehat{s'}|^2}(\boldsymbol{u},f)$ *with* $m_{|\widehat{s'}|^2}$ *defined*

in (37) *can be factorized as in* (42)*, where function* $\boldsymbol{u} \mapsto \xi_{i,j}(\boldsymbol{u}) \geq 0$ *is twice continuously differentiable, and function* $f \mapsto \chi(f) \geq 0$ *is smooth. For any sensors* $i, j \in \{1 \dots I\}$*, let* $\gamma_{i,j}(t_1, t_2)$ *be the function defined in* (11)*. Then when* $t \to +\infty$*,* $\forall f \in \mathbb{R}$*,*

$$\mathcal{W}_{\gamma_{i,i}}(t,f) = \pi\lambda c\beta_2 \frac{e^{-2\widehat{\alpha}^{\inf} t}}{t} \left(\chi(f) \sum_{k\in\mathcal{K}} \frac{\xi_{i,i}(\boldsymbol{u}_k)}{\sqrt{\widehat{\alpha}_k}} + O(\tfrac{1}{t}) \right), \tag{55}$$

the time-frequency correlation introduced in Definition 5 is such that

$$\rho_{i,j}(t,f,\boldsymbol{x}_j-\boldsymbol{x}_i) = \sum_{k\in\mathcal{K}} a_k(\boldsymbol{x}_j-\boldsymbol{x}_i) e^{-2\imath\pi f \tau_k(\boldsymbol{x}_j-\boldsymbol{x}_i)} + O\left(\tfrac{1}{\sqrt{t}}\right) \tag{56}$$

where $\forall k \in \mathcal{K}$*,* $\tau_k(\boldsymbol{x}_j - \boldsymbol{x}_i) = \frac{\boldsymbol{u}_k^\top(\boldsymbol{x}_j-\boldsymbol{x}_i)}{c} \in [-\frac{D}{c}, \frac{D}{c}]$ *and*

$$a_k(\boldsymbol{r}) = \frac{\beta_k(\boldsymbol{r})}{\beta_2} \frac{\frac{\xi_{i,j}(\boldsymbol{u}_k)}{\sqrt{\widehat{\alpha}_k}}}{\sqrt{\sum_{l\in\mathcal{K}} \frac{\xi_{i,i}(\boldsymbol{u}_l)}{\sqrt{\widehat{\alpha}_l}}} \sqrt{\sum_{l\in\mathcal{K}} \frac{\xi_{j,j}(\boldsymbol{u}_l)}{\sqrt{\widehat{\alpha}_l}}}} \geq 0,$$

where $\beta_k(\boldsymbol{r})$ *is defined in* (51)*. Finally, the temporal support of the asymptotic correlation function introduced in Definition 6 lies in* $[-\frac{D}{c}, \frac{D}{c}]$*:*

$$\sigma_{i,j}(\tau, \boldsymbol{x}_j - \boldsymbol{x}_i) = \sum_{k\in\mathcal{K}} a_k(\boldsymbol{x}_j - \boldsymbol{x}_i)\ \delta(\tau - \tau_k(\boldsymbol{x}_j - \boldsymbol{x}_i)). \tag{57}$$

Corollary 2 is proved in Appendix G.5. Again, note that the additional assumption in Corollary 2 is necessary to conclude that the asymptotic correlation function $\sigma_{i,j}(\tau, \boldsymbol{x}_j - \boldsymbol{x}_i)$ is nonnegative and that its temporal support lies in $[-\frac{D}{c}, \frac{D}{c}]$. Under the more general assumptions of Proposition 4, these properties may not hold.

E. Conclusions of the asymptotic analysis

Let us conclude Section III with a brief discussion about the various orders of convergence that appear in Propositions 3 and 4, and in Corollaries 1 and 2. First, in Proposition 3 and Corollary 1 in Section III-C, we observe that:

- $\mathrm{var}[h_i(t)]$ and $\mathcal{W}_{\gamma_{i,i}}(t,f)$ are in closed-form $\forall t \geq T$;
- if $i \neq j$, $\mathcal{W}_{\gamma_{i,j}}(t,f)$ and $\rho_{i,j}(t,f,\boldsymbol{x}_j - \boldsymbol{x}_i)$ converge to their asymptotic forms as $O(\frac{1}{t})$.

Second, in Proposition 4 and Corollary 2 in Section III-D, we observe that:

- $\mathrm{var}[h_i(t)]$ and $\mathcal{W}_{\gamma_{i,i}}(t,f)$ converge to their asymptotic forms as $O(\frac{1}{t})$;
- if $i \neq j$, $\mathcal{W}_{\gamma_{i,j}}(t,f)$ and $\rho_{i,j}(t,f,\boldsymbol{x}_j - \boldsymbol{x}_i)$ converge to their asymptotic forms as $O(\frac{1}{\sqrt{t}})$.

Finally, we can make two additional observations:

- in all cases, the convergence to the asymptotic form is faster in Proposition 3 than in Proposition 4, which justifies the terms *early* and *late asymptotic states*;
- the convergence speed of $O(\frac{1}{t})$ is obtained in *late* asymptotic state for $\mathrm{var}[h_i(t)]$ and $\mathcal{W}_{\gamma_{i,i}}(t,f)$, and in *early* asymptotic state for $\mathcal{W}_{\gamma_{i,j}}(t,f)$ and $\rho_{i,j}(t,f,\boldsymbol{x}_j - \boldsymbol{x}_i)$.

This last observation is very important: in the case of real RIRs obtained from real measurements as in Section IV-B, the RIRs are observed on a limited time interval, because the measurement noise ends up dominating the reverberation after a while. It appears that a convergence speed of $O(\frac{1}{\sqrt{t}})$ is too slow to permit the asymptotic form to be reached within the reverberation time. Therefore we will not be able to observe the asymptotic forms (56) and (57) of $\rho_{i,j}(t,f,\boldsymbol{x}_j - \boldsymbol{x}_i)$ and $\sigma_{i,j}(\tau, \boldsymbol{x}_j - \boldsymbol{x}_i)$ in late asymptotic state. However, a convergence speed of $O(\frac{1}{t})$ is fast enough to permit the asymptotic form to be observed within the reverberation time. This explains why in real conditions, the observed behavior of $\mathrm{var}[h_i(t)]$ and $\mathcal{W}_{\gamma_{i,i}}(t,f)$ will match the predictions of the late asymptotic state, whereas the behavior of $\rho_{i,j}(t,f,\boldsymbol{x}_j - \boldsymbol{x}_i)$ and $\sigma_{i,j}(\tau, \boldsymbol{x}_j - \boldsymbol{x}_i)$ will match the predictions of the early asymptotic state.

IV. Experimental results

In this section, we will study both synthetic and real room impulse responses[4], and for each of them, we will check whether their asymptotic statistical behavior corresponds to one of the following states:

- diffuse acoustic field (characterized in Proposition 2);
- early asymptotic state of non-diffuse acoustic field (characterized in Proposition 3 and Corollary 1), in the particular symmetric or isotropic cases, or in the general anisotropic case;
- late asymptotic state of non-diffuse acoustic field (characterized in Proposition 4 and Corollary 2).

In order to perform this classification, we will consider the four following *statistical signatures of reverberation*[5]:

- *temporal power profile*: $\mathrm{var}[h_i(t)]$;
- *time-frequency power profile*: $\mathcal{W}_{\gamma_{i,i}}(t,f)$;
- *time-frequency correlation*: $\rho_{i,j}(t,f,\boldsymbol{x}_j - \boldsymbol{x}_i)$ in (10);
- *asymptotic correlation function*: $\sigma_{i,j}(\tau, \boldsymbol{x}_j - \boldsymbol{x}_i)$ in (12).

In Table I, we summarize some results obtained in Propositions 2, 3 and 4 and in Corollaries 1 and 2. Remember that the results in Corollaries 1 and 2 hold when $\widehat{g_i'}(\boldsymbol{u},f)\widehat{g_j'}(\boldsymbol{u},f)m_{|\widehat{s'}|^2}(\boldsymbol{u},f)$ can be factorized as $\xi_{i,j}(\boldsymbol{u})\,\chi(f)$, with $\xi_{i,j}(\boldsymbol{u}) \geq 0$ and $\chi(f) \geq 0$. This assumption holds in various setups:

1) if the source response does not depend on frequency and if the microphones' responses are nonnegative and do not depend on frequency either, we get $\xi_{i,j}(\boldsymbol{u}) = \widehat{g_i'}(\boldsymbol{u})\widehat{g_j'}(\boldsymbol{u})m_{|\widehat{s'}|^2}(\boldsymbol{u}) \geq 0$ and $\chi(f) = 1$ (as illustrated in Section IV-A);
2) in the isotropic case, if the microphones are omnidirectional and have the same response g, we get $\xi_{i,j}(\boldsymbol{u}) = 1$

[4]The Matlab code generating all the figures in Section IV is available at https://perso.telecom-paristech.fr/rbadeau/techreport2019-04-code.zip.

[5]Note that the four signatures of reverberation are based on the second order moments of the RIR. In the following experiments, we will display neither the expected values nor the higher order cumulants of $h_i(t)$: the zero mean and asymptotic Gaussianity of RIRs (which are mathematically proved in Propositions 1, 3 and 4) are well-known experimental facts.

Convergence speed to asymptotic state	**Diffuse acoustic field** (Proposition 2)	**Non-diffuse acoustic field, early asymptotic state** (Proposition 3 & Corollary 1)			**Non-diffuse acoustic field, late asymptotic state** (Proposition 4 & Corollary 2)	
	Omnidirectional source Same omnidirectional sensors	Anisotropic (general case)	Symmetric ($\xi_{i,j}$ even)	Isotropic ($\xi_{i,j}$ constant)		
Immediate ($\forall t \geq T + \frac{D}{2c}$)	$\mathrm{var}[h_i(t)] \propto e^{-2\widehat{\alpha}^{\inf} t}$ $\mathcal{W}_{\gamma_{i,i}}(t,f) \propto e^{-2\widehat{\alpha}^{\inf} t}\chi(f)$ $\rho_{i,j} = \frac{\widehat{b}(f,D)}{\beta_2} \underset{D\to 0}{\longrightarrow} \mathrm{sinc}(\frac{2\pi f D}{c})$ $\sigma_{i,j} = \frac{b(\tau,D)}{\beta_2} \underset{D\to 0}{\sim} \frac{c}{2D}\mathbf{1}_{[-\frac{D}{c},\frac{D}{c}]}(\tau)$	$\mathrm{var}[h_i(t)] \propto e^{-2\widehat{\alpha}^{\inf} t}$ $\mathcal{W}_{\gamma_{i,i}}(t,f) \propto e^{-2\widehat{\alpha}^{\inf} t}\chi(f)$				
$\boldsymbol{O}\left(\frac{1}{t}\right)$ (fast)		$\lim_{t\to+\infty} \rho_{i,j}$ smooth, even symmetric; $\sigma_{i,j} \geq 0$, continuous within support $]-\frac{D}{c},\frac{D}{c}[$	$\lim_{t\to+\infty} \rho_{i,j}$ real; $\sigma_{i,j}$ even	$\rho_{i,j} \underset{t\to+\infty}{\longrightarrow} \frac{\widehat{b}(f,D)}{\beta_2}$ $\sigma_{i,j} = \frac{b(\tau,D)}{\beta_2}$	$\mathrm{var}[h_i(t)] \propto \frac{e^{-2\widehat{\alpha}^{\inf} t}}{t}$	$\mathcal{W}_{\gamma_{i,i}}(t,f) \propto \frac{e^{-2\widehat{\alpha}^{\inf} t}}{t}\chi(f)$
Observed before RT_{60} in:		Shoebox room, Great Hall (Sections IV-A & IV-B3)	Octagon room (Section IV-B2)	Classroom (Section IV-B1)	All rooms (Section IV)	Shoebox room (Section IV-A)
$\boldsymbol{O}\left(\frac{1}{\sqrt{t}}\right)$ (slow)					$\rho_{i,j} \underset{t\to+\infty}{\longrightarrow} \sum_{k\in\mathcal{K}} a_k e^{-2i\pi f \tau_k}$ $\sigma_{i,j} = \sum_{k\in\mathcal{K}} a_k \delta(\tau - \tau_k)$	
Observed after RT_{60} in:					Shoebox room (Section IV-A)	

TABLE I
THE FOUR STATISTICAL SIGNATURES OF REVERBERATION IN VARIOUS EXPERIMENTAL SETUPS

and $\chi(f) = |\widehat{g'}(f)|^2 m_{|\widehat{s'}|^2}(f) \geq 0$ (as illustrated in Section IV-B1);

3) if the microphones are omnidirectional and have the same response g, and if $m_{|\widehat{s'}|^2}(\boldsymbol{u},f) \geq 0$ can be factorized as $m_{|\widehat{s'}|^2}(\boldsymbol{u},f) = \xi_s(\boldsymbol{u})\,\chi_s(f)$ with $\xi_s(\boldsymbol{u}) \geq 0$ and $\chi_s(f) \geq 0$, we get $\xi_{i,j}(\boldsymbol{u}) = \xi_s(\boldsymbol{u}) \geq 0$ and $\chi(f) = |\widehat{g'}(f)|^2\chi_s(f) \geq 0$ (as illustrated in Sections IV-B2 and IV-B3).

In the following sections, the four statistical signatures of reverberation are estimated from a pair ($I = 2$) of L observed room impulse responses $h_1^{(l)}(t)$ and $h_2^{(l)}(t)$ for $l \in \{1 \dots L\}$, that are such that $\boldsymbol{x}_2 - \boldsymbol{x}_1$ is fixed. For $i \in \{1,2\}$, the temporal power profile $\mathrm{var}[h_i(t)]$ is thus estimated as $\frac{1}{L}\sum_{l=1}^{L} |h_i^{(l)}(t)|^2$. The Wigner distributions $\mathcal{W}_{\gamma_{i,i}}(t,f)$ and $\mathcal{W}_{\gamma_{1,2}}(t,f)$ are estimated as $\widehat{\mathcal{W}}_{\gamma_{i,i}}(t,f) = \frac{1}{L}\sum_{l=1}^{L} |S_{h_i}^{(l)}(t,f)|^2$ and $\widehat{\mathcal{W}}_{\gamma_{1,2}}(t,f) = \frac{1}{L}\sum_{l=1}^{L} S_{h_1}^{(l)}(t,f) S_{h_2}^{(l)}(t,f)$, where $S_{h_1}^{(l)}(t,f)$ (resp. $S_{h_2}^{(l)}(t,f)$) is the short time Fourier transform (STFT) of $h_1^{(l)}(t)$ (resp. $h_2^{(l)}(t)$). The distributions $\widehat{\mathcal{W}}_{\gamma_{i,i}}(t,f)$ and $\widehat{\mathcal{W}}_{\gamma_{1,2}}(t,f)$ obtained in this way are smoothed estimates of $\mathcal{W}_{\gamma_{i,i}}(t,f)$ and $\mathcal{W}_{\gamma_{1,2}}(t,f)$ in the time-frequency domain [14]. Then the time-frequency correlation $\rho_{1,2}(t,f,\boldsymbol{x}_2 - \boldsymbol{x}_1)$ is estimated as

$$\widehat{\rho}_{1,2}(t,f,\boldsymbol{x}_2 - \boldsymbol{x}_1) = \frac{\widehat{\mathcal{W}}_{\gamma_{1,2}}(t,f)}{\sqrt{\widehat{\mathcal{W}}_{\gamma_{1,1}}(t,f)\widehat{\mathcal{W}}_{\gamma_{2,2}}(t,f)}}.$$

The asymptotic correlation function $\sigma_{1,2}(\tau, \boldsymbol{x}_2 - \boldsymbol{x}_1)$ is estimated as the inverse discrete Fourier transform (DFT)[6] of

$$\frac{1}{|\mathcal{T}|}\sum_{t\in\mathcal{T}} \widehat{\rho}_{1,2}(t,f,\boldsymbol{x}_2 - \boldsymbol{x}_1) \tag{58}$$

where $\mathcal{T}$ is a time interval of length $|\mathcal{T}|$, on which $\widehat{\rho}_{1,2}(t,f,\boldsymbol{x}_2 - \boldsymbol{x}_1)$ is approximately stationary (*i.e.* does not depend on t) on average.

A. Numerical simulation

We first considered synthetic RIRs generated by the Roomsimove toolbox [15], which is a state-of-the-art RIR generator based on the source image principle. Roomsimove is dedicated to parallelepipedic ("shoebox") rooms and applies high-pass filtering above 20 Hz. We used it with the default physical parameters (humidity: 40%, temperature: 20°C, speed of sound: c = 343 m/s), and we removed the modeling of absorption due to the air[7]. We thus simulated a shoebox room having the same volume as the classroom described in [12, p. 84]: 200 m^3 (the room dimensions are 7.4 m × 9 m × 3 m). The values of the absorption coefficients for the six room surfaces are described in Table II.

Surface	$x=0$	$x=7.4$	$y=0$	$y=9$	$z=0$	$z=3$
Absorption	0.25	0.3	0.35	0.4	0.5	0.6

TABLE II
ABSORPTION COEFFICIENTS FOR THE SIX ROOM SURFACES

Let RT_{60} denote the reverberation time, defined as the time the sound pressure level takes to reduce by 60 dB. For this setup, RT_{60} = 0.23 s. We considered omnidirectional sources and directional (cardioid) microphones. The distance between the two microphones is 20 cm, and the vector $\boldsymbol{x}_2 - \boldsymbol{x}_1$, pointing from the first microphone to the second one, is in

[6]In Section IV-B, in order to denoise the estimate of $\sigma_{1,2}(\tau, \boldsymbol{x}_2 - \boldsymbol{x}_1)$, (58) will be truncated to the frequency band [-5000 Hz, +5000 Hz] before computing the inverse DFT, which is equivalent to smoothing in time domain.

[7]The modeling of absorption due to the air involves a frequency-varying attenuation, which is not accounted for by the model presented in this research report. However, frequency-varying attenuations are handled by the general stochastic reverberation model introduced in [13], and will be analyzed both mathematically and experimentally in future work.

the horizontal plane, forming an angle of $50°$ from the x-axis and $40°$ from the y-axis. We used the sensor orientations described in Table III.

Sensor	Azimuth	Elevation	Roll offset
Sensor 1	15°	25°	35°
Sensor 2	45°	55°	65°

TABLE III
SENSOR ORIENTATIONS (AZIMUTH, ELEVATION AND ROLL OFFSET IN DEGREES, POSITIVE FOR SLEW LEFT, NOSE UP OR RIGHT WING DOWN)

We thus generated $L = 1000$ RIRs sampled at 16 kHz, with random source positions and random middle positions of the sensors (both uniformly distributed inside the room volume). We computed all the STFTs with a 128-sample-long Hann window and an overlap of 64 samples in the time domain.

Note that the particular numerical values of the parameters used in this simulation are only provided here for the sake of reproducible research. They were not chosen for their realism, but rather for reducing the computation time and for improving visualization. The observations that we will make below regarding the four signatures of reverberation would qualitatively be the same with different numerical values.

Besides, in the Roomsimove toolbox, the source response does not depend on frequency and the microphones' responses are nonnegative and do not depend on frequency either, thus $\forall i, j \in \{1 \dots I\}$, $\widehat{g_i'}(\boldsymbol{u}, f)\widehat{g_j'}(\boldsymbol{u}, f)m_{|\widehat{s'}|^2}(\boldsymbol{u}, f)$ can be factorized as in Corollaries 1 and 2 as $\xi_{i,j}(\boldsymbol{u})\,\chi(f)$, with $\xi_{i,j}(\boldsymbol{u}) = \widehat{g_i'}(\boldsymbol{u})\widehat{g_j'}(\boldsymbol{u})m_{|\widehat{s'}|^2}(\boldsymbol{u}) \geq 0$ and $\chi(f) = 1$. Thus we expect the measurements on the data to match the results in Table I with $\chi(f) = 1\ \forall f \in \mathbb{R}$.

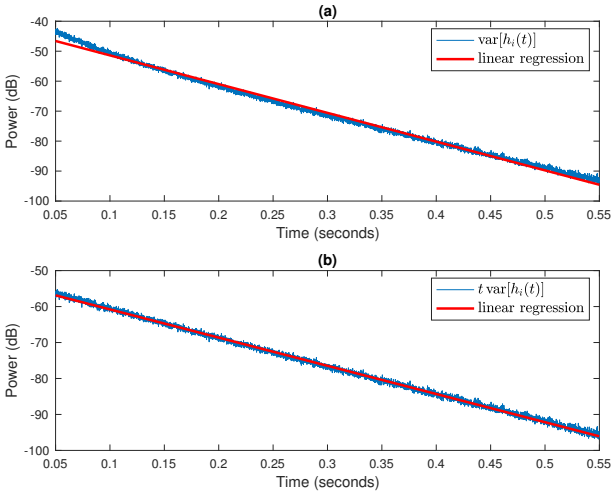

Fig. 1. Temporal power profile $\mathrm{var}[h_i(t)]$ in the shoebox room

Fig. 1-(a) represents the temporal power profile $\mathrm{var}[h_i(t)]$ in dB (blue curve), superimposed with a straight red line obtained by linear regression. We can observe that the temporal power profile is slightly bent compared with the straight line, so we are neither in a diffuse acoustic field, nor in the early asymptotic state of a non-diffuse acoustic field in Table I (otherwise, we would have $\ln(\mathrm{var}[h_i(t)]) \overset{c}{=} -2\widehat{\alpha}^{\mathrm{inf}}t$). Fig. 1-(b) represents $t\,\mathrm{var}[h_i(t)]$ in dB (blue curve), and a straight red line obtained by linear regression. This time the blue curve is not bent and matches the output of linear regression much better. This corresponds to the behavior predicted by the late asymptotic state of a non-diffuse acoustic field in Table I: $\ln(t\,\mathrm{var}[h_i(t)]) \overset{c}{=} -2\widehat{\alpha}^{\mathrm{inf}}t$.

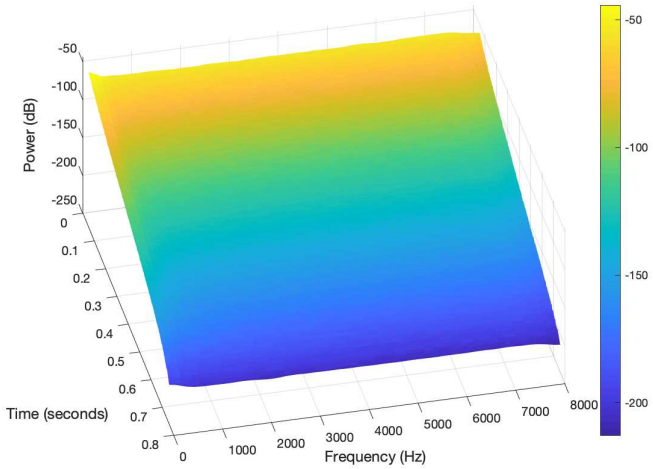

Fig. 2. Time-frequency power profile $\mathcal{W}_{\gamma_{i,i}}(t, f)$ in the shoebox room

Fig. 2 represents the time-frequency power profile $\mathcal{W}_{\gamma_{i,i}}(t, f)$ in dB. We note that it can be approximately factorized as a function of time multiplied by a fixed spectrum, which is the behavior predicted by the reverberation model in all asymptotic states in Table I. Due to the projection property (3), the function of time is necessarily proportional to the temporal power profile: $\frac{e^{-2\widehat{\alpha}^{\mathrm{inf}}t}}{t}$, which corresponds to the late asymptotic state. Besides, we observe that the fixed spectrum is approximately constant, which is again the behavior predicted by the reverberation model in all asymptotic states, since $\chi(f) = 1\ \forall f \in \mathbb{R}$. Finally, we can conclude that the time-frequency power profile is the one predicted by the late asymptotic state of a non-diffuse acoustic field (*cf.* Table I).

Fig. 3 (resp. Fig. 4) represents the real part (resp. the imaginary part) of the time-frequency correlation $\rho_{1,2}(t, f, \boldsymbol{x}_2 - \boldsymbol{x}_1)$. A very interesting phenomenon can be observed: the time-frequency correlation is not stationary, its "spectrum" evolving from a shape similar to that of a cardinal sine (at low values of t in Fig. 3), to the shape of a sine wave (at high values of t in Fig. 3 and 4). Note that the time axis goes up to 0.8 s, far beyond the RT_{60} = 0.23 s (we have deliberately modified Roomsimove's code in order to synthesize such long RIRs). Fig. 5 and 6 will help us understand what is at stake here.

The blue curve in Fig. 5-(a) (resp. Fig. 5-(b)) represents the real part (resp. the imaginary part) of the last spectrum of the time-frequency correlation $\rho_{1,2}(t, f, \boldsymbol{x}_2 - \boldsymbol{x}_1)$ in Fig. 3 (resp. Fig. 4). The red curves in these figures represent the asymptotic time-frequency correlation predicted by the late

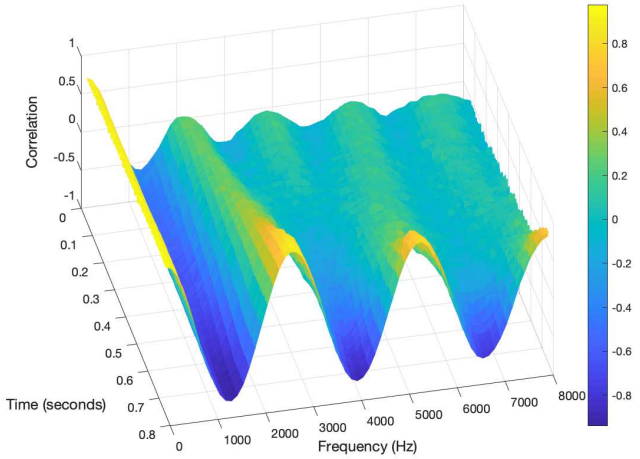

Fig. 3. Real part of the time-frequency correlation $\rho_{1,2}(t, f, \boldsymbol{x}_2 - \boldsymbol{x}_1)$ in the shoebox room

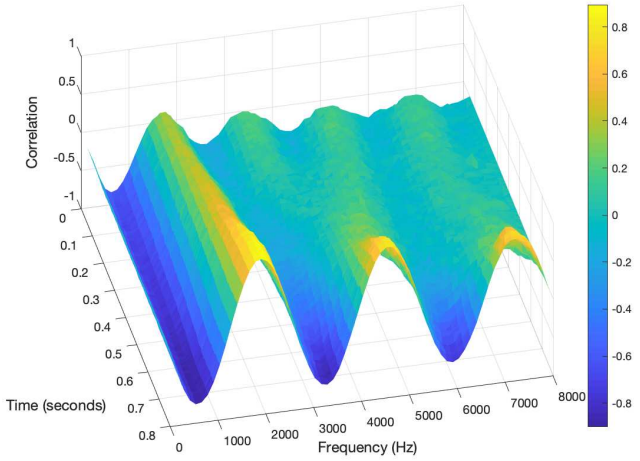

Fig. 4. Imaginary part of the time-frequency correlation $\rho_{1,2}(t, f, \boldsymbol{x}_2 - \boldsymbol{x}_1)$ in the shoebox room

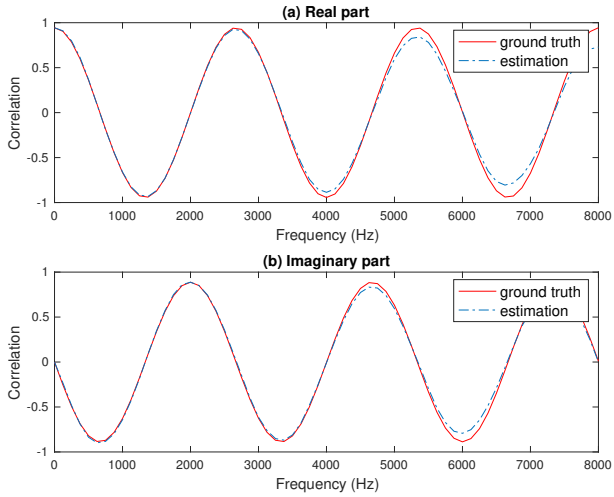

Fig. 5. Last time-frequency correlation $\rho_{1,2}(t, f, \boldsymbol{x}_2 - \boldsymbol{x}_1)$ in the shoebox room (late asymptotic state)

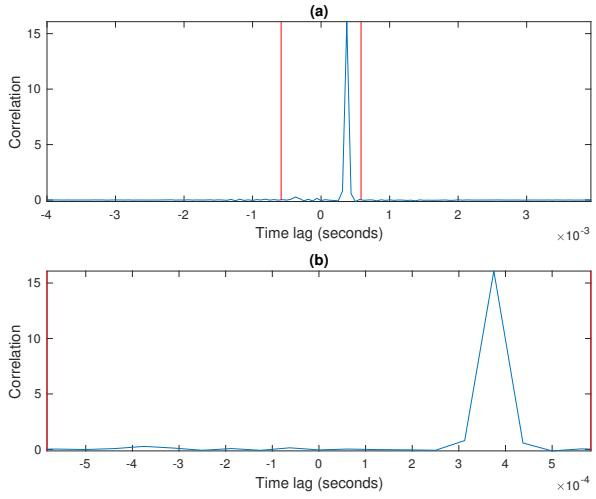

Fig. 6. Normalized asymptotic correlation function $\frac{2D}{c}\sigma_{1,2}(\tau, \boldsymbol{x}_2 - \boldsymbol{x}_1)$ in the shoebox room (late asymptotic state)

asymptotic state of a non-diffuse acoustic field (*cf.* Table I). Indeed, it appears that the minimum of function $\boldsymbol{u} \mapsto \widehat{\alpha}(\boldsymbol{u})$ is reached at a single direction $\boldsymbol{u}_0$. Consequently, the real (resp. imaginary) part of $\lim_{t\to+\infty} \rho_{1,2}(t, f, \boldsymbol{x}_2 - \boldsymbol{x}_1)$ in (56) is a cosine function (resp. a sine function). The good match between the ground truth and the estimation in Fig. 5 shows that the time-frequency correlation in Fig. 3 and 4 does converge to the behavior predicted by the late asymptotic state of a non-diffuse acoustic field[8].

[8]Since the acoustic field in this rectangular room is not isotropic, it is not *diffuse*. The reader might notice that yet, we used a simulated shoebox room in the experimental section of [2] to illustrate the properties of a diffuse acoustic field. Actually, we made the experimental setup isotropic in [2] by randomizing the orientation of vector $\boldsymbol{x}_2^{(l)} - \boldsymbol{x}_1^{(l)}$ according to a uniform probability distribution, and by averaging the results.

The blue curve in Fig. 6-(a) represents the correlation function $\sigma_{1,2}(\tau, \boldsymbol{x}_2 - \boldsymbol{x}_1)$, obtained by computing the inverse Fourier transform of the last spectrum of the time-frequency correlation $\rho_{1,2}(t, f, \boldsymbol{x}_2 - \boldsymbol{x}_1)$. We observe that it is formed of a single peak lying in the interval $[-\frac{D}{c}, \frac{D}{c}]$ (whose boundaries are represented by red vertical lines and which is zoomed in in Fig. 6-(b)), as predicted in (57), which confirms what we already observed in Fig. 5.

However, up to the reverberation time RT_{60} = 0.23 s, the average spectrum in Fig. 3 and 4 behaves very differently. The blue curve in Fig. 7-(a) represents the correlation function $\sigma_{1,2}(\tau, \boldsymbol{x}_2 - \boldsymbol{x}_1)$, obtained by computing the inverse Fourier transform of the time-frequency correlation $\rho_{1,2}(t, f, \boldsymbol{x}_2 - \boldsymbol{x}_1)$ averaged from 0 to 0.23 s. We observe that the temporal support of this correlation function approximately lies in the interval $[-\frac{D}{c}, \frac{D}{c}]$ (whose boundaries are represented by red

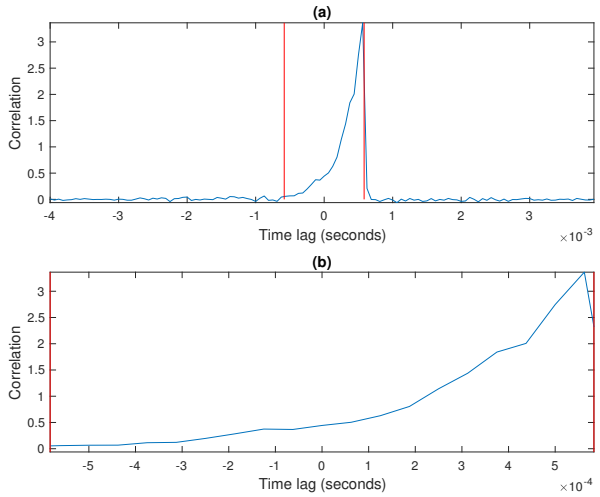

Fig. 7. Normalized asymptotic correlation function $\frac{2D}{c}\sigma_{1,2}(\tau, \boldsymbol{x}_2 - \boldsymbol{x}_1)$ in the shoebox room (early asymptotic state)

vertical lines), as predicted by the reverberation model in all asymptotic states (*cf.* Table I). Moreover, within this temporal support (Fig. 7-(b) represents a zoom in on this interval), the correlation function is nonnegative and not even, and it has continuous variations, as predicted by the anisotropic case of the *early* asymptotic state of a non-diffuse acoustic field in Table I.

We can conclude that up to the RT_{60}, the time-frequency correlation $\rho_{1,2}(t, f, \boldsymbol{x}_2 - \boldsymbol{x}_1)$ represented in Fig. 3 and 4 actually behaves as in the early asymptotic state, whereas the late asymptotic state is actually reached much later. This makes a difference with the temporal power profile $\mathrm{var}[h_i(t)]$ in Fig. 1 and the time-frequency power profile $\mathcal{W}_{\gamma_{i,i}}(t, f)$ in Fig. 2, which match the predictions of the late asymptotic state almost right from the beginning.

This remark confirms our conclusions in Section III-E regarding the asymptotic analysis in Section III. When we will analyze real RIRs in Section IV-B, obtained from measurements in real acoustic environments, we will not be able to estimate the time-frequency correlation $\rho_{1,2}(t, f, \boldsymbol{x}_2 - \boldsymbol{x}_1)$ beyond the reverberation time, because the measurement noise ends up dominating the reverberation. Therefore we will never be able to observe the late asymptotic state in the time-frequency correlation, which stays stuck in early asymptotic state in its temporal observation interval. This explains why in real conditions, the behavior of the first two reverberation signatures (temporal power profile $\mathrm{var}[h_i(t)]$ and time-frequency power profile $\mathcal{W}_{\gamma_{i,i}}(t, f)$) will match the predictions of the late asymptotic state, whereas the last two signatures (time-frequency correlation $\rho_{1,2}(t, f, \boldsymbol{x}_2 - \boldsymbol{x}_1)$ and asymptotic correlation function $\sigma_{1,2}(\tau, \boldsymbol{x}_2 - \boldsymbol{x}_1)$) will match the predictions of the early asymptotic state.

B. Real RIR measurements

We used the collection of room impulse responses measured in a classroom, the Octagon room, and the Great Hall at the Mile End campus of Queen Mary, University of London in 2008 [16]. The measurements were created using a sine sweep technique [17] with a Genelec 8250A loudspeaker (which forms a directive sound source) and two microphones, an omnidirectional DPA 4006 and a B-format Soundfield SPS422B. Each measurement has source and receiver heights of 1.5 m. We used the RIRs measured with the omnidirectional microphone. We resampled the RIRs at 48 kHz, and we truncated them so as to remove both their beginning (formed of early reflections) in order to focus on late reverberation only, and their end, which is dominated by the measurement noise. All STFTs are computed by means of Hann windows of length 2400 samples, with a 95% overlap.

As we will show in the following subsections, the acoustic field in the three rooms is uniform and non-diffuse. Even though we did not report here the results in order to avoid overloading this document, the uniformity of the acoustic field over space was checked by computing the four reverberation signatures (temporal power profile $\mathrm{var}[h_i(t)]$, time-frequency power profile $\mathcal{W}_{\gamma_{i,i}}(t, f)$, time-frequency correlation $\rho_{1,2}(t, f, \boldsymbol{x}_2 - \boldsymbol{x}_1)$, and asymptotic correlation function $\sigma_{1,2}(\tau, \boldsymbol{x}_2 - \boldsymbol{x}_1)$) through space averages in different parts of the rooms (we separated the half-left side from the half-right side, and the half-up side from the half-bottom side, along the two horizontal directions). We thus observed a remarkably accurate match of the four signatures in the different parts of the room, which permitted us to conclude that the acoustic field is uniform (at least in the space areas where the measurements were carried out). In the following subsections, the reported signatures are computed through space averages over all available measurements in the rooms.

1) Classroom: In the *QMUL Classroom Impulse Response* "Omni" dataset, 130 RIRs were measured within a classroom. As described in [16], the room measures 7.5 × 9 × 3.5 m (236 m^3) with reflective surfaces of a linoleum floor, painted plaster walls and ceiling, and a large whiteboard. Measurements were 50 cm apart arranged in 10 rows and 13 columns (over a 9 m × 12 m area) relative to the speaker, with the 7th column directly on axis with the speaker. For this setup, the average measured reverberation time RT_{30} is about 1.8 s around 1000 Hz [16, Fig. 4]. For the correlation measurements (time-frequency correlation $\rho_{1,2}(t, f, \boldsymbol{x}_2 - \boldsymbol{x}_1)$ and asymptotic correlation function $\sigma_{1,2}(\tau, \boldsymbol{x}_2 - \boldsymbol{x}_1)$), we computed space averages over all pairs of microphones placed 50 cm apart, and such that the vector $\boldsymbol{x}_2 - \boldsymbol{x}_1$, pointing from the first microphone to the second one, is in the horizontal plane, in the direction of the y-axis.

Fig. 8 represents the temporal power profile $\mathrm{var}[h_i(t)]$. As for the simulated shoebox room (*cf.* Fig. 1), we observe that its behavior is predicted by the late asymptotic state of a non-diffuse acoustic field: $\mathrm{var}[h_i(t)]$ does not decrease as $e^{-2\widehat{\alpha}^{\inf}t}$, but rather as $\frac{e^{-2\widehat{\alpha}^{\inf}t}}{t}$ (*cf.* Table I).

Fig. 9 represents the time-frequency power profile $\mathcal{W}_{\gamma_{i,i}}(t, f)$. We observe that this power profile can no longer be approximately factorized as a function of time multiplied

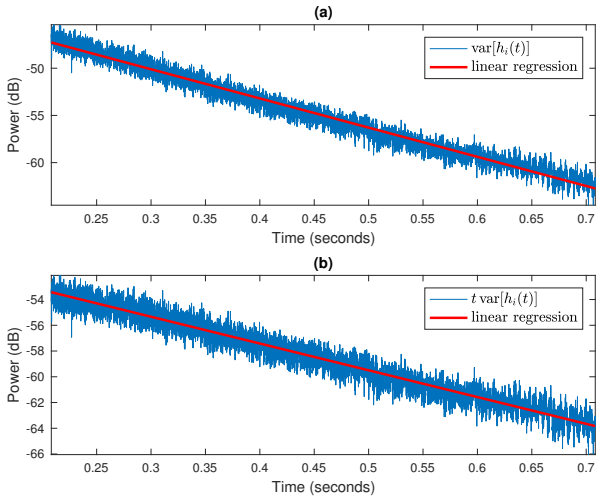

Fig. 8. Temporal power profile $\mathrm{var}[h_i(t)]$ in the classroom

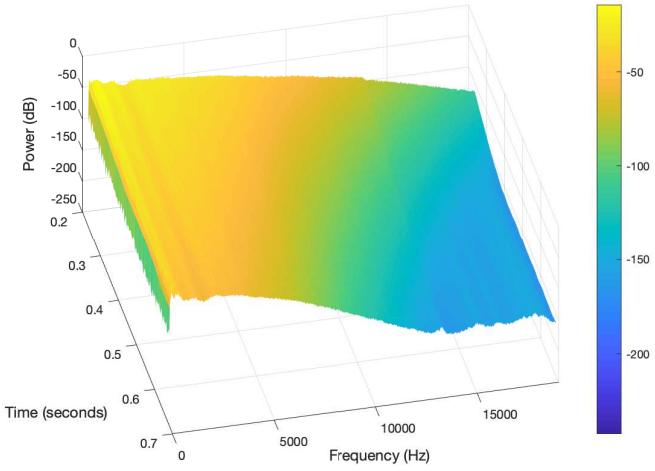

Fig. 9. Time-frequency power profile $\mathcal{W}_{\gamma_{i,i}}(t,f)$ in the classroom

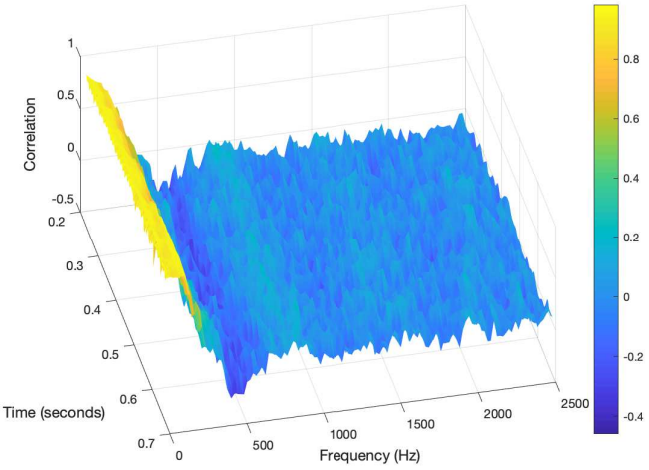

Fig. 10. Real part of the time-frequency correlation $\rho_{1,2}(t,f,\boldsymbol{x}_2-\boldsymbol{x}_1)$ in the classroom

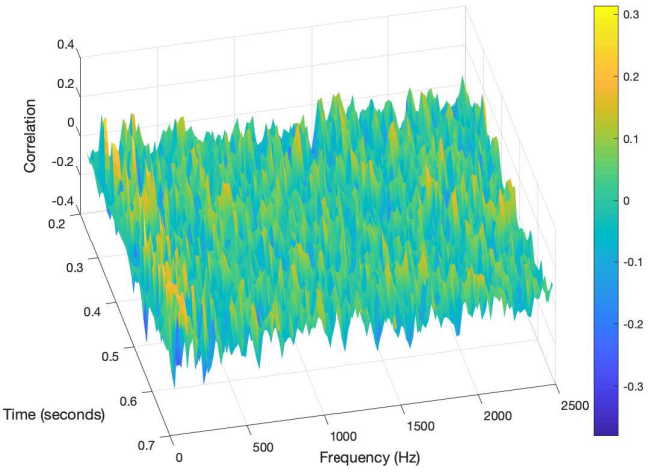

Fig. 11. Imaginary part of the time-frequency correlation $\rho_{1,2}(t,f,\boldsymbol{x}_2-\boldsymbol{x}_1)$ in the classroom

by a fixed spectrum: the temporal decrease rate depends on frequency, which is not predicted by the reverberation model studied in this research report. Indeed, remember that we simplified the general stochastic reverberation model introduced in [13] by removing the dependency of vector $\widehat{\boldsymbol{\alpha}}$ on frequency f, in order to simplify the mathematical analysis of the model (*cf.* Sections I and II). Actually, the general model introduced in [13] does account for a frequency-varying decrease rate, but its mathematical analysis is left for future work.

Fig. 10 (resp. Fig. 11) represents the real part (resp. the imaginary part) of the time-frequency correlation $\rho_{1,2}(t,f,\boldsymbol{x}_2-\boldsymbol{x}_1)$. We notice that the imaginary part is zero on average (the surface in Fig. 11 looks like centered noise), and that the real part is approximately stationary (it does not depend on time), as predicted by the reverberation model in all asymptotic states (*cf.* Table I).

The blue curve in Fig. 12-(a) (resp. Fig. 12-(b)) represents the average over time of the real part (resp. the imaginary part) of the time-frequency correlation $\rho_{1,2}(t,f,\boldsymbol{x}_2-\boldsymbol{x}_1)$ in Fig. 10 (resp. Fig. 11). The red curve in Fig. 12-(a) represents the cardinal sine function $\mathrm{sinc}\left(\frac{2\pi f D}{c}\right)$ with c = 343 m/s and D = 50 cm, whereas the red curve in Fig. 12-(b) represents the zero prediction. We thus observe that the shape of the time-frequency correlation is well predicted by the isotropic case of the early asymptotic state of a non-diffuse acoustic field when $D \to 0$ (*cf.* Table I).

Indeed, the results of Corollary 1 hold in this experimental setup, because in this dataset, the microphones are omnidirectional and have the same response g. In addition, if we assume

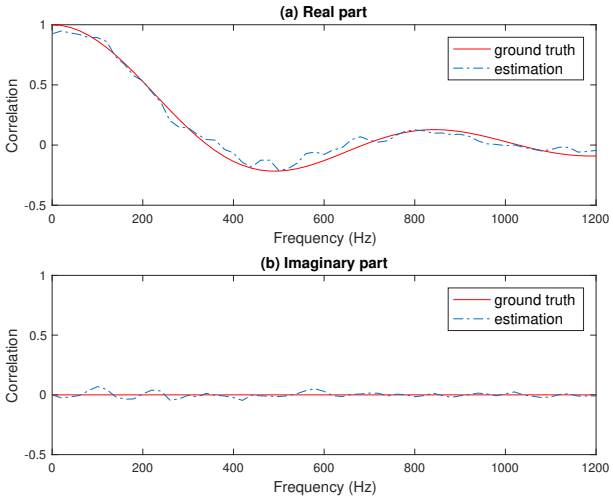

Fig. 12. Average over time of the time-frequency correlation $\rho_{1,2}(t, f, \boldsymbol{x}_2 - \boldsymbol{x}_1)$ in the classroom

that the second-order source response $m_{|\widehat{s'}|^2}$ is also omnidirectional, then $\forall i, j \in \{1 \dots I\}$, $\widehat{g'_i}(\boldsymbol{u}, f)\overline{\widehat{g'_j}(\boldsymbol{u}, f)} m_{|\widehat{s'}|^2}(\boldsymbol{u}, f)$ can be factorized as $\xi_{i,j}(\boldsymbol{u})\,\chi(f)$, with $\xi_{i,j}(\boldsymbol{u}) = 1$ and $\chi(f) = |\widehat{g'}(f)|^2 m_{|\widehat{s'}|^2}(f) \geq 0$, which corresponds to the isotropic case of the early asymptotic state in Corollary 1.

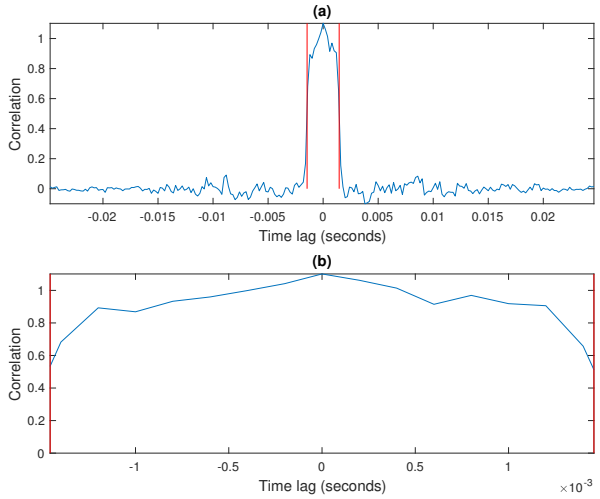

Fig. 13. Normalized asymptotic correlation function $\frac{2D}{c}\sigma_{1,2}(\tau, \boldsymbol{x}_2 - \boldsymbol{x}_1)$ in the classroom

The blue curve in Fig. 13-(a) represents the asymptotic correlation function $\sigma_{1,2}(\tau, \boldsymbol{x}_2 - \boldsymbol{x}_1)$. We observe that the temporal support of this correlation function lies in the interval $[-\frac{D}{c}, \frac{D}{c}]$ (whose boundaries are represented by red vertical lines), as predicted by the reverberation model in all asymptotic states. Moreover, within this temporal support (Fig. 13-(b) represents a zoom in on this interval), the correlation function is nearly constant, as predicted in the isotropic case of the early asymptotic state when $D \to 0$, which confirms what we already observed in Fig. 12. However, the assumption $D \to 0$ does not seem to hold completely, because in Fig. 13-(a), the shape of the asymptotic correlation function $\sigma_{1,2}(\tau, \boldsymbol{x}_2 - \boldsymbol{x}_1) = \frac{b(\tau, D)}{\beta_2}$ is rather peaky at $\tau = 0$. This behavior confirms the prediction of Lemma 3, which states that function $\tau \mapsto b(\tau, D)$ reaches its maximum at $\tau = 0$, and is not differentiable at $\tau = 0$.

We repeated the correlation measurements represented in Fig. 13 with different experimental setups: we tested various distances between microphones, and orientations of the vector $\boldsymbol{x}_2 - \boldsymbol{x}_1$, pointing from the first microphone to the second one. We did not include here all the results in order to avoid overloading this document, but all experimental setups led to figures looking like Fig. 13. This confirms that, regarding the time-frequency correlation between sensors, the reverberation in the classroom behaves as in the isotropic case of the early asymptotic state of a non-diffuse acoustic field.

2) Octagon room: In the *QMUL Octagon Impulse Response* "Omni" dataset, 169 RIRs were measured in the center of the Octagon room (a Victorian building completed in 1888 and originally designed to be a library). As described in [16], the walls of the room are lined with books, with a wooden floor and plaster ceiling. The room has eight walls each 7.5 m in length and a domed ceiling reaching 21 m over the floor, with an approximate volume of 9500 m^3. Measurements were 1 m apart arranged in 13 rows and 13 columns (over a 12 m $\times$ 12 m area) relative to the speaker, with the 7th column directly on axis with the speaker. For this setup, the average measured reverberation time RT_{30} is about 2 s around 1000 Hz [16, Fig. 4]. For the correlation measurements (time-frequency correlation $\rho_{1,2}(t, f, \boldsymbol{x}_2 - \boldsymbol{x}_1)$ and asymptotic correlation function $\sigma_{1,2}(\tau, \boldsymbol{x}_2 - \boldsymbol{x}_1)$), we computed space averages over all pairs of microphones placed 1 m apart, and such that the vector $\boldsymbol{x}_2 - \boldsymbol{x}_1$, pointing from the first microphone to the second one, is in the horizontal plane, in the direction of the x-axis.

Fig. 14 to Fig. 17 respectively represent the temporal power profile $\mathrm{var}[h_i(t)]$, the time-frequency power profile $\mathcal{W}_{\gamma_{i,i}}(t, f)$, and the real and imaginary parts of the time-frequency correlation $\rho_{1,2}(t, f, \boldsymbol{x}_2 - \boldsymbol{x}_1)$. All observations made in Section IV-B1 still hold here.

Regarding the asymptotic correlation function $\sigma_{1,2}(\tau, \boldsymbol{x}_2 - \boldsymbol{x}_1)$ represented in Fig. 18-(a), the observations are a bit different. First, the temporal support of this correlation function still essentially lies in the interval $[-\frac{D}{c}, \frac{D}{c}]$ (whose boundaries are represented by red vertical lines). Besides, Fig. 18-(b) shows that within this interval, the correlation function is still nonnegative and has continuous variations, but it can no longer be considered as approximately constant. Instead, it looks approximately even, which suggests that function $\boldsymbol{u} \mapsto \xi_{1,2}(\boldsymbol{u})$ may also be even, as stated in Corollary 1. Therefore, contrary to what we observed in the classroom, the observations in the Octagon room can no longer by explained by the isotropic case, but rather by the symmetric case of the early asymptotic state of a non-diffuse acoustic field (*cf.* Table I).

Indeed, the results of Corollary 1 hold in this experimental setup, because in this dataset, the microphones are omnidirec-

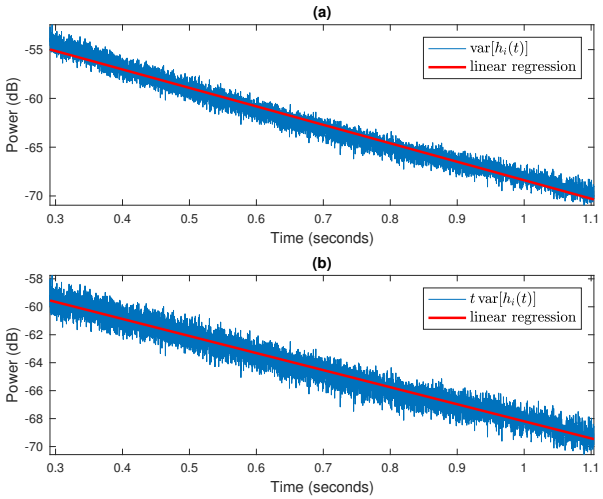

Fig. 14. Temporal power profile var$[h_i(t)]$ in the Octagon room

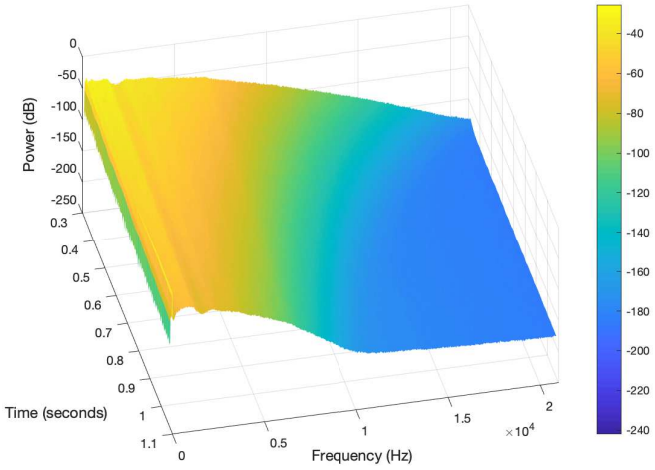

Fig. 15. Time-frequency power profile $\mathcal{W}_{\gamma_{i,i}}(t,f)$ in the Octagon room

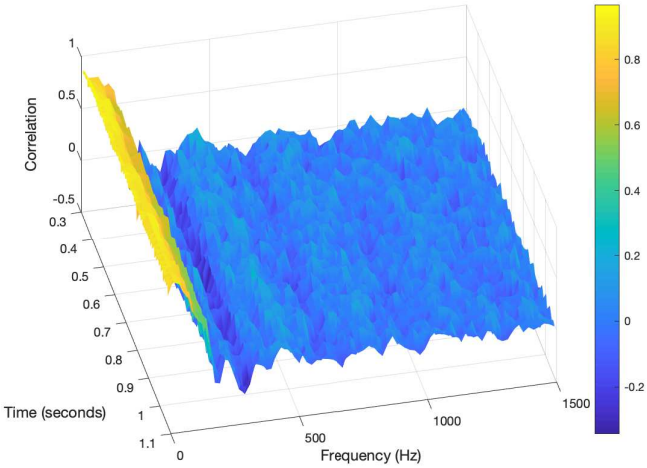

Fig. 16. Real part of the time-frequency correlation $\rho_{1,2}(t,f,\boldsymbol{x}_2-\boldsymbol{x}_1)$ in the Octagon room

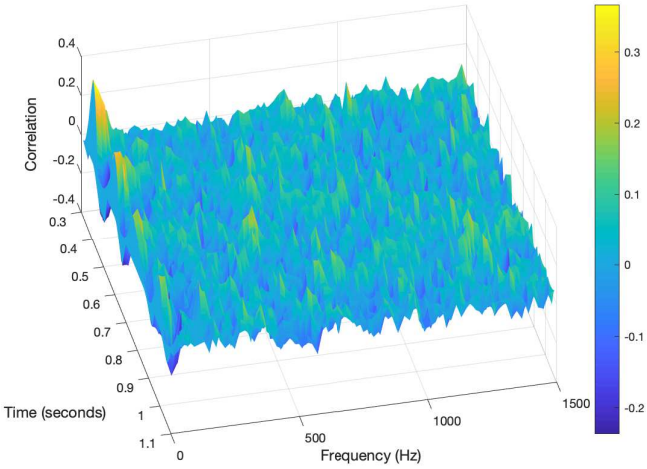

Fig. 17. Imaginary part of the time-frequency correlation $\rho_{1,2}(t,f,\boldsymbol{x}_2-\boldsymbol{x}_1)$ in the Octagon room

tional and have the same response g. In addition, if we assume that the second-order source response $m_{|\widehat{s'}|^2}(\boldsymbol{u},f) \geq 0$ can be approximately factorized as $m_{|\widehat{s'}|^2}(\boldsymbol{u},f) \approx \xi_s(\boldsymbol{u})\,\chi_s(f)$ where $\chi_s(f) \geq 0$ and function $\boldsymbol{u} \mapsto \xi_s(\boldsymbol{u}) \geq 0$ is even, then $\forall i,j \in \{1\dots I\}$, $\widehat{g_i'}(\boldsymbol{u},f)\overline{\widehat{g_j'}(\boldsymbol{u},f)}m_{|\widehat{s'}|^2}(\boldsymbol{u},f)$ can be factorized as $\xi_{i,j}(\boldsymbol{u})\,\chi(f)$, where $\chi(f) = |\widehat{g'}(f)|^2\chi_s(f) \geq 0$ and function $\boldsymbol{u} \mapsto \xi_{i,j}(\boldsymbol{u}) = \xi_s(\boldsymbol{u}) \geq 0$ is even, which corresponds to the symmetric case in Corollary 1.

However, outside the interval $[-\frac{D}{c},\frac{D}{c}]$, the estimated correlation represented in Fig. 18-(a) has a particular shape that cannot be modeled as centered noise, whereas Corollary 1 predicts that it should be zero. This discrepancy may be explained by the inaccuracy of the approximation $m_{|\widehat{s'}|^2}(\boldsymbol{u},f) \approx \xi_s(\boldsymbol{u})\,\chi_s(f)$.

We repeated the correlation measurements represented in Fig. 18 for other experimental setups: we tested various distances between microphones, and orientations of the vector $\boldsymbol{x}_2-\boldsymbol{x}_1$, pointing from the first microphone to the second one. Again we did not include here all the results in order to avoid overloading this document, but to put it simply, we obtained correlation functions $\sigma_{1,2}(\tau,\boldsymbol{x}_2-\boldsymbol{x}_1)$ whose support still essentially lies in the interval $[-\frac{D}{c},\frac{D}{c}]$, and still with nonnegative values and continuous variations, but with different shapes within this support. Therefore the asymptotic correlation function does depend on vector $\boldsymbol{x}_2-\boldsymbol{x}_1$, as predicted by Corollary 1.

3) Great hall: In the *QMUL Great Hall Impulse Response* "Omni" dataset, 169 RIRs were measured within the Great

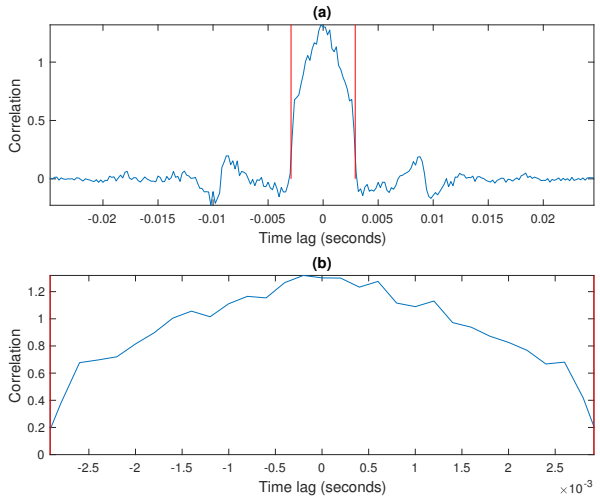

Fig. 18. Normalized asymptotic correlation function $\frac{2D}{c}\sigma_{1,2}(\tau, \boldsymbol{x}_2 - \boldsymbol{x}_1)$ in the Octagon room

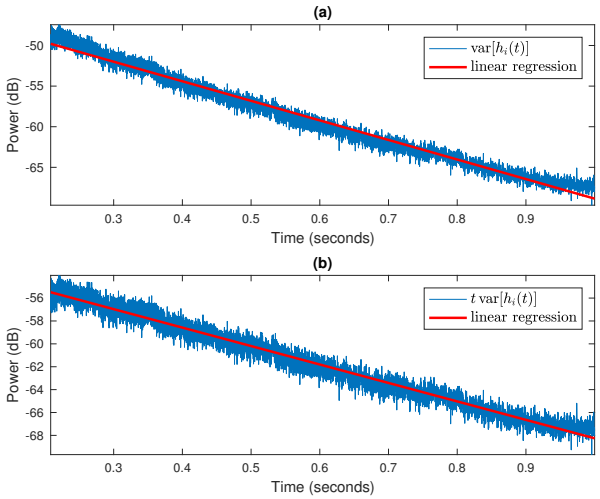

Fig. 19. Temporal power profile $\mathrm{var}[h_i(t)]$ in the Great Hall

Hall (a multipurpose hall that can hold approximately 800 seats). As described in [16], the hall has a stage and seating areas on the floor and a balcony. The microphones were placed in the seating area on the floor, approximately a 23 m $\times$ 16 m area, but the room is significantly bigger as the balcony extends 20 m past the rear wall. Measurements were 1 m apart arranged in 13 rows and 13 columns (over a 12 m $\times$ 12 m area) relative to the speaker, with the 7th column directly on axis with the speaker. For this setup, the average measured reverberation time RT_{30} is about 2 s around 1000 Hz [16, Fig. 4]. For the correlation measurements (time-frequency correlation $\rho_{1,2}(t, f, \boldsymbol{x}_2 - \boldsymbol{x}_1)$ and asymptotic correlation function $\sigma_{1,2}(\tau, \boldsymbol{x}_2 - \boldsymbol{x}_1)$), we computed space averages over all pairs of microphones placed 1 m apart, and such that the vector $\boldsymbol{x}_2 - \boldsymbol{x}_1$, pointing from the first microphone to the second one, is in the horizontal plane, in the direction of the y-axis.

Fig. 19 to 22 respectively represent the temporal power profile $\mathrm{var}[h_i(t)]$, the time-frequency power profile $\mathcal{W}_{\gamma_{i,i}}(t, f)$, and the real and imaginary parts of the time-frequency correlation $\rho_{1,2}(t, f, \boldsymbol{x}_2 - \boldsymbol{x}_1)$. All observations made in Section IV-B1 still hold here. Note however that the imaginary part of the time-frequency correlation in Fig. 22 is not approximately zero at low frequencies, thus the real-valued asymptotic correlation function in Fig. 23 is not even, as in the case of the shoebox room (*cf.* Section IV-A, Fig 6). Therefore function $\xi_{1,2}(\boldsymbol{u})$ is not even either, as showed in Corollary 1. This behavior corresponds to the anisotropic case of the early asymptotic state of a non-diffuse acoustic field (*cf.* Table I).

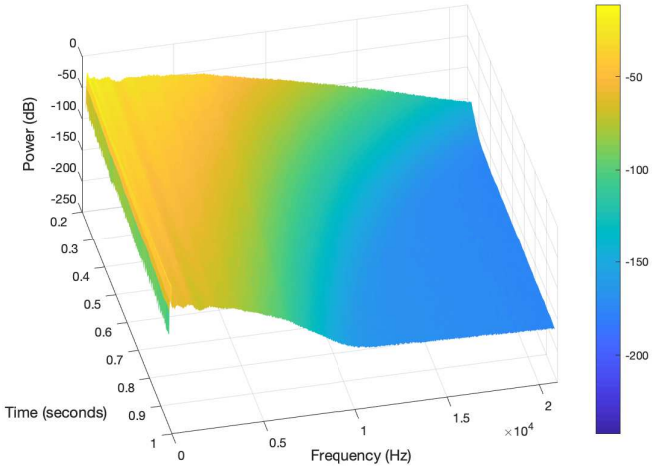

Fig. 20. Time-frequency power profile $\mathcal{W}_{\gamma_{i,i}}(t, f)$ in the Great Hall

V. Conclusion and Perspectives

In this research report, we extended the mathematical analysis of the stochastic model initially proposed in [1], [2], which was dedicated to the particular case of diffuse acoustic fields, omnidirectional sources and microphones, and constant attenuation w.r.t frequency, to the more general case of uniform and non-diffuse acoustic fields, and directive sources and microphones. The experiments confirmed that the predictions of the generalized stochastic model introduced in [13] match the observations, based on both synthetic and real room impulse responses, measured in various acoustic environments.

The next step in this research project will be the extension of both the mathematical analysis and the experimental validation to the more realistic case of frequency-varying attenuation coefficients, before addressing the most general case of non-uniform acoustic fields. Our purpose is then to develop efficient algorithms for estimating the model parameters, in order to investigate the potential of the general stochastic reverberation model in various signal processing applications.

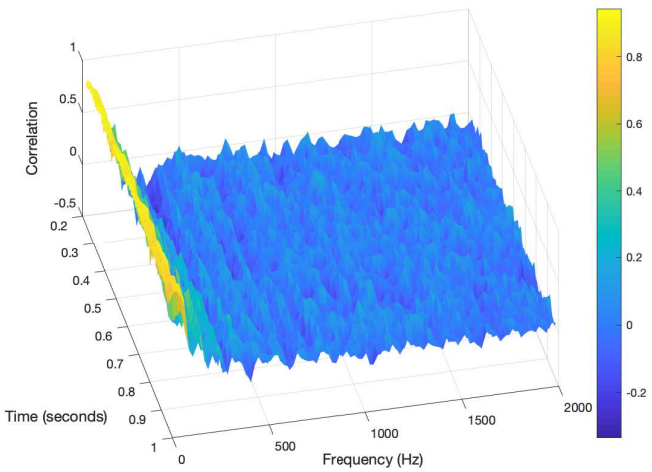

Fig. 21. Real part of the time-frequency correlation $\rho_{1,2}(t, f, \boldsymbol{x}_2 - \boldsymbol{x}_1)$ in the Great Hall

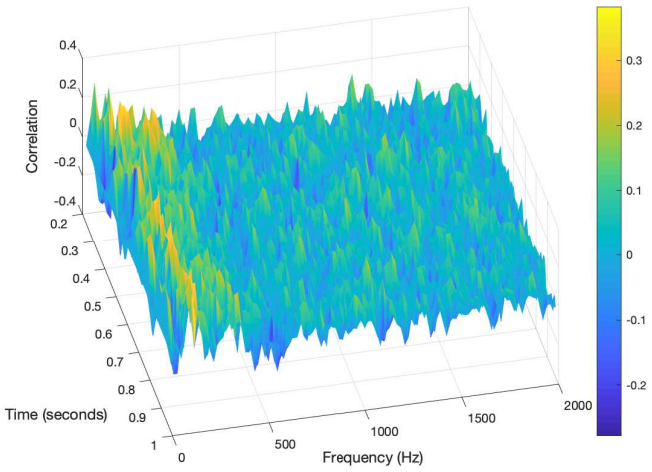

Fig. 22. Imaginary part of the time-frequency correlation $\rho_{1,2}(t, f, \boldsymbol{x}_2 - \boldsymbol{x}_1)$ in the Great Hall

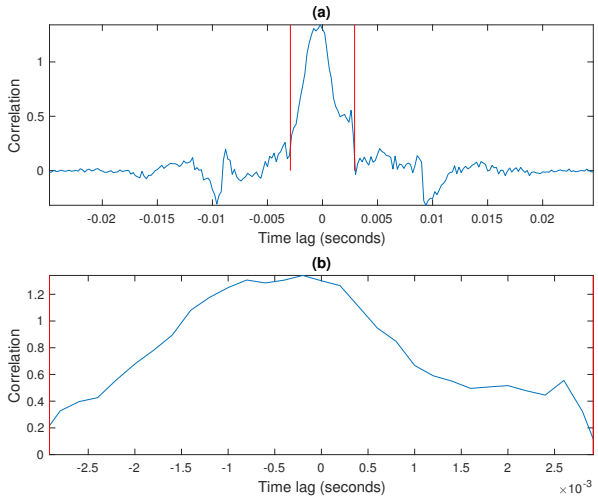

Fig. 23. Normalized asymptotic correlation function $\frac{2D}{c}\sigma_{1,2}(\tau, \boldsymbol{x}_2 - \boldsymbol{x}_1)$ in the Great Hall

APPENDIX A
GENERAL STATISTICAL PROPERTIES

In this appendix, we introduce a common formulation of the two equations (5) and (6) in Definition 1, which are expressed in the temporal and the spectral domains, respectively. This will permit us to prove general results that hold in both domains.

A.1. Common formulation of temporal and spectral equations

Lemma 4. *Both* (5) *and* (6) *in Definition 1 can be written in the form*

$$h_i = \int_{\boldsymbol{x}\in\mathbb{R}^3}\int_{\boldsymbol{y}\in\mathbb{R}^M} \frac{V_i(\boldsymbol{x},\boldsymbol{y};\boldsymbol{y}-\boldsymbol{q}(\boldsymbol{x}-\boldsymbol{x}_i))\varphi_i(\boldsymbol{x},\boldsymbol{y};\boldsymbol{x}-\boldsymbol{x}_i)e^{-\frac{\boldsymbol{y}^\top\widehat{\boldsymbol{\alpha}}}{c}}}{\|\boldsymbol{x}-\boldsymbol{x}_i\|_2} dN(\boldsymbol{x},\boldsymbol{y}), \tag{59}$$

where $\varphi_i(\boldsymbol{x}, \boldsymbol{y}; \boldsymbol{r})$ *is a random field on* $\mathbb{R}^3 \times \mathbb{R}^M$ *whose distribution is parameterized by* $\boldsymbol{r} \in \mathbb{R}^3$ *and is i.i.d. w.r.t.* $(\boldsymbol{x}, \boldsymbol{y})$*, and such that*

$$\|\varphi_i\|_\infty = \sup_{\mathbb{R}^3\times\mathbb{R}^M\times\mathbb{R}^3} |\varphi_i(\boldsymbol{x}, \boldsymbol{y}; \boldsymbol{r})| < +\infty.$$

Proof. With $\boldsymbol{r} = \boldsymbol{x} - \boldsymbol{x}_i$, (5) is derived by applying (59) to

$$\varphi_i(\boldsymbol{x}, \boldsymbol{y}; \boldsymbol{r}) = g_i\left(\frac{\boldsymbol{r}}{\|\boldsymbol{r}\|_2}, .\right) \overset{t}{*} s\left(\Theta(\boldsymbol{x}, \boldsymbol{y})\frac{\boldsymbol{r}}{\|\boldsymbol{r}\|_2}, t - \frac{\|\boldsymbol{r}\|_2}{c}\right), \tag{60}$$

where $\forall(\boldsymbol{x}, \boldsymbol{y}) \in \mathbb{R}^3 \times \mathbb{R}^M$, $\forall \boldsymbol{r} \in \mathbb{R}^3$,

$$|\varphi_i(\boldsymbol{x}, \boldsymbol{y}; \boldsymbol{r})| \leq \begin{array}{l} \min(T_g, T_s)\sup_{\boldsymbol{u}\in\mathcal{S}^2, t\in[0,T_g]} |g_i(\boldsymbol{u}, t)| \\ \sup_{\boldsymbol{u}\in\mathcal{S}^2, t\in[0,T_s]} |s(\boldsymbol{u}, t)|, \end{array}$$

and (6) is derived by applying (59) to

$$\varphi_i(\boldsymbol{x}, \boldsymbol{y}; \boldsymbol{r}) = \widehat{g}_i\left(\frac{\boldsymbol{r}}{\|\boldsymbol{r}\|_2}, f\right)\widehat{s}\left(\Theta(\boldsymbol{x}, \boldsymbol{y})\frac{\boldsymbol{r}}{\|\boldsymbol{r}\|_2}, f\right)e^{-\frac{2\imath\pi f\|\boldsymbol{r}\|_2}{c}}, \tag{61}$$

where $\forall(\boldsymbol{x}, \boldsymbol{y}) \in \mathbb{R}^3 \times \mathbb{R}^M$, $\forall \boldsymbol{r} \in \mathbb{R}^3$,

$$|\varphi_i(\boldsymbol{x}, \boldsymbol{y}; \boldsymbol{r})| \leq \sup_{\boldsymbol{u}\in\mathcal{S}^2, f\in\mathbb{R}} |\widehat{g}_i(\boldsymbol{u}, f)| \sup_{\boldsymbol{u}\in\mathcal{S}^2, f\in\mathbb{R}} |\widehat{s}(\boldsymbol{u}, f)|.$$

□

A.2. First order moments

Proposition 5. *Considering the stochastic reverberation model in Definition 1, the expected value of* (59) *for any sensor* $i \in \{1 \dots I\}$ *is*

$$\mathbb{E}[h_i] = \lambda\beta_1 \int_{\boldsymbol{r}\in\mathbb{R}^3} \frac{m_{\varphi_i}(\boldsymbol{r})e^{-\frac{\widehat{\alpha}(\boldsymbol{r})}{c}}}{\|\boldsymbol{r}\|_2} d\boldsymbol{r} < +\infty \tag{62}$$

where function $\widehat{\alpha}(.)$ *is defined in* (7)*,* β_1 *is defined in* (13) *for* $n = 1$*, and* $\forall \boldsymbol{x}, \boldsymbol{y} \in \mathbb{R}^3 \times \mathbb{R}^M$*,* $\forall \boldsymbol{r} \in \mathbb{R}^3$*,*

$$m_{\varphi_i}(\boldsymbol{r}) = \mathbb{E}[\varphi_i(\boldsymbol{x}, \boldsymbol{y}; \boldsymbol{r})] \in L^\infty(\mathbb{R}^3). \tag{63}$$

Proof. First, we note that β_1 is finite, as proved in Lemma 1. We also note that $m_{\varphi_i} \in L^\infty(\mathbb{R}^3)$ because $\|\varphi_i\|_\infty < +\infty$, and $\widehat{\alpha}^{\inf} = \inf_{\boldsymbol{u}\in\mathcal{S}^2} \alpha(\boldsymbol{u}) > 0$, so that $\forall \boldsymbol{r} \in \mathbb{R}^3$,

$$\left| \frac{m_{\varphi_i}(\boldsymbol{r}) e^{-\frac{\widehat{\alpha}(\boldsymbol{r})}{c}}}{\|\boldsymbol{r}\|_2} \right| \leq \frac{\|m_{\varphi_i}\|_\infty e^{-\frac{\widehat{\alpha}^{\inf}\|\boldsymbol{r}\|}{c}}}{\|\boldsymbol{r}\|_2},$$

which proves that the integral in (62) converges.

Let us now prove (62). The expected value of (59) can be written as $\mathbb{E}[h_i] = \mathbb{E}[I]$, where the mathematical expectation is w.r.t. the three random fields φ_i, V_i and dN on $\mathbb{R}^3 \times \mathbb{R}^M$, with $I = \int_{\boldsymbol{x}\in\mathbb{R}^3} \int_{\boldsymbol{y}\in\mathbb{R}^M} \psi(\boldsymbol{x},\boldsymbol{y}) dN(\boldsymbol{x},\boldsymbol{y})$, and

$$\psi(\boldsymbol{x},\boldsymbol{y}) = \frac{V_i(\boldsymbol{x},\boldsymbol{y};\boldsymbol{y}-\boldsymbol{q}(\boldsymbol{x}-\boldsymbol{x}_i))\varphi_i(\boldsymbol{x},\boldsymbol{y};\boldsymbol{x}-\boldsymbol{x}_i) e^{-\frac{\boldsymbol{y}^\top \widehat{\boldsymbol{\alpha}}}{c}}}{\|\boldsymbol{x}-\boldsymbol{x}_i\|_2}. \quad (64)$$

By applying Proposition 4 in [2] to $\Lambda(\boldsymbol{x},\boldsymbol{y}) = \lambda$ and I defined above, equation (B4) in [2] yields

$$\mathbb{E}[I] = \lambda \mathbb{E}\left[\int_{\boldsymbol{x}\in\mathbb{R}^3} \int_{\boldsymbol{y}\in\mathbb{R}^M} \psi(\boldsymbol{x},\boldsymbol{y}) d\boldsymbol{x} d\boldsymbol{y} \right], \quad (65)$$

where the mathematical expectation is now w.r.t. the two random fields φ_i and V_i only. Substituting (64) into (65) yields

$$\mathbb{E}[h_i] = \lambda \mathbb{E}\left[\int_{\boldsymbol{x}\in\mathbb{R}^3} \int_{\boldsymbol{y}\in\mathbb{R}^M} \frac{V_i(\boldsymbol{x},\boldsymbol{y};\boldsymbol{y}-\boldsymbol{q}(\boldsymbol{x}-\boldsymbol{x}_i))\varphi_i(\boldsymbol{x},\boldsymbol{y};\boldsymbol{x}-\boldsymbol{x}_i) e^{-\frac{\boldsymbol{y}^\top \widehat{\boldsymbol{\alpha}}}{c}}}{\|\boldsymbol{x}-\boldsymbol{x}_i\|_2} d\boldsymbol{x} d\boldsymbol{y} \right]. \quad (66)$$

With the change of variable $\boldsymbol{r} = \boldsymbol{x} - \boldsymbol{x}_i$, which is such that $d\boldsymbol{r} = d\boldsymbol{x}$, since $\mathbb{E}[V_i(\boldsymbol{x},\boldsymbol{y};\boldsymbol{y}-\boldsymbol{q}(\boldsymbol{r}))] = p(1;\boldsymbol{y}-\boldsymbol{q}(\boldsymbol{r}))$ and $\mathbb{E}[\varphi_i(\boldsymbol{x},\boldsymbol{y};\boldsymbol{r})] = m_{\varphi_i}(\boldsymbol{r})$ as defined in (63), (66) yields

$$\mathbb{E}[h_i] = \lambda \int_{\boldsymbol{r}\in\mathbb{R}^3} \int_{\boldsymbol{y}\in\mathbb{R}^M} \frac{p(1;\boldsymbol{y}-\boldsymbol{q}(\boldsymbol{r})) m_{\varphi_i}(\boldsymbol{r}) e^{-\frac{\boldsymbol{y}^\top \widehat{\boldsymbol{\alpha}}}{c}}}{\|\boldsymbol{r}\|_2} d\boldsymbol{r} d\boldsymbol{y}. \quad (67)$$

Finally, with the change of variable $\boldsymbol{z} = \boldsymbol{y} - \boldsymbol{q}(\boldsymbol{r})$, which is such that $d\boldsymbol{z} = d\boldsymbol{y}$, and by substituting (7) and (13) for $n = 1$ into (67), we get (62). □

A.3. Second order moments

Proposition 6. *Considering the stochastic reverberation model in Definition 1, the covariance of* (59) *for any sensors* $i, j \in \{1 \dots I\}$ *is*

$$\operatorname{cov}[h_i, h_j] = \lambda \int_{\boldsymbol{x}\in\mathbb{R}^3} \beta(\boldsymbol{q}(\boldsymbol{x}-\boldsymbol{x}_i) - \boldsymbol{q}(\boldsymbol{x}-\boldsymbol{x}_j)) \frac{m_{\varphi_i,\overline{\varphi_j}}(\boldsymbol{x}-\boldsymbol{x}_i, \boldsymbol{x}-\boldsymbol{x}_j) e^{-\frac{\widehat{\alpha}(\boldsymbol{x}-\boldsymbol{x}_i)+\widehat{\alpha}(\boldsymbol{x}-\boldsymbol{x}_j)}{c}}}{\|\boldsymbol{x}-\boldsymbol{x}_i\|_2 \|\boldsymbol{x}-\boldsymbol{x}_j\|_2} d\boldsymbol{x} < +\infty \quad (68)$$

where function $\widehat{\alpha}(.)$ *is defined in* (7)*, function* $\beta(.)$ *is defined in* (17)*, and* $\forall (\boldsymbol{x},\boldsymbol{y}) \in \mathbb{R}^3 \times \mathbb{R}^M$*,* $\forall \boldsymbol{r}_i, \boldsymbol{r}_j \in \mathbb{R}^3$*,*

$$m_{\varphi_i,\overline{\varphi_j}}(\boldsymbol{r}_i, \boldsymbol{r}_j) = \mathbb{E}\left[\varphi_i(\boldsymbol{x},\boldsymbol{y};\boldsymbol{r}_i) \overline{\varphi_j(\boldsymbol{x},\boldsymbol{y};\boldsymbol{r}_j)} \right] \in L^\infty(\mathbb{R}^3 \times \mathbb{R}^3). \quad (69)$$

Proof. First, Lemma 2 shows that function $\beta(.)$ in (17) is upper bounded by β_2; however β_2 is finite, as proved in Lemma 1. We also note that $m_{\varphi_i,\overline{\varphi_j}} \in L^\infty(\mathbb{R}^3 \times \mathbb{R}^3)$ because $\|\varphi_i\|_\infty < +\infty$, and $\widehat{\alpha}^{\inf} = \inf_{\boldsymbol{u}\in\mathcal{S}^2} \alpha(\boldsymbol{u}) > 0$, so that $\forall \boldsymbol{x} \in \mathbb{R}^3$,

$$\left| \frac{\beta(\boldsymbol{q}(\boldsymbol{x}-\boldsymbol{x}_i)-\boldsymbol{q}(\boldsymbol{x}-\boldsymbol{x}_j)) m_{\varphi_i,\overline{\varphi_j}}(\boldsymbol{x}-\boldsymbol{x}_i, \boldsymbol{x}-\boldsymbol{x}_j) e^{-\frac{\widehat{\alpha}(\boldsymbol{x}-\boldsymbol{x}_i)+\widehat{\alpha}(\boldsymbol{x}-\boldsymbol{x}_j)}{c}}}{\|\boldsymbol{x}-\boldsymbol{x}_i\|_2 \|\boldsymbol{x}-\boldsymbol{x}_j\|_2} \right| \leq \frac{\beta_2 \|m_{\varphi_i,\overline{\varphi_j}}\|_\infty e^{-\frac{\widehat{\alpha}^{\inf}(\|\boldsymbol{x}-\boldsymbol{x}_i\|_2 + \|\boldsymbol{x}-\boldsymbol{x}_j\|_2)}{c}}}{\|\boldsymbol{x}-\boldsymbol{x}_i\|_2 \|\boldsymbol{x}-\boldsymbol{x}_j\|_2},$$

which proves that the integral in (68) converges.

Let us now prove (68). For $k \in \{1, 2\}$, let

$$I_k = \int_{\boldsymbol{x}\in\mathbb{R}^3} \int_{\boldsymbol{y}\in\mathbb{R}^M} \psi_k(\boldsymbol{x},\boldsymbol{y}) dN(\boldsymbol{x},\boldsymbol{y}),$$

with

$$\begin{aligned} \psi_1(\boldsymbol{x},\boldsymbol{y}) &= \frac{V_i(\boldsymbol{x},\boldsymbol{y};\boldsymbol{y}-\boldsymbol{q}(\boldsymbol{x}-\boldsymbol{x}_i))\varphi_i(\boldsymbol{x},\boldsymbol{y};\boldsymbol{x}-\boldsymbol{x}_i) e^{-\frac{\boldsymbol{y}^\top \widehat{\boldsymbol{\alpha}}}{c}}}{\|\boldsymbol{x}-\boldsymbol{x}_i\|_2}, \\ \psi_2(\boldsymbol{x},\boldsymbol{y}) &= \frac{V_j(\boldsymbol{x},\boldsymbol{y};\boldsymbol{y}-\boldsymbol{q}(\boldsymbol{x}-\boldsymbol{x}_j))\varphi_j(\boldsymbol{x},\boldsymbol{y};\boldsymbol{x}-\boldsymbol{x}_j) e^{-\frac{\boldsymbol{y}^\top \widehat{\boldsymbol{\alpha}}}{c}}}{\|\boldsymbol{x}-\boldsymbol{x}_j\|_2}. \end{aligned} \quad (70)$$

We note that

$$\mathbb{E}[I_1 \overline{I_2}] = \operatorname{cov}[I_1, I_2] + \mathbb{E}[I_1]\mathbb{E}[\overline{I_2}], \quad (71)$$

where the mathematical expectation is w.r.t. the random fields φ_i, φ_j, V_i, V_j and dN on $\mathbb{R}^3 \times \mathbb{R}^M$. By applying Proposition 4 in [2] to $\Lambda(\boldsymbol{x},\boldsymbol{y}) = \lambda$ and I_1 and I_2 defined above, equation (B4) in [2] yields

$$\begin{aligned} \mathbb{E}[I_1] &= \lambda \mathbb{E}\left[\int_{\boldsymbol{x}\in\mathbb{R}^3} \int_{\boldsymbol{y}\in\mathbb{R}^M} \psi_1(\boldsymbol{x},\boldsymbol{y}) d\boldsymbol{x} d\boldsymbol{y} \right], \\ \mathbb{E}[I_2] &= \lambda \mathbb{E}\left[\int_{\boldsymbol{x}\in\mathbb{R}^3} \int_{\boldsymbol{y}\in\mathbb{R}^M} \psi_2(\boldsymbol{x},\boldsymbol{y}) d\boldsymbol{x} d\boldsymbol{y} \right], \end{aligned} \quad (72)$$

where the mathematical expectations in the right members of these equalities are now w.r.t. the random fields φ_i, φ_j and V_i, V_j only. In the same way, by applying Proposition 5 in [2] to $\Lambda(\boldsymbol{x},\boldsymbol{y}) = \lambda$ and I_1 and I_2 defined above, equation (B8) [9] in [2] yields

$$\operatorname{cov}[I_1, I_2] = \lambda \mathbb{E}\left[\int_{\boldsymbol{x}\in\mathbb{R}^3} \int_{\boldsymbol{y}\in\mathbb{R}^M} \psi_1(\boldsymbol{x},\boldsymbol{y}) \overline{\psi_2(\boldsymbol{x},\boldsymbol{y})} d\boldsymbol{x} d\boldsymbol{y} \right]. \quad (73)$$

By substituting (72) and (73) into (71), we get

$$\begin{aligned} \mathbb{E}[I_1 \overline{I_2}] = \; & \lambda \mathbb{E}\left[\int_{\boldsymbol{x}\in\mathbb{R}^3} \int_{\boldsymbol{y}\in\mathbb{R}^M} \psi_1(\boldsymbol{x},\boldsymbol{y}) \overline{\psi_2(\boldsymbol{x},\boldsymbol{y})} d\boldsymbol{x} d\boldsymbol{y} \right] \\ & + \lambda^2 \mathbb{E}\Big[\int_{\boldsymbol{x}_1\in\mathbb{R}^3} \int_{\boldsymbol{y}_1\in\mathbb{R}^M} \psi_1(\boldsymbol{x}_1,\boldsymbol{y}_1) d\boldsymbol{x}_1 d\boldsymbol{y}_1 \\ & \int_{\boldsymbol{x}_2\in\mathbb{R}^3} \int_{\boldsymbol{y}_2\in\mathbb{R}^M} \overline{\psi_2(\boldsymbol{x}_2,\boldsymbol{y}_2)} d\boldsymbol{x}_2 d\boldsymbol{y}_2 \Big]. \end{aligned} \quad (74)$$

However, since the random increments $\psi_1(\boldsymbol{x}_1,\boldsymbol{y}_1)$ and $\psi_2(\boldsymbol{x}_2,\boldsymbol{y}_2)$ are independent when $(\boldsymbol{x}_1,\boldsymbol{y}_1) \neq (\boldsymbol{x}_2,\boldsymbol{y}_2)$, we get $\forall \boldsymbol{x}_1, \boldsymbol{x}_2 \in \mathbb{R}^3$, $\forall \boldsymbol{y}_1, \boldsymbol{y}_2 \in \mathbb{R}^M$,

$$\begin{aligned} & \lambda^2 \mathbb{E}\left[\psi_1(\boldsymbol{x}_1,\boldsymbol{y}_1) \overline{\psi_2(\boldsymbol{x}_2,\boldsymbol{y}_2)} \right] \\ = \; & \lambda^2 \operatorname{cov}[\psi_1(\boldsymbol{x}_1,\boldsymbol{y}_1), \psi_2(\boldsymbol{x}_2,\boldsymbol{y}_2)] \delta_{\boldsymbol{x}_1,\boldsymbol{x}_2} \delta_{\boldsymbol{y}_1,\boldsymbol{y}_2} \\ & + \lambda^2 \mathbb{E}\left[\psi_1(\boldsymbol{x}_1,\boldsymbol{y}_1)\right] \mathbb{E}\left[\overline{\psi_2(\boldsymbol{x}_2,\boldsymbol{y}_2)} \right], \end{aligned} \quad (75)$$

where $\delta_{x,y}$ denotes the Kronecker delta: $\delta_{x,y} = 1$ if $x = y$, or $\delta_{x,y} = 0$ if $x \neq y$. Since the Lebesgue measure of the support

[9] Equation (B8) was proved in [2] in the real case; we use here its extension to the complex case, which is straightforward.

of $\delta_{\boldsymbol{x}_1,\boldsymbol{x}_2}\delta_{\boldsymbol{y}_1,\boldsymbol{y}_2}$ is zero in $(\mathbb{R}^3\times\mathbb{R}^M)^2$, integrating (75) over $(\mathbb{R}^3\times\mathbb{R}^M)^2$ yields

$$\begin{aligned}&\lambda^2\int_{\boldsymbol{x}_1,\boldsymbol{y}_1,\boldsymbol{x}_2,\boldsymbol{y}_2}\mathbb{E}\left[\psi_1(\boldsymbol{x}_1,\boldsymbol{y}_1)\overline{\psi_2(\boldsymbol{x}_2,\boldsymbol{y}_2)}\right]d\boldsymbol{x}_1d\boldsymbol{y}_1d\boldsymbol{x}_2d\boldsymbol{y}_2\\&=\lambda^2\int_{\boldsymbol{x}_1,\boldsymbol{y}_1,\boldsymbol{x}_2,\boldsymbol{y}_2}\mathbb{E}[\psi_1(\boldsymbol{x}_1,\boldsymbol{y}_1)]\mathbb{E}[\overline{\psi_2(\boldsymbol{x}_2,\boldsymbol{y}_2)}]d\boldsymbol{x}_1d\boldsymbol{y}_1d\boldsymbol{x}_2d\boldsymbol{y}_2\\&=\mathbb{E}[I_1]\mathbb{E}[\overline{I_2}],\end{aligned}\tag{76}$$

where we have used (72). By substituting (74) and (76) into (71), we get

$$\begin{aligned}\operatorname{cov}[I_1,I_2]=&\ \mathbb{E}[I_1\overline{I_2}]-\mathbb{E}[I_1]\mathbb{E}[\overline{I_2}]\\=&\ \lambda\mathbb{E}\left[\int_{\boldsymbol{x}\in\mathbb{R}^3}\int_{\boldsymbol{y}\in\mathbb{R}^M}\psi_1(\boldsymbol{x},\boldsymbol{y})\overline{\psi_2(\boldsymbol{x},\boldsymbol{y})}d\boldsymbol{x}d\boldsymbol{y}\right].\end{aligned}\tag{77}$$

Since $\forall(\boldsymbol{x},\boldsymbol{y})\in\mathbb{R}^3\times\mathbb{R}^M$,

$$\begin{aligned}&\mathbb{E}\left[V_i(\boldsymbol{x},\boldsymbol{y};\boldsymbol{y}-\boldsymbol{q}(\boldsymbol{x}-\boldsymbol{x}_i))V_j(\boldsymbol{x},\boldsymbol{y};\boldsymbol{y}-\boldsymbol{q}(\boldsymbol{x}-\boldsymbol{x}_j))\right]\\=&\ p(1,1;\boldsymbol{y}-\boldsymbol{q}(\boldsymbol{x}-\boldsymbol{x}_i),\boldsymbol{y}-\boldsymbol{q}(\boldsymbol{x}-\boldsymbol{x}_j))\end{aligned}$$

and

$$\mathbb{E}\left[\varphi_i(\boldsymbol{x},\boldsymbol{y};\boldsymbol{x}\text{-}\boldsymbol{x}_i)\overline{\varphi_j(\boldsymbol{x},\boldsymbol{y};\boldsymbol{x}\text{-}\boldsymbol{x}_j)}\right]=m_{\varphi_i,\overline{\varphi_j}}(\boldsymbol{x}\text{-}\boldsymbol{x}_i,\boldsymbol{x}\text{-}\boldsymbol{x}_j)$$

as defined in (69), by substituting (70) into (77), we get

$$\begin{aligned}&\operatorname{cov}[I_1,I_2]=\lambda\int_{\boldsymbol{x}\in\mathbb{R}^3}\int_{\boldsymbol{y}\in\mathbb{R}^M}\\&\frac{p(1,1;\boldsymbol{y}-\boldsymbol{q}(\boldsymbol{x}-\boldsymbol{x}_i),\boldsymbol{y}-\boldsymbol{q}(\boldsymbol{x}-\boldsymbol{x}_j))m_{\varphi_i,\overline{\varphi_j}}(\boldsymbol{x}-\boldsymbol{x}_i,\boldsymbol{x}-\boldsymbol{x}_j)e^{-\frac{2\boldsymbol{y}^\top\hat{\boldsymbol{\alpha}}}{c}}}{\|\boldsymbol{x}-\boldsymbol{x}_i\|_2\|\boldsymbol{x}-\boldsymbol{x}_j\|_2}d\boldsymbol{x}d\boldsymbol{y}.\end{aligned}\tag{78}$$

Finally, with the change of variable $\boldsymbol{z}=\boldsymbol{y}-\frac{\boldsymbol{q}(\boldsymbol{x}-\boldsymbol{x}_i)+\boldsymbol{q}(\boldsymbol{x}-\boldsymbol{x}_j)}{2}$, which is such that $d\boldsymbol{z}=d\boldsymbol{y}$, and by substituting (7) and (17) into (78), we get (68). □

A.4. Characteristic function

Proposition 7. *Considering the stochastic reverberation model in Definition 1, for any sensors $i,j\in\{1\dots I\}$, the characteristic function*

$$\phi_{h_i,h_j}(\theta_1,\theta_2)=\mathbb{E}\left[e^{\imath\left(Re(\overline{\theta_1}h_i+\overline{\theta_2}h_j)\right)}\right]\quad\forall\theta_1,\theta_2\in\mathbb{C}\tag{79}$$

of the random vector $[h_i,h_j]^\top$ with h_i and h_j defined in (59) *is such that*

$$\begin{aligned}&\ln\phi_{h_i,h_j}(\theta_1,\theta_2)=\lambda\int_{\boldsymbol{x}\in\mathbb{R}^3}\int_{\boldsymbol{y}\in\mathbb{R}^M}\\&p(1,1;\boldsymbol{y}-\boldsymbol{q}(\boldsymbol{x}-\boldsymbol{x}_i),\boldsymbol{y}-\boldsymbol{q}(\boldsymbol{x}-\boldsymbol{x}_j))\\&\left(\phi_{\varphi_i(\boldsymbol{x}-\boldsymbol{x}_i),\varphi_j(\boldsymbol{x}-\boldsymbol{x}_j)}\left(\frac{\theta_1e^{-\frac{\boldsymbol{y}^\top\hat{\boldsymbol{\alpha}}}{c}}}{\|\boldsymbol{x}-\boldsymbol{x}_i\|_2},\frac{\theta_2e^{-\frac{\boldsymbol{y}^\top\hat{\boldsymbol{\alpha}}}{c}}}{\|\boldsymbol{x}-\boldsymbol{x}_j\|_2}\right)-1\right)\\&+p(1,0;\boldsymbol{y}-\boldsymbol{q}(\boldsymbol{x}-\boldsymbol{x}_i),\boldsymbol{y}-\boldsymbol{q}(\boldsymbol{x}-\boldsymbol{x}_j))\\&\left(\phi_{\varphi_i(\boldsymbol{x}-\boldsymbol{x}_i)}\left(\frac{\theta_1e^{-\frac{\boldsymbol{y}^\top\hat{\boldsymbol{\alpha}}}{c}}}{\|\boldsymbol{x}-\boldsymbol{x}_i\|_2}\right)-1\right)\\&+p(0,1;\boldsymbol{y}-\boldsymbol{q}(\boldsymbol{x}-\boldsymbol{x}_i),\boldsymbol{y}-\boldsymbol{q}(\boldsymbol{x}-\boldsymbol{x}_j))\\&\left(\phi_{\varphi_j(\boldsymbol{x}-\boldsymbol{x}_j)}\left(\frac{\theta_2e^{-\frac{\boldsymbol{y}^\top\hat{\boldsymbol{\alpha}}}{c}}}{\|\boldsymbol{x}-\boldsymbol{x}_j\|_2}\right)-1\right)d\boldsymbol{x}d\boldsymbol{y}.\end{aligned}\tag{80}$$

Proof. By substituting (59) into (79) we get

$$\phi_{h_i,h_j}(\theta_1,\theta_2)=\mathbb{E}[e^{\imath\theta I}],$$

where the mathematical expectation is w.r.t. the random fields φ_i, φ_j, V_i, V_j and dN on $\mathbb{R}^3\times\mathbb{R}^M$, with $\theta=1$, $I=\int_{\boldsymbol{x}\in\mathbb{R}^3}\int_{\boldsymbol{y}\in\mathbb{R}^M}\psi(\boldsymbol{x},\boldsymbol{y})dN(\boldsymbol{x},\boldsymbol{y})$, and

$$\begin{aligned}\psi(\boldsymbol{x},\boldsymbol{y})=&\ Re\Big(\overline{\theta_1}\tfrac{V_i(\boldsymbol{x},\boldsymbol{y};\boldsymbol{y}-\boldsymbol{q}(\boldsymbol{x}-\boldsymbol{x}_i))\varphi_i(\boldsymbol{x},\boldsymbol{y};\boldsymbol{x}-\boldsymbol{x}_i)}{\|\boldsymbol{x}-\boldsymbol{x}_i\|_2}\\&+\overline{\theta_2}\tfrac{V_j(\boldsymbol{x},\boldsymbol{y};\boldsymbol{y}-\boldsymbol{q}(\boldsymbol{x}-\boldsymbol{x}_j))\varphi_j(\boldsymbol{x},\boldsymbol{y};\boldsymbol{x}-\boldsymbol{x}_j)}{\|\boldsymbol{x}-\boldsymbol{x}_j\|_2}\Big)e^{-\frac{\boldsymbol{y}^\top\hat{\boldsymbol{\alpha}}}{c}}.\end{aligned}\tag{81}$$

By applying Proposition 4 in [2] to $\Lambda(\boldsymbol{x},\boldsymbol{y})=\lambda$, and θ, I defined above, equation (B1) in [2] yields

$$\begin{aligned}&\phi_{h_i,h_j}(\theta_1,\theta_2)=\mathbb{E}\left[e^{\lambda\int_{\boldsymbol{x}\in\mathbb{R}^3}\int_{\boldsymbol{y}\in\mathbb{R}^M}(e^{\imath\psi(\boldsymbol{x},\boldsymbol{y})}-1)d\boldsymbol{x}d\boldsymbol{y}}\right]\\&=\textstyle\sum_{n=0}^{+\infty}\frac{1}{n!}\mathbb{E}\left[\left(\lambda\int_{\boldsymbol{x}\in\mathbb{R}^3}\int_{\boldsymbol{y}\in\mathbb{R}^M}(e^{\imath\psi(\boldsymbol{x},\boldsymbol{y})}-1)d\boldsymbol{x}d\boldsymbol{y}\right)^n\right],\end{aligned}\tag{82}$$

where the mathematical expectation is now w.r.t. the random fields φ_i, φ_j, V_i, and V_j only. Since the random increments $\psi(\boldsymbol{x}_1,\boldsymbol{y}_1)$ and $\psi(\boldsymbol{x}_2,\boldsymbol{y}_2)$ are independent when $(\boldsymbol{x}_1,\boldsymbol{y}_1)\neq(\boldsymbol{x}_2,\boldsymbol{y}_2)$, we get

$$\begin{aligned}&\mathbb{E}\left[\left(\lambda\int_{\boldsymbol{x}\in\mathbb{R}^3}\int_{\boldsymbol{y}\in\mathbb{R}^M}(e^{\imath\psi(\boldsymbol{x},\boldsymbol{y})}-1)d\boldsymbol{x}d\boldsymbol{y}\right)^n\right]\\&=\left(\mathbb{E}\left[\lambda\int_{\boldsymbol{x}\in\mathbb{R}^3}\int_{\boldsymbol{y}\in\mathbb{R}^M}(e^{\imath\psi(\boldsymbol{x},\boldsymbol{y})}-1)d\boldsymbol{x}d\boldsymbol{y}\right]\right)^n\end{aligned}\tag{83}$$

because when developing the product in the left member, all terms but the one in the right member are zero, since they result from integrations on Borel sets whose Lebesgue measure is zero in $(\mathbb{R}^3\times\mathbb{R}^M)^n$ (we use here the same argument as in the proof of Proposition 6). Substituting (83) into (82) yields

$$\begin{aligned}&\phi_{h_i,h_j}(\theta_1,\theta_2)\\&=\textstyle\sum_{n=0}^{+\infty}\frac{1}{n!}\left(\mathbb{E}\left[\lambda\int_{\boldsymbol{x}\in\mathbb{R}^3}\int_{\boldsymbol{y}\in\mathbb{R}^M}(e^{\imath\psi(\boldsymbol{x},\boldsymbol{y})}-1)d\boldsymbol{x}d\boldsymbol{y}\right]\right)^n\\&=e^{\lambda\int_{\boldsymbol{x}\in\mathbb{R}^3}\int_{\boldsymbol{y}\in\mathbb{R}^M}\left(\mathbb{E}\left[e^{\imath\psi(\boldsymbol{x},\boldsymbol{y})}\right]-1\right)d\boldsymbol{x}d\boldsymbol{y}}.\end{aligned}\tag{84}$$

By substituting (81) into (84), we get:

$$\begin{aligned}&\ln\phi_{h_i,h_j}(\theta_1,\theta_2)=\lambda\int_{\boldsymbol{x}\in\mathbb{R}^3}\int_{\boldsymbol{y}\in\mathbb{R}^M}\\&\mathbb{E}\Big[e^{\imath Re\left(\overline{\theta_1}\frac{V_i(\boldsymbol{x},\boldsymbol{y};\boldsymbol{y}-\boldsymbol{q}(\boldsymbol{x}-\boldsymbol{x}_i))\varphi_i(\boldsymbol{x},\boldsymbol{y};\boldsymbol{x}-\boldsymbol{x}_i)}{\|\boldsymbol{x}-\boldsymbol{x}_i\|_2}\right)e^{-\frac{\boldsymbol{y}^\top\hat{\boldsymbol{\alpha}}}{c}}}\\&e^{\imath Re\left(\overline{\theta_2}\frac{V_j(\boldsymbol{x},\boldsymbol{y};\boldsymbol{y}-\boldsymbol{q}(\boldsymbol{x}-\boldsymbol{x}_j))\varphi_j(\boldsymbol{x},\boldsymbol{y};\boldsymbol{x}-\boldsymbol{x}_j)}{\|\boldsymbol{x}-\boldsymbol{x}_j\|_2}\right)e^{-\frac{\boldsymbol{y}^\top\hat{\boldsymbol{\alpha}}}{c}}}\Big]-1d\boldsymbol{x}d\boldsymbol{y}.\end{aligned}$$

Then, by considering the conditional expectation given $V_i(\boldsymbol{x},\boldsymbol{y};\boldsymbol{y}-\boldsymbol{q}(\boldsymbol{x}-\boldsymbol{x}_i))$ and $V_j(\boldsymbol{x},\boldsymbol{y};\boldsymbol{y}-\boldsymbol{q}(\boldsymbol{x}-\boldsymbol{x}_j))$, we get

$$\begin{aligned}&\ln\phi_{h_i,h_j}(\theta_1,\theta_2)=\lambda\int_{\boldsymbol{x}\in\mathbb{R}^3}\int_{\boldsymbol{y}\in\mathbb{R}^M}\\&p(1,1;\boldsymbol{y}-\boldsymbol{q}(\boldsymbol{x}-\boldsymbol{x}_i),\boldsymbol{y}-\boldsymbol{q}(\boldsymbol{x}-\boldsymbol{x}_j))\\&\left(\mathbb{E}\left[e^{\imath Re\left(\overline{\theta_1}\frac{\varphi_i(\boldsymbol{x},\boldsymbol{y};\boldsymbol{x}-\boldsymbol{x}_i)}{\|\boldsymbol{x}-\boldsymbol{x}_i\|_2}+\overline{\theta_2}\frac{\varphi_j(\boldsymbol{x},\boldsymbol{y};\boldsymbol{x}-\boldsymbol{x}_j)}{\|\boldsymbol{x}-\boldsymbol{x}_j\|_2}\right)e^{-\frac{\boldsymbol{y}^\top\hat{\boldsymbol{\alpha}}}{c}}}\right]-1\right)\\&+p(1,0;\boldsymbol{y}-\boldsymbol{q}(\boldsymbol{x}-\boldsymbol{x}_i),\boldsymbol{y}-\boldsymbol{q}(\boldsymbol{x}-\boldsymbol{x}_j))\\&\left(\mathbb{E}\left[e^{\imath Re\left(\overline{\theta_1}\frac{\varphi_i(\boldsymbol{x},\boldsymbol{y};\boldsymbol{x}-\boldsymbol{x}_i)}{\|\boldsymbol{x}-\boldsymbol{x}_i\|_2}\right)e^{-\frac{\boldsymbol{y}^\top\hat{\boldsymbol{\alpha}}}{c}}}\right]-1\right)\\&+p(0,1;\boldsymbol{y}-\boldsymbol{q}(\boldsymbol{x}-\boldsymbol{x}_i),\boldsymbol{y}-\boldsymbol{q}(\boldsymbol{x}-\boldsymbol{x}_j))\\&\left(\mathbb{E}\left[e^{\imath Re\left(\overline{\theta_2}\frac{\varphi_j(\boldsymbol{x},\boldsymbol{y};\boldsymbol{x}-\boldsymbol{x}_j)}{\|\boldsymbol{x}-\boldsymbol{x}_j\|_2}\right)e^{-\frac{\boldsymbol{y}^\top\hat{\boldsymbol{\alpha}}}{c}}}\right]-1\right)d\boldsymbol{x}d\boldsymbol{y},\end{aligned}$$

where the mathematical expectation is now w.r.t. the random fields φ_i and φ_j only, which finally proves (80). □

Note that Proposition 7 provides a straightforward proof for Proposition 1 in [13]. Indeed, equation (8) in [13] can be proved by applying Proposition 7 to $\theta_1 = \theta$, $\theta_2 = 0$, $\widehat{\boldsymbol{\alpha}} = \mathbf{0}$, $\boldsymbol{x}_i = \mathbf{0}$, and $\forall \boldsymbol{x}, \boldsymbol{y} \in \mathbb{R}^3 \times \mathbb{R}^M$, $\varphi_i(\boldsymbol{x}, \boldsymbol{y}; \boldsymbol{r}) = \|\boldsymbol{r}\|_2 \psi(\boldsymbol{r}) \in L^\infty(\mathbb{R}^3 \times \mathbb{R}^M \times \mathbb{R}^3)$ since $\psi \in L^\infty(\mathbb{R}^3)$ has compact support.

APPENDIX B
GEOMETRY WITH TWO MICROPHONES

B.1. Computation of integrals over space

We consider two sensor locations $\boldsymbol{x}_i$, $\boldsymbol{x}_j \in \mathbb{R}^3$ and $D = \|\boldsymbol{x}_i - \boldsymbol{x}_j\|_2$. In Appendices E to G, we will need to compute several integrals of the form:

$$J_\xi = \int_{\boldsymbol{x} \in \mathbb{R}^3} \frac{\xi(\boldsymbol{x}-\boldsymbol{x}_i, \boldsymbol{x}-\boldsymbol{x}_j)}{\|\boldsymbol{x}-\boldsymbol{x}_i\|_2 \|\boldsymbol{x}-\boldsymbol{x}_j\|_2} d\boldsymbol{x}, \tag{85}$$

where $\boldsymbol{x} \mapsto \xi(\boldsymbol{x} - \boldsymbol{x}_i, \boldsymbol{x} - \boldsymbol{x}_j) \in L^1(\mathbb{R}^3) \cap L^\infty(\mathbb{R}^3)$.

In the particular case $i = j$, let $\boldsymbol{r} = \boldsymbol{x} - \boldsymbol{x}_i$ and

$$J_\xi = \int_{\boldsymbol{r} \in \mathbb{R}^3} \frac{\xi(\boldsymbol{r})}{\|\boldsymbol{r}\|_2^2} d\boldsymbol{r}, \tag{86}$$

where $\xi \in L^1(\mathbb{R}^3) \cap L^\infty(\mathbb{R}^3)$.

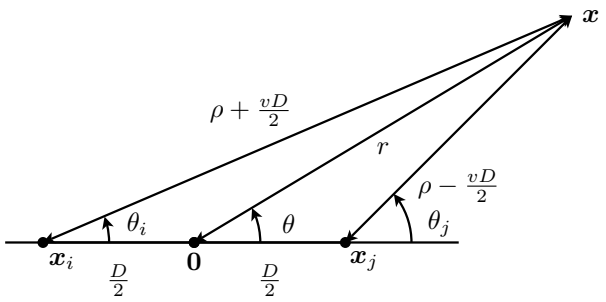

Fig. 24. Geometry with two microphones at $\boldsymbol{x}_i$, $\boldsymbol{x}_j$ and a source image at $\boldsymbol{x}$.

To compute such integrals, we will use the spherical coordinates (θ, φ, r), as illustrated in Fig. 24, where $\theta = 0$ corresponds to the direction of vector $\boldsymbol{x}_j - \boldsymbol{x}_i$, and the origin of the coordinates is the middle of the line segment $[\boldsymbol{x}_i,\ \boldsymbol{x}_j]$ (so that $\frac{\boldsymbol{x}_i + \boldsymbol{x}_j}{2} = \mathbf{0}$ as represented in Fig. 24). We thus get $\boldsymbol{x} = [r\sin(\theta)\cos(\varphi), r\sin(\theta)\sin(\varphi), r\cos(\theta)]^\top$ and $d\boldsymbol{x} = r^2 dr \sin(\theta) d\theta d\varphi$, with $r \in \mathbb{R}_+$, $\theta \in [0, \pi]$ and $\varphi \in [0, 2\pi]$. Moreover, as can be deduced from Fig. 24,

- $\|\boldsymbol{x} - \boldsymbol{x}_i\|_2 = \sqrt{r^2 + \frac{D^2}{4} + rD\cos(\theta)}$,
- $\|\boldsymbol{x} - \boldsymbol{x}_j\|_2 = \sqrt{r^2 + \frac{D^2}{4} - rD\cos(\theta)}$,
- $\theta_i = \operatorname{acos}\left(\frac{r\cos(\theta) + D/2}{\sqrt{r^2 + \frac{D^2}{4} + rD\cos(\theta)}}\right)$,
- $\theta_j = \operatorname{acos}\left(\frac{r\cos(\theta) - D/2}{\sqrt{r^2 + \frac{D^2}{4} - rD\cos(\theta)}}\right)$.

By substitution into (85), we get

$$J_\xi = \int_{r=0}^{+\infty} \int_{\theta=0}^{\pi} \int_{\varphi=0}^{2\pi} \frac{\xi\left(\theta_i, \varphi, \sqrt{r^2 + \frac{D^2}{4} + rD\cos(\theta)}, \theta_j, \varphi, \sqrt{r^2 + \frac{D^2}{4} - rD\cos(\theta)}\right)}{\sqrt{r^2 + \frac{D^2}{4} + rD\cos(\theta)}\sqrt{r^2 + \frac{D^2}{4} - rD\cos(\theta)}} r^2 dr \sin(\theta) d\theta d\varphi. \tag{87}$$

Note that in (87), the two arguments of function ξ have been replaced by their spherical coordinates. In the rest of this research report, we will continue using this notation without any further notice, as long as it is not ambiguous.

Finally, we make a last change of variables, that is also illustrated in Fig. 24:

$$\begin{aligned} \rho &= \frac{\|\boldsymbol{x}-\boldsymbol{x}_i\|_2 + \|\boldsymbol{x}-\boldsymbol{x}_j\|_2}{2} = \frac{\sqrt{r^2 + \frac{D^2}{4} + rD\cos(\theta)} + \sqrt{r^2 + \frac{D^2}{4} - rD\cos(\theta)}}{2}, \\ v &= \frac{\|\boldsymbol{x}-\boldsymbol{x}_i\|_2 - \|\boldsymbol{x}-\boldsymbol{x}_j\|_2}{D} = \frac{\sqrt{r^2 + \frac{D^2}{4} + rD\cos(\theta)} - \sqrt{r^2 + \frac{D^2}{4} - rD\cos(\theta)}}{D}, \end{aligned} \tag{88}$$

which is such that $\rho \in \left[\frac{D}{2}, +\infty\right[$, $v \in [-1, 1]$, $\theta_i = \operatorname{acos}\left(\frac{2\rho v + D}{2\rho + vD}\right)$, $\theta_j = \operatorname{acos}\left(\frac{2\rho v - D}{2\rho - vD}\right)$, and

$$\frac{r^2 dr \sin(\theta) d\theta}{\sqrt{r^2 + \frac{D^2}{4} + rD\cos(\theta)}\sqrt{r^2 + \frac{D^2}{4} - rD\cos(\theta)}} = d\rho dv. \tag{89}$$

Indeed, we note that (88) implies that $r\cos(\theta) = \rho v$ and $r^2 = \rho^2 - (1 - v^2)\frac{D^2}{4}$, thus

$$\boldsymbol{x} = \begin{bmatrix} \sqrt{\rho^2 - \frac{D^2}{4}}\sqrt{1 - v^2}\cos(\varphi) \\ \sqrt{\rho^2 - \frac{D^2}{4}}\sqrt{1 - v^2}\sin(\varphi) \\ \rho v \end{bmatrix}, \tag{90}$$

and $d\boldsymbol{x} = \sqrt{\rho^2 - (\frac{vD}{2})^2} d\rho dv d\varphi$, which proves (89).

Therefore substituting (88) and (89) into (87) yields

$$J_\xi = \int_{\rho=\frac{D}{2}}^{+\infty} \int_{v=-1}^{1} \int_{\varphi=0}^{2\pi} \xi\left(\frac{2\rho v + D}{2\rho + vD}, \varphi, \rho + \frac{vD}{2}, \frac{2\rho v - D}{2\rho - vD}, \varphi, \rho - \frac{vD}{2}\right) d\rho dv d\varphi. \tag{91}$$

Again, note that compared with (87), in (91) the angles θ_i and θ_j have been replaced by their cosine. In the rest of this research report, we will continue using this notation without any further notice, as long as it is not ambiguous since $\theta_i, \theta_j \in [0, \pi]$ and the cosine function takes values in $[-1, 1]$.

Finally, in the particular case $i = j$ (*i.e.* $D = 0$), (91) shows that (86) is equivalent to

$$J_\xi = \int_{r=0}^{+\infty} \int_{v=-1}^{1} \int_{\varphi=0}^{2\pi} \xi(v, \varphi, r)\, dr dv d\varphi. \tag{92}$$

B.2. Differentiation of function $\boldsymbol{q}(.)$ on $\mathcal{S}^2$

In Appendix G, we will need to express the quantity $\beta\left(\boldsymbol{q}(v,\varphi)\, vD + \frac{\partial \boldsymbol{q}(v,\varphi)}{\partial v}(1 - v^2)D\right)$ as a function of $\boldsymbol{u} \triangleq \frac{\boldsymbol{x}}{\|\boldsymbol{x}\|_2} \in \mathcal{S}^2$ when $\rho \to +\infty$ (which is equivalent to $r \to +\infty$), where $\boldsymbol{q}(v, \varphi)$ denotes $\boldsymbol{q}(\boldsymbol{u})$. To that end, we first note that (90) implies $\boldsymbol{x}^\top(\boldsymbol{x}_j - \boldsymbol{x}_i) = \rho v D$, therefore

$$vD = \boldsymbol{u}^\top(\boldsymbol{x}_j - \boldsymbol{x}_i)\left(1 + O(\tfrac{D^2}{\rho^2})\right). \tag{93}$$

Moreover, $\forall \boldsymbol{x} \in \mathbb{R}^3$, $\frac{\partial \boldsymbol{q}}{\partial v}(\boldsymbol{x}) = \mathbf{J}_{\boldsymbol{q}}(\boldsymbol{x}) \frac{\partial \boldsymbol{x}}{\partial v}$, where $\mathbf{J}_{\boldsymbol{q}}(\boldsymbol{x})$ denotes the Jacobian matrix of function $\boldsymbol{q}(.)$ at $\boldsymbol{x} \in \mathbb{R}^3$, and (90) implies

$$\frac{\partial \boldsymbol{x}}{\partial v} = \begin{bmatrix} -\sqrt{\rho^2 - \frac{D^2}{4}} \frac{v}{\sqrt{1-v^2}} \cos(\varphi) \\ -\sqrt{\rho^2 - \frac{D^2}{4}} \frac{v}{\sqrt{1-v^2}} \sin(\varphi) \\ \rho \end{bmatrix}. \tag{94}$$

However, by noting that function $\boldsymbol{q}(.)$ is 1-homogeneous, we have $\mathbf{J}_{\boldsymbol{q}}(\boldsymbol{x}) = \mathbf{J}_{\boldsymbol{q}}(\boldsymbol{u})$, since $\mathbf{J}_{\boldsymbol{q}}(\boldsymbol{x})$ does not depend on $\|\boldsymbol{x}\|_2$. Therefore we can write

$$\tfrac{\partial \boldsymbol{q}}{\partial v}(\boldsymbol{x}) = \mathbf{J}_{\boldsymbol{q}}(\boldsymbol{u}) \tfrac{\partial \boldsymbol{x}}{\partial v}. \tag{95}$$

We note that (90) and (94) imply

$$\frac{1}{\rho}\left((1-v^2)D\frac{\partial \boldsymbol{x}}{\partial v} + vD\boldsymbol{x}\right) = \begin{bmatrix} 0 \\ 0 \\ D \end{bmatrix} = \boldsymbol{x}_j - \boldsymbol{x}_i.$$

Substituting (93) into this last equation, we get

$$\frac{1}{\rho}(1-v^2)D\frac{\partial \boldsymbol{x}}{\partial v} = \left(\boldsymbol{I} - \boldsymbol{u}\boldsymbol{u}^\top\right)(\boldsymbol{x}_j - \boldsymbol{x}_i) + O(\tfrac{D^3}{\rho^2}). \tag{96}$$

By multiplying (95) with $\frac{1}{\rho}(1-v^2)D$, and by substituting (96), we get

$$\tfrac{1}{\rho}\tfrac{\partial \boldsymbol{q}}{\partial v}(\boldsymbol{x})(1-v^2)D = \mathbf{J}_{\boldsymbol{q}}(\boldsymbol{u})\left(\boldsymbol{I} - \boldsymbol{u}\boldsymbol{u}^\top\right)(\boldsymbol{x}_j - \boldsymbol{x}_i) + O(\tfrac{D^3}{\rho^2}).$$

Since function $\boldsymbol{q}(.)$ is 1-homogeneous, we note that $\frac{1}{\rho}\frac{\partial \boldsymbol{q}}{\partial v}(\boldsymbol{x}) = \frac{\partial \boldsymbol{q}}{\partial v}(\boldsymbol{u}) + O(\frac{D^2}{\rho^2})$, therefore we end up with

$$\tfrac{\partial \boldsymbol{q}}{\partial v}(\boldsymbol{u})(1-v^2)D = \mathring{\mathbf{J}}_{\boldsymbol{q}}(\boldsymbol{u})(\boldsymbol{x}_j - \boldsymbol{x}_i) + O(\tfrac{D^3}{\rho^2}),$$

where matrix $\mathring{\mathbf{J}}_{\boldsymbol{q}}(\boldsymbol{u})$ is defined in (48). Finally, this last equation and (93) yield

$$\begin{aligned} &\boldsymbol{q}(v,\varphi)\, vD + \tfrac{\partial \boldsymbol{q}}{\partial v}(v,\varphi)\,(1-v^2)D \\ &= \left(\boldsymbol{q}(\boldsymbol{u})\boldsymbol{u}^\top + \mathring{\mathbf{J}}_{\boldsymbol{q}}(\boldsymbol{u})\right)(\boldsymbol{x}_j - \boldsymbol{x}_i) + O(\tfrac{D^3}{\rho^2}). \end{aligned} \tag{97}$$

Since function $\beta(.)$ is continuous and differentiable almost everywhere in $\mathbb{R}^M$, and all its partial derivatives belong to $L^\infty(\mathbb{R}^M)$ as shown in Lemma 2, then (97) implies

$$\begin{aligned} &\beta\left(\boldsymbol{q}(v,\varphi)\, vD + \tfrac{\partial \boldsymbol{q}}{\partial v}(v,\varphi)\,(1-v^2)D\right) \\ &= \beta\left(\left(\boldsymbol{q}(\boldsymbol{u})\boldsymbol{u}^\top + \mathring{\mathbf{J}}_{\boldsymbol{q}}(\boldsymbol{u})\right)(\boldsymbol{x}_j - \boldsymbol{x}_i)\right) + O(\tfrac{D^2}{\rho^2}). \end{aligned} \tag{98}$$

Appendix C
Asymptotic expansion

Proposition 8. *Considering the stochastic reverberation model in Definition 1, suppose that the attenuation function* $\widehat{\alpha}(.)$ *defined in* (7) *is regular (*cf. *Definition 7). Let* $\forall x \in \mathbb{R}$,

$$I(x) = \int_{\boldsymbol{u} \in \mathcal{S}^2} \psi(\boldsymbol{u}) e^{-\widehat{\alpha}(\boldsymbol{u})x} d\boldsymbol{u}, \tag{99}$$

where ψ *is a continuous function on* $\mathcal{S}^2$. *Then when* $x \to +\infty$,

$$I(x) = \frac{e^{-\widehat{\alpha}^{\inf} x}}{x}\left(\sum_{k \in \mathcal{K}} \frac{2\pi\psi(\boldsymbol{u}_k)}{\sqrt{\ddot{\widehat{\alpha}}_k}} + o(1)\right). \tag{100}$$

In addition, if ψ *is differentiable almost everywhere on* $\mathcal{S}^2$, *and all its partial derivatives belong to* $L^\infty(\mathcal{S}^2)$, *then*

$$I(x) = \frac{e^{-\widehat{\alpha}^{\inf} x}}{x}\left(\sum_{k \in \mathcal{K}} \frac{2\pi\psi(\boldsymbol{u}_k)}{\sqrt{\ddot{\widehat{\alpha}}_k}} + O\left(\frac{1}{\sqrt{x}}\right)\right). \tag{101}$$

Finally, if ψ *is twice (or more) continuously differentiable, then*

$$I(x) = \frac{e^{-\widehat{\alpha}^{\inf} x}}{x}\left(\sum_{k \in \mathcal{K}} \frac{2\pi\psi(\boldsymbol{u}_k)}{\sqrt{\ddot{\widehat{\alpha}}_k}} + O\left(\frac{1}{x}\right)\right). \tag{102}$$

Proof. Since vectors $\{\boldsymbol{u}_k\}_{k \in \mathcal{K}}$ are distinct, let $\{\mathcal{S}_k^2\}_{k \in \mathcal{K}}$ be a partition of $\mathcal{S}^2$, such that every $\boldsymbol{u}_k$ is in the interior of $\mathcal{S}_k^2$. Then $I(x) = \sum_{k \in \mathcal{K}} I_k(x)$, where

$$I_k(x) = \int_{\boldsymbol{u} \in \mathcal{S}_k^2} \psi(\boldsymbol{u}) e^{-\widehat{\alpha}(\boldsymbol{u})x} d\boldsymbol{u}. \tag{103}$$

Since $\boldsymbol{u}_k$ is the unique global minimum of the four times continuously differentiable function $\hat{\alpha}(.)$ in the two-dimensional (2D) Riemannian manifold $\mathcal{S}_k^2$, the following second order expansion holds:

$$\widehat{\alpha}(\boldsymbol{u}) = \widehat{\alpha}^{\inf} + (\boldsymbol{u} - \boldsymbol{u}_k)^\top \frac{\ddot{\boldsymbol{A}}_k}{2}(\boldsymbol{u} - \boldsymbol{u}_k) + O(\|\boldsymbol{u} - \boldsymbol{u}_k\|_2^3), \tag{104}$$

where the 3×3 Hessian matrix $\ddot{\boldsymbol{A}}_k$ has rank 2 (with two positive eigenvalues and one zero eigenvalue), and $\mathrm{span}(\ddot{\boldsymbol{A}}_k) = \mathrm{span}(\boldsymbol{u}_k)^\perp$ is the tangent space of the Riemannian manifold $\mathcal{S}^2$ at point $\boldsymbol{u}_k$. By substituting (104) into (103), we get

$$I_k(x) = \int_{\boldsymbol{u} \in \mathcal{S}_k^2} \psi(\boldsymbol{u}) e^{-\left(\widehat{\alpha}^{\inf} + (\boldsymbol{u} - \boldsymbol{u}_k)^\top \frac{\ddot{\boldsymbol{A}}_k}{2}(\boldsymbol{u} - \boldsymbol{u}_k) + O(\|\boldsymbol{u} - \boldsymbol{u}_k\|_2^3)\right)x} d\boldsymbol{u}.$$

With the change of variable $\boldsymbol{v} = \sqrt{x}(\boldsymbol{u} - \boldsymbol{u}_k)$, the surface element becomes $d\boldsymbol{v} = x\, d\boldsymbol{u}$, thus

$$I_k(x) = \frac{e^{-\widehat{\alpha}^{\inf} x}}{x} \int_{\boldsymbol{v} \in \sqrt{x}(\mathcal{S}_k^2 - \boldsymbol{u}_k)} \psi(\boldsymbol{u}_k + \tfrac{\boldsymbol{v}}{\sqrt{x}}) e^{-\boldsymbol{v}^\top \frac{\ddot{\boldsymbol{A}}_k}{2}\boldsymbol{v} + O\left(\frac{\|\boldsymbol{v}\|_2^3}{\sqrt{x}}\right)} d\boldsymbol{v}. \tag{105}$$

If ψ is continuous, when $x \to +\infty$, since $\mathrm{span}(\boldsymbol{u}_k)^\perp = \mathrm{span}(\ddot{\boldsymbol{A}}_k)$, we get the asymptotic form

$$\begin{aligned} I_k(x) &= \frac{e^{-\widehat{\alpha}^{\inf} x}}{x}\left(\psi(\boldsymbol{u}_k) \int_{\boldsymbol{v} \in \mathrm{span}(\ddot{\boldsymbol{A}}_k)} e^{-\boldsymbol{v}^\top \frac{\ddot{\boldsymbol{A}}_k}{2}\boldsymbol{v}} d\boldsymbol{v} + o(1)\right) \\ &= \frac{e^{-\widehat{\alpha}^{\inf} x}}{x}\left(\psi(\boldsymbol{u}_k)\frac{2\pi}{\sqrt{\ddot{\widehat{\alpha}}_k}} + o(1)\right), \end{aligned} \tag{106}$$

where $\ddot{\widehat{\alpha}}_k > 0$ is the Hessian of function $\widehat{\alpha}(.)$ at $\boldsymbol{u}_k$, *i.e.* the product of the two positive eigenvalues of the Hessian matrix $\ddot{\boldsymbol{A}}_k$.

In addition, if ψ is differentiable almost everywhere on $\mathcal{S}^2$, and all its partial derivatives belong to $L^\infty(\mathcal{S}^2)$, then the next term in the Taylor series expansion of $\psi(\boldsymbol{u}_k +$

$\frac{\boldsymbol{v}}{\sqrt{x}}$)$e^{-\boldsymbol{v}^\top \frac{\ddot{\boldsymbol{A}}_k}{2}\boldsymbol{v}+O\left(\frac{\|\boldsymbol{v}\|_2^3}{\sqrt{x}}\right)}$ in (105) is of order $\frac{1}{\sqrt{x}}$. By integrating over $\mathrm{span}(\ddot{\boldsymbol{A}}_k)$, we get

$$I_k(x) = \frac{e^{-\widehat{\alpha}^{\inf}x}}{x}\left(\psi(\boldsymbol{u}_k)\frac{2\pi}{\sqrt{\ddot{\widehat{\alpha}}_k}} + O(\tfrac{1}{\sqrt{x}})\right). \tag{107}$$

Finally, if ψ is twice (or more) continuously differentiable, then the term of order $\frac{1}{\sqrt{x}}$ in the Taylor series expansion of $\psi(\boldsymbol{u}_k + \frac{\boldsymbol{v}}{\sqrt{x}})e^{-\boldsymbol{v}^\top \frac{\ddot{\boldsymbol{A}}_k}{2}\boldsymbol{v}+O\left(\frac{\|\boldsymbol{v}\|_2^3}{\sqrt{x}}\right)}$ in (105) is odd w.r.t. $\boldsymbol{v}$, thus its integral over $\mathrm{span}(\ddot{\boldsymbol{A}}_k)$ is zero. The following term is of order $\frac{1}{x}$, and since it is even w.r.t. $\boldsymbol{v}$, its integral over $\mathrm{span}(\ddot{\boldsymbol{A}}_k)$ is not zero in general. Therefore we can write

$$I_k(x) = \frac{e^{-\widehat{\alpha}^{\inf}x}}{x}\left(\psi(\boldsymbol{u}_k)\frac{2\pi}{\sqrt{\ddot{\widehat{\alpha}}_k}} + O(\tfrac{1}{x})\right). \tag{108}$$

By summing (106) (resp. (107) and (108)) for all $k \in \mathcal{K}$, we finally get (100) (resp. (101) and (102)). □

APPENDIX D
PROPERTIES OF PROBABILITY DISTRIBUTION p

Lemma 5. *Let $p(b, \boldsymbol{z})$ (where $b \in \{0,1\}$ and $\boldsymbol{z} \in \mathbb{R}^M$) and $p(b_i, b_j, \boldsymbol{z}_i, \boldsymbol{z}_j)$ (where $b_i, b_j \in \{0,1\}$ and $\boldsymbol{z}_i, \boldsymbol{z}_j \in \mathbb{R}^M$) be the probability distributions introduced in Definition 1. Then function $(\boldsymbol{z}_1, \boldsymbol{z}_2) \mapsto p(1,1;\boldsymbol{z}_1,\boldsymbol{z}_2)$ is not differentiable at any point $(\boldsymbol{z},\boldsymbol{z})$ such that $\nabla p(1;\boldsymbol{z}) \neq \boldsymbol{0}$.*

Proof. First, since $V_i(\boldsymbol{x},\boldsymbol{y};\boldsymbol{z}_i)$ and $V_j(\boldsymbol{x},\boldsymbol{y};\boldsymbol{z}_j)$ are Booleans,

$$V_i(\boldsymbol{x},\boldsymbol{y};\boldsymbol{z}_i)V_j(\boldsymbol{x},\boldsymbol{y};\boldsymbol{z}_j) \leq \min\left(V_i(\boldsymbol{x},\boldsymbol{y};\boldsymbol{z}_i), V_j(\boldsymbol{x},\boldsymbol{y};\boldsymbol{z}_j)\right).$$

By applying the mathematical expectation to both members of this inequality, we get

$$p(1,1;\boldsymbol{z}_i,\boldsymbol{z}_j) \leq \min\left(p(1;\boldsymbol{z}_i), p(1;\boldsymbol{z}_j)\right). \tag{109}$$

In other respects, since function $\boldsymbol{z} \mapsto p(1;\boldsymbol{z})$ is continuously differentiable and it is not constant, then there is $\boldsymbol{z} \in \mathbb{R}^M$ such that $\boldsymbol{h} \triangleq \nabla p(1;\boldsymbol{z}) \neq \boldsymbol{0}$. Then $\forall t > 0$, since we have both (9) and $p(1,1;\boldsymbol{z}_i,\boldsymbol{z}_j) \leq p(1;\boldsymbol{z}_j)$, we get

$$\tfrac{p(1,1;\boldsymbol{z}+t\boldsymbol{h},\boldsymbol{z}-t\boldsymbol{h})-p(1,1;\boldsymbol{z},\boldsymbol{z})}{t} \leq \tfrac{p(1;\boldsymbol{z}-t\boldsymbol{h})-p(1;\boldsymbol{z})}{t}.$$

Therefore

$$\limsup_{t\to 0, t>0} \tfrac{p(1,1;\boldsymbol{z}+t\boldsymbol{h},\boldsymbol{z}-t\boldsymbol{h})-p(1,1;\boldsymbol{z},\boldsymbol{z})}{t} \leq -\boldsymbol{h}^\top \nabla p(1;\boldsymbol{z}) = -\|\boldsymbol{h}\|_2^2.$$

In the same way, $\forall t < 0$, since we have both (9) and $p(1,1;\boldsymbol{z}_i,\boldsymbol{z}_j) \leq p(1;\boldsymbol{z}_i)$, we get

$$\tfrac{p(1,1;\boldsymbol{z}+t\boldsymbol{h},\boldsymbol{z}-t\boldsymbol{h})-p(1,1;\boldsymbol{z},\boldsymbol{z})}{t} \geq \tfrac{p(1;\boldsymbol{z}+t\boldsymbol{h})-p(1;\boldsymbol{z})}{t}.$$

Therefore

$$\liminf_{t\to 0, t<0} \tfrac{p(1,1;\boldsymbol{z}+t\boldsymbol{h},\boldsymbol{z}-t\boldsymbol{h})-p(1,1;\boldsymbol{z},\boldsymbol{z})}{t} \geq \boldsymbol{h}^\top \nabla p(1;\boldsymbol{z}) = \|\boldsymbol{h}\|_2^2.$$

Consequently, the limit of $\frac{p(1,1;\boldsymbol{z}+t\boldsymbol{h},\boldsymbol{z}-t\boldsymbol{h})-p(1,1;\boldsymbol{z},\boldsymbol{z})}{t}$ when $t \to 0$ and $t \in \mathbb{R}$ does not exist, thus function $(\boldsymbol{z}_1,\boldsymbol{z}_2) \mapsto p(1,1;\boldsymbol{z}_1,\boldsymbol{z}_2)$ is not differentiable at $(\boldsymbol{z},\boldsymbol{z})$. □

Nevertheless, it is still possible to assume that function $(\boldsymbol{z}_1,\boldsymbol{z}_2) \mapsto p(1,1;\boldsymbol{z}_1,\boldsymbol{z}_2)$ is continuous and differentiable almost everywhere in $\mathbb{R}^M \times \mathbb{R}^M$, and that all its partial derivatives belong to $L^\infty(\mathbb{R}^M \times \mathbb{R}^M)$, as we did in Definition 1.

Proof of Lemma 1. We have assumed in Definition 1 that the support of $\boldsymbol{z} \mapsto p(1;\boldsymbol{z})$ is left-bounded, *i.e.* $\forall m \in \{1 \dots M\}$, $\exists z_m^{\inf} < 0$ such that $\forall \boldsymbol{z} \in \mathbb{R}^M$, if $\exists m \in \{1 \dots M\}$ such that $z_m < z_m^{\inf}$, then $p(1;\boldsymbol{z}) = 0$. Since $\forall \boldsymbol{z} \in \mathbb{R}^M$, $p(1;\boldsymbol{z}) \in [0,1]$, (13) implies the majoration $\forall n \in \mathbb{N}\backslash\{0\}$,

$$\begin{aligned}\beta_n \leq & \int_{\boldsymbol{z}\geq \boldsymbol{z}^{\inf}} e^{-n\frac{\boldsymbol{z}^\top \widehat{\boldsymbol{\alpha}}}{c}} d\boldsymbol{z} \\ = & \frac{c^M}{\prod_{m=1}^M \widehat{\alpha}_m} \frac{e^{n\frac{|\boldsymbol{z}^{\inf}|^\top \widehat{\boldsymbol{\alpha}}}{c}}}{n^M} \\ = & O\left(\frac{e^{n\frac{|\boldsymbol{z}^{\inf}|^\top \widehat{\boldsymbol{\alpha}}}{c}}}{n^M}\right),\end{aligned}$$

where symbol $\geq$ between two vectors is applied entrywise.

Moreover, $\beta_n > 0$ in (13) because function $\boldsymbol{z} \mapsto p(1;\boldsymbol{z})$ is continuous, nonnegative, and not identically zero. □

Proof of Lemma 2. First, function $\boldsymbol{e} \mapsto \beta(\boldsymbol{e})$ is even because function $(\boldsymbol{z},\boldsymbol{z}') \mapsto p(1,1;\boldsymbol{z},\boldsymbol{z}')$ is symmetric, since in Definition 1, p is invariant under a permutation of the two sensors i and j.

Moreover, we have assumed in Definition 1 that the support of $\boldsymbol{z} \mapsto p(1;\boldsymbol{z})$ is left-bounded, *i.e.* $\forall m \in \{1 \dots M\}$, $\exists z_m^{\inf} < 0$ such that $\forall \boldsymbol{z} \in \mathbb{R}^M$, if $\exists m \in \{1 \dots M\}$ such that $z_m < z_m^{\inf}$, then $p(1;\boldsymbol{z}) = 0$. Consequently, $(\boldsymbol{z},\boldsymbol{z}') \mapsto p(1,1;\boldsymbol{z},\boldsymbol{z}')$ is also left-bounded: $\forall \boldsymbol{z},\boldsymbol{z}' \in \mathbb{R}^M$, if $\exists m \in \{1 \dots M\}$ such that $z_m < z_m^{\inf}$ or $z'_m < z_m^{\inf}$, then $p(1,1;\boldsymbol{z},\boldsymbol{z}') = 0$. Therefore $\forall \boldsymbol{z} \in \mathbb{R}^M$, if $\exists m \in \{1 \dots M\}$ such that $z_m < z_m^{\inf}$, then $\forall \boldsymbol{e} \in \mathbb{R}^M$, $p(1,1;\boldsymbol{z}-\frac{\boldsymbol{e}}{2},\boldsymbol{z}+\frac{\boldsymbol{e}}{2}) = 0$. Finally, function $(\boldsymbol{e},\boldsymbol{z}) \mapsto p(1,1;\boldsymbol{z}-\frac{\boldsymbol{e}}{2},\boldsymbol{z}+\frac{\boldsymbol{e}}{2})e^{-\frac{2\boldsymbol{z}^\top \widehat{\boldsymbol{\alpha}}}{c}}$ is continuous w.r.t. $\boldsymbol{e}$, and it is dominated by the integrable function $\boldsymbol{z} \mapsto e^{-\frac{2\boldsymbol{z}^\top \widehat{\boldsymbol{\alpha}}}{c}} \prod_{m=1}^M \mathbf{1}_{[z_m^{\inf},+\infty[}(z_m)$. Therefore the theorem of continuity under the integral sign proves that function $\boldsymbol{e} \mapsto \beta(\boldsymbol{e})$ defined in (17) is continuous on $\mathbb{R}^M$. In the same way, function $(\boldsymbol{e},\boldsymbol{z}) \mapsto p(1,1;\boldsymbol{z}-\frac{\boldsymbol{e}}{2},\boldsymbol{z}+\frac{\boldsymbol{e}}{2})e^{-\frac{2\boldsymbol{z}^\top \widehat{\boldsymbol{\alpha}}}{c}}$ is differentiable w.r.t. $\boldsymbol{e}$ almost everywhere in $\mathbb{R}^M$, and all its partial derivatives w.r.t. $\boldsymbol{e}$ are dominated by a constant multiplied by the integrable function $\boldsymbol{z} \mapsto e^{-\frac{2\boldsymbol{z}^\top \widehat{\boldsymbol{\alpha}}}{c}} \prod_{m=1}^M \mathbf{1}_{[z_m^{\inf},+\infty[}(z_m)$. Therefore the theorem of differentiability under the integral sign proves that function $\boldsymbol{e} \mapsto \beta(\boldsymbol{e})$ defined in (17) is differentiable almost everywhere in $\mathbb{R}^M$, and all its partial derivatives belong to $L^\infty(\mathbb{R}^M)$.

Besides, applying (17) to $\boldsymbol{e} = \boldsymbol{0}$ and substituting (9) yields $\beta(\boldsymbol{0}) = \beta_2$, with β_2 defined in (13) for $n = 2$.

With the change of variables $\boldsymbol{z} = \frac{\boldsymbol{z}_i+\boldsymbol{z}_j}{2}$ and $\boldsymbol{e} = \boldsymbol{z}_j - \boldsymbol{z}_i$, which is such that $d\boldsymbol{z}d\boldsymbol{e} = d\boldsymbol{z}_i d\boldsymbol{z}_j$, by multiplying both members of (109) with $e^{-\frac{2\boldsymbol{z}^\top \widehat{\boldsymbol{\alpha}}}{c}}$, integrating over $\boldsymbol{z}$, and substituting (17) and (13) for $n = 2$, we get (18). Since $\boldsymbol{z}_i, \boldsymbol{z}_j$ can take any value in $\mathbb{R}^M$, (18) holds $\forall \boldsymbol{e} \in \mathbb{R}^M$. In particular, function $\boldsymbol{e} \mapsto \beta(\boldsymbol{e})$ is not differentiable at $\boldsymbol{e} = 0$ (otherwise, with $\boldsymbol{e} = \boldsymbol{q}c\tau$ and $\tau \in \mathbb{R}$, we would have $\lim_{\tau\to 0,\tau>0} \frac{\beta(\boldsymbol{q}c\tau)-\beta(\boldsymbol{0})}{\tau} \leq -\beta_2\widehat{\alpha}^{\inf}$ and $\lim_{\tau\to 0,\tau<0} \frac{\beta(\boldsymbol{q}c\tau)-\beta(\boldsymbol{0})}{\tau} \geq +\beta_2\widehat{\alpha}^{\inf}$, so the two limits cannot be equal). □

APPENDIX E
FIRST ORDER MOMENTS

Proof of Proposition 1.
Temporal domain: Substituting (60) and (63) into (62) yields

$$\mathbb{E}[h_i(t)] = \lambda\beta_1 \int_{\boldsymbol{r}\in\mathbb{R}^3} \frac{g_i\left(\frac{\boldsymbol{r}}{\|\boldsymbol{r}\|_2},.\right) \overset{t}{*} m_s(\frac{\boldsymbol{r}}{\|\boldsymbol{r}\|_2}, t-\frac{\|\boldsymbol{r}\|_2}{c}) e^{-\frac{\widehat{\alpha}(\boldsymbol{r})}{c}}}{\|\boldsymbol{r}\|_2} d\boldsymbol{r}$$

where function $\widehat{\alpha}(.)$ and β_1 are defined in (7) and (13) for $n=1$, and $\forall \boldsymbol{u}\in\mathcal{S}^2$, $\forall t\in\mathbb{R}$, $\forall(\boldsymbol{x},\boldsymbol{y})\in\mathbb{R}^3\times\mathbb{R}^M$,

$$m_s(\boldsymbol{u},t) = \mathbb{E}\left[s\left(\Theta(\boldsymbol{x},\boldsymbol{y})\boldsymbol{u},t\right)\right].$$

Besides, $\mathbb{E}[h_i(t)] = \lambda\beta_1 J_\xi$ where J_ξ is defined in (86) and

$$\xi(\boldsymbol{r}) = \|\boldsymbol{r}\|_2\, g_i\left(\frac{\boldsymbol{r}}{\|\boldsymbol{r}\|_2},.\right) \overset{t}{*} m_s(\frac{\boldsymbol{r}}{\|\boldsymbol{r}\|_2}, t-\frac{\|\boldsymbol{r}\|_2}{c})\, e^{-\frac{\widehat{\alpha}(\boldsymbol{r})}{c}}$$

belongs to $L^1(\mathbb{R}^3)\cap L^\infty(\mathbb{R}^3)$. Thus (92) yields

$$\begin{aligned}&\mathbb{E}[h_i(t)] = \lambda\beta_1 \int_{r=0}^{+\infty}\int_{v=-1}^{1}\int_{\varphi=0}^{2\pi}\\ &g_i\left(v,\varphi,.\right) \overset{t}{*} m_s(v,\varphi,t-\tfrac{r}{c}) e^{-\widehat{\alpha}(v,\varphi)\frac{r}{c}} r dr dv d\varphi.\end{aligned}$$

Let $m_{g_i'*s'}(v,\varphi,.) = \left(g_i(v,\varphi,.) \overset{t}{*} m_s(v,\varphi,.)\right) e^{\widehat{\alpha}(v,\varphi)t} = g_i'(v,\varphi,.) \overset{t}{*} m_s'(v,\varphi,.)$ and let $T = T_g + T_s$.

With the change of variable $\tau = t - \frac{r}{c}$, which is such that $d\tau = \frac{dr}{c}$, we get $\forall t \geq T$,

$$\begin{aligned}&\mathbb{E}[h_i(t)] = \lambda c^2\beta_1 \int_{v=-1}^{1}\int_{\varphi=0}^{2\pi} e^{-\widehat{\alpha}(v,\varphi)t}\\ &\left(t\int_{\tau\in\mathbb{R}} m_{g_i'*s'}(v,\varphi,\tau)\, d\tau - \int_{\tau\in\mathbb{R}} m_{g_i'*s'}(v,\varphi,\tau)\,\tau d\tau\right) dv d\varphi\\ &= \lambda c^2\beta_1 \int_{v=-1}^{1}\int_{\varphi=0}^{2\pi} e^{-\widehat{\alpha}(v,\varphi)t}\\ &\left(t\,\widehat{m_{g_i'*s'}}(v,\varphi,0) - \tfrac{\imath}{2\pi}\frac{\partial \widehat{m_{g_i'*s'}}}{\partial f}(v,\varphi,0)\right) dv d\varphi,\end{aligned} \tag{110}$$

where $\widehat{m_{g_i'*s'}}(v,\varphi,f) = \widehat{g_i'}(v,\varphi,f)\, m_{\widehat{s'}}(v,\varphi,f)$ with $m_{\widehat{s'}}$ defined in (8). Note that we have proved in Section II that function $f\mapsto \widehat{g_i'}(\boldsymbol{u},f)$ is smooth. Moreover, $\forall\Theta(\boldsymbol{x},\boldsymbol{y})\in SO(3)$, $\forall\boldsymbol{u}\in\mathcal{S}^2$, $\forall q\in\mathbb{N}$, function $f\mapsto \widehat{s'}(\Theta(\boldsymbol{x},\boldsymbol{y})\boldsymbol{u},f)$ is q times continuously differentiable and $\frac{\partial^q \widehat{s'}(\Theta(\boldsymbol{x},\boldsymbol{y})\boldsymbol{u},f)}{\partial f^q}$ is dominated by $\|t^q s'(\boldsymbol{u},t)\|_1$. Since $SO(3)$ is a compact set, the differentiability under the integral sign theorem proves that function $f\mapsto m_{\widehat{s'}}(\boldsymbol{u},f)$ is smooth. Therefore functions $\widehat{m_{g_i'*s'}}(v,\varphi,f)$ and $\frac{\partial \widehat{m_{g_i'*s'}}}{\partial f}(v,\varphi,f)$ are well-defined.

Finally, both $\widehat{m_{g_i'*s'}}(v,\varphi,0) = 0$ and $\frac{\partial \widehat{m_{g_i'*s'}}}{\partial f}(v,\varphi,0) = 0$, since we have assumed in Definition 1 that at least one of the following properties holds $\forall\boldsymbol{u}\in\mathcal{S}^2$ at $f=0$:

- $\forall i\in\{1\dots I\}$, $\widehat{g_i'}(\boldsymbol{u},0)=0$ and $m_{\widehat{s'}}(\boldsymbol{u},0)=0$;
- $\forall i\in\{1\dots I\}$, $\widehat{g_i'}(\boldsymbol{u},0)=0$ and $\frac{\partial g_i'}{\partial f}(\boldsymbol{u},0)=0$;
- $m_{\widehat{s'}}(\boldsymbol{u},0)=0$ and $\frac{\partial m_{\widehat{s'}}}{\partial f}(\boldsymbol{u},0)=0$.

Therefore (110) proves that $\forall t\geq T$, $\mathbb{E}[h_i(t)]=0$.

Spectral domain: First, $\forall\Theta(\boldsymbol{x},\boldsymbol{y})\in SO(3)$, $\forall f\in\mathbb{R}$, function $\boldsymbol{u}\mapsto \widehat{s}(\Theta(\boldsymbol{x},\boldsymbol{y})\boldsymbol{u},f)$ is twice continuously differentiable, and all its second order derivatives are bounded on $\mathcal{S}^2$. Since $SO(3)$ is a compact set, the differentiability under the integral sign theorem proves that function $\boldsymbol{u}\mapsto m_{\widehat{s}}(\boldsymbol{u},f)$ defined in (15) is twice continuously differentiable. Second, $\forall\Theta(\boldsymbol{x},\boldsymbol{y})\in SO(3)$, $\forall\boldsymbol{u}\in\mathcal{S}^2$, $\forall q\in\mathbb{N}$, function $f\mapsto \widehat{s}(\Theta(\boldsymbol{x},\boldsymbol{y})\boldsymbol{u},f)$ is q times continuously differentiable and $\frac{\partial^q \widehat{s}(\Theta(\boldsymbol{x},\boldsymbol{y})\boldsymbol{u},f)}{\partial f^q}$ is dominated by $\|t^q s(\boldsymbol{u},t)\|_1$. Since $SO(3)$ is a compact set, the differentiability under the integral sign theorem proves that function $f\mapsto m_{\widehat{s}}(\boldsymbol{u},f)$ is smooth.

By substituting (61) and (63) into (62), we get

$$\mathbb{E}[\widehat{h_i}(f)] = \lambda\beta_1 \int_{\boldsymbol{r}\in\mathbb{R}^3} \frac{\widehat{g_i}\left(\frac{\boldsymbol{r}}{\|\boldsymbol{r}\|_2},f\right) m_{\widehat{s}}\left(\frac{\boldsymbol{r}}{\|\boldsymbol{r}\|_2},f\right) e^{-\frac{\widehat{\alpha}(\boldsymbol{r})+2\imath\pi f\|\boldsymbol{r}\|_2}{c}}}{\|\boldsymbol{r}\|_2} d\boldsymbol{r}$$

where function $\widehat{\alpha}(.)$ and β_1 are defined in (7) and (13) for $n=1$. We note that $\mathbb{E}[\widehat{h_i}(f)] = \lambda\beta_1 J_\xi$ where J_ξ is defined in (86) and

$$\xi(\boldsymbol{r}) = \|\boldsymbol{r}\|_2\, \widehat{g_i}\left(\frac{\boldsymbol{r}}{\|\boldsymbol{r}\|_2},f\right) m_{\widehat{s}}\left(\frac{\boldsymbol{r}}{\|\boldsymbol{r}\|_2},f\right) e^{-\frac{\widehat{\alpha}(\boldsymbol{r})+2\imath\pi f\|\boldsymbol{r}\|_2}{c}}$$

belongs to $L^1(\mathbb{R}^3)\cap L^\infty(\mathbb{R}^3)$. Thus (92) yields

$$\begin{aligned}\mathbb{E}[\widehat{h_i}(f)] &= \lambda\beta_1 \int_{v=-1}^{1}\int_{\varphi=0}^{2\pi} \widehat{g_i}\left(v,\varphi,f\right) m_{\widehat{s}}\left(v,\varphi,f\right)\\ &\quad \int_{r=0}^{+\infty} r e^{-(\widehat{\alpha}(v,\varphi)+2\imath\pi f)\frac{r}{c}} dr dv d\varphi.\\ &= \lambda c^2\beta_1 \int_{v=-1}^{1}\int_{\varphi=0}^{2\pi} \tfrac{\widehat{g_i}(v,\varphi,f) m_{\widehat{s}}(v,\varphi,f)}{(\widehat{\alpha}(v,\varphi)+2\imath\pi f)^2} dv d\varphi,\end{aligned}$$

which proves (16). Finally, $\mathbb{E}[\widehat{h_i}(f)]$ is obtained as the integral over the compact set $\mathcal{S}^2$ of a function of $(\boldsymbol{u},f)$ which is smooth w.r.t. f, and whose derivatives of all orders are bounded; therefore the differentiation under the integral sign theorem proves that function $f\mapsto\mathbb{E}[\widehat{h_i}(f)]$ is smooth. □

APPENDIX F
SECOND ORDER MOMENTS

Proof of Lemma 3. First, function $\tau\mapsto b(\tau,D)$ defined in (19) is even because Lemma 2 shows that function $\beta(.)$ is even. As a consequence, function $f\mapsto\widehat{b}(f,D)$ is real-valued.

Second, function $\tau\mapsto b(\tau,D)$ is continuous and differentiable almost everywhere in the interior of its support, and $\frac{\partial b}{\partial\tau}(\tau,D)\in L^\infty(]-\frac{D}{c},+\frac{D}{c}[)$, because Lemma 2 shows that function $\beta(.)$ is continuous and differentiable almost everywhere in $\mathbb{R}^M$, and all its partial derivatives belong to $L^\infty(\mathbb{R}^M)$. As a consequence, function $f\mapsto\widehat{b}(f,D)$ is smooth.

Besides, applying (18) in Lemma 2 to $\boldsymbol{e}=\boldsymbol{q}c\tau$ leads to $\beta(\boldsymbol{q}c\tau)\leq\beta_2\, e^{-\widehat{\alpha}^{\inf}|\tau|}$, which proves (20). In particular, function $\tau\mapsto b(\tau,D)$ reaches its maximum at $\tau=0$, and it is not differentiable at $\tau=0$ (otherwise we would have $\lim_{\tau\to0,\tau>0}\frac{b(\tau,D)-b(0,D)}{\tau} = \frac{\partial b}{\partial\tau}(0,D)\leq-\beta_2\widehat{\alpha}^{\inf}$ and $\lim_{\tau\to0,\tau<0}\frac{b(\tau,D)-b(0,D)}{\tau} = \frac{\partial b}{\partial\tau}(0,D)\geq+\beta_2\widehat{\alpha}^{\inf}$). Moreover, $\forall f\in\mathbb{R}$, $|\widehat{b}(f,D)|\leq\int_{\tau\in\mathbb{R}} b(\tau,D)d\tau$, thus (20) implies (21).

If $D\to0$, since function $\beta(.)$ is continuous and differentiable almost everywhere in $\mathbb{R}^M$, and all its partial derivatives belong to $L^\infty(\mathbb{R}^M)$, we have $\beta(\boldsymbol{q}c\tau)=\beta_2+O(\tau)$ $\forall\tau\in[-\frac{D}{c},\frac{D}{c}]$. Therefore (19) yields (22), whose Fourier transform leads to (23). □

Proof of Proposition 2.
Temporal domain: Substituting (60) and (69) into (68) yields

$$\begin{aligned}&\gamma_{i,j}(t_1,t_2)=\lambda\int_{\boldsymbol{x}\in\mathbb{R}^3}\beta(\boldsymbol{q}(\boldsymbol{x}-\boldsymbol{x}_i)-\boldsymbol{q}(\boldsymbol{x}-\boldsymbol{x}_j))\\&\frac{e^{-\frac{\widehat{\alpha}(\boldsymbol{x}-\boldsymbol{x}_i)+\widehat{\alpha}(\boldsymbol{x}-\boldsymbol{x}_j)}{c}}g_i\left(\frac{\boldsymbol{x}-\boldsymbol{x}_i}{\|\boldsymbol{x}-\boldsymbol{x}_i\|_2},t_1\right)g_j\left(\frac{\boldsymbol{x}-\boldsymbol{x}_j}{\|\boldsymbol{x}-\boldsymbol{x}_j\|_2},t_2\right)}{\|\boldsymbol{x}-\boldsymbol{x}_i\|_2\|\boldsymbol{x}-\boldsymbol{x}_j\|_2}\overset{t_1}{*}\overset{t_2}{*}\\&m_{s,s}\left(\frac{\boldsymbol{x}-\boldsymbol{x}_i}{\|\boldsymbol{x}-\boldsymbol{x}_i\|_2},t_1-\frac{\|\boldsymbol{x}-\boldsymbol{x}_i\|_2}{c},\frac{\boldsymbol{x}-\boldsymbol{x}_j}{\|\boldsymbol{x}-\boldsymbol{x}_j\|_2},t_2-\frac{\|\boldsymbol{x}-\boldsymbol{x}_j\|_2}{c}\right)d\boldsymbol{x}\end{aligned}\tag{111}$$

where functions $\widehat{\alpha}(.)$ and $\beta(.)$ are defined in (7) and (17), and $\forall \boldsymbol{u}_1,\boldsymbol{u}_2\in\mathcal{S}^2$, $\forall t_1,t_2\in\mathbb{R}$, $\forall(\boldsymbol{x},\boldsymbol{y})\in\mathbb{R}^3\times\mathbb{R}^M$,

$$m_{s,s}(\boldsymbol{u}_1,t_1,\boldsymbol{u}_2,t_2)=\mathbb{E}[s\left(\Theta(\boldsymbol{x},\boldsymbol{y})\boldsymbol{u}_1,t_1\right)s\left(\Theta(\boldsymbol{x},\boldsymbol{y})\boldsymbol{u}_2,t_2\right)].\tag{112}$$

Note that $\gamma_{i,j}(t_1,t_2)=\lambda\,J_\xi$ with J_ξ defined in (85), and

$$\begin{aligned}\xi(\boldsymbol{r}_1,\boldsymbol{r}_2)=\quad&\beta(\boldsymbol{q}(\boldsymbol{r}_1)-\boldsymbol{q}(\boldsymbol{r}_2))e^{-\frac{\widehat{\alpha}(\boldsymbol{r}_1)+\widehat{\alpha}(\boldsymbol{r}_2)}{c}}\\&g_i\left(\frac{\boldsymbol{r}_1}{\|\boldsymbol{r}_1\|_2},t_1\right)g_j\left(\frac{\boldsymbol{r}_2}{\|\boldsymbol{r}_2\|_2},t_2\right)\overset{t_1}{*}\overset{t_2}{*}\\&m_{s,s}\left(\frac{\boldsymbol{r}_1}{\|\boldsymbol{r}_1\|_2},t_1-\frac{\|\boldsymbol{r}_1\|_2}{c},\frac{\boldsymbol{r}_2}{\|\boldsymbol{r}_2\|_2},t_2-\frac{\|\boldsymbol{r}_2\|_2}{c}\right)\end{aligned}$$

is such that $\boldsymbol{x}\mapsto\xi\left(\boldsymbol{x}-\boldsymbol{x}_i,\boldsymbol{x}-\boldsymbol{x}_j\right)\in L^1(\mathbb{R}^3)\cap L^\infty(\mathbb{R}^3)$. Thus (91) yields

$$\begin{aligned}&\gamma_{i,j}(t_1,t_2)=\lambda\int_{\rho=\frac{D}{2}}^{+\infty}\int_{v=-1}^{1}\int_{\varphi=0}^{2\pi}\\&\beta\left(\boldsymbol{q}\left(\frac{2\rho v+D}{2\rho+vD},\varphi\right)(\rho+\tfrac{vD}{2})-\boldsymbol{q}\left(\frac{2\rho v-D}{2\rho-vD},\varphi\right)(\rho-\tfrac{vD}{2})\right)\\&e^{-\frac{\widehat{\alpha}\left(\frac{2\rho v+D}{2\rho+vD},\varphi\right)(\rho+\frac{vD}{2})+\widehat{\alpha}\left(\frac{2\rho v-D}{2\rho-vD},\varphi\right)(\rho-\frac{vD}{2})}{c}}\\&g_i\left(\frac{2\rho v+D}{2\rho+vD},\varphi,t_1\right)g_j\left(\frac{2\rho v-D}{2\rho-vD},\varphi,t_2\right)\overset{t_1}{*}\overset{t_2}{*}\\&m_{s,s}\left(\frac{2\rho v+D}{2\rho+vD},\varphi,t_1-\frac{\rho+\frac{vD}{2}}{c},\frac{2\rho v-D}{2\rho-vD},\varphi,t_2-\frac{\rho-\frac{vD}{2}}{c}\right)d\rho dv d\varphi.\end{aligned}\tag{113}$$

If the acoustic field is diffuse (*cf.* Definition 2) and if the microphones and the source are omnidirectional (*cf.* Definitions 3 and 4), we get the simplification

$$\begin{aligned}&\gamma_{i,j}(t_1,t_2)=2\pi\lambda\int_{\rho=\frac{D}{2}}^{+\infty}\int_{v=-1}^{1}\beta\left(\boldsymbol{q}vD\right)e^{-\frac{2\widehat{\alpha}^{\inf}\rho}{c}}\\&(g_i*s)\left(t_1-\frac{\rho+\frac{vD}{2}}{c}\right)(g_j*s)\left(t_2-\frac{\rho-\frac{vD}{2}}{c}\right)d\rho dv.\end{aligned}\tag{114}$$

With the changes of variables $t=\frac{t_1+t_2}{2}-\frac{\rho}{c}$ and $\tau=\frac{vD}{c}$, which are such that $dt=\frac{d\rho}{c}$ and $d\tau=\frac{D}{c}dv$, and by substituting (19) into (114), we get (24). Moreover, if $D>0$, $b(.,D)\in L^1(\mathbb{R})$ and has compact support, or if $D=0$, $b(.,0)=\beta_2\delta(.)$. In both cases, since functions g_i' and s' are continuous with compact support, then function $b(.,D)*g_i'*\widetilde{g_j'}*s'*\widetilde{s'}$ is also continuous with compact support. Therefore function $(t_1,t_2)\mapsto\gamma_{i,j}(t_1,t_2)$ is continuous.

In particular, if $i=j$ and $t_1=t_2=t$, we get (25), hence the expression of the temporal correlation in (26).

Spectral domain: Substituting (61) and (69) into (68) yields

$$\begin{aligned}&\mathrm{cov}[\widehat{h}_i(f_1),\widehat{h}_j(f_2)]=\lambda\int_{\boldsymbol{x}\in\mathbb{R}^3}\\&\overline{\beta(\boldsymbol{q}(\boldsymbol{x}-\boldsymbol{x}_i)-\boldsymbol{q}(\boldsymbol{x}-\boldsymbol{x}_j))\widehat{g}_i(\frac{\boldsymbol{x}-\boldsymbol{x}_i}{\|\boldsymbol{x}-\boldsymbol{x}_i\|_2},f_1)}\\&\widehat{g}_j(\frac{\boldsymbol{x}-\boldsymbol{x}_j}{\|\boldsymbol{x}-\boldsymbol{x}_j\|_2},f_2)m_{\widehat{s},\overline{\widehat{s}}}(\frac{\boldsymbol{x}-\boldsymbol{x}_i}{\|\boldsymbol{x}-\boldsymbol{x}_i\|_2},f_1,\frac{\boldsymbol{x}-\boldsymbol{x}_j}{\|\boldsymbol{x}-\boldsymbol{x}_j\|_2},f_2)\\&\frac{e^{-\frac{\widehat{\alpha}(\boldsymbol{x}-\boldsymbol{x}_i)+2\imath\pi f_1\|\boldsymbol{x}-\boldsymbol{x}_i\|_2+\widehat{\alpha}(\boldsymbol{x}-\boldsymbol{x}_j)-2\imath\pi f_2\|\boldsymbol{x}-\boldsymbol{x}_j\|_2}{c}}}{\|\boldsymbol{x}-\boldsymbol{x}_i\|_2\|\boldsymbol{x}-\boldsymbol{x}_j\|_2}d\boldsymbol{x}\end{aligned}$$

where functions $\widehat{\alpha}(.)$ and $\beta(.)$ are defined in (7) and (17), and $\forall \boldsymbol{u}_1,\boldsymbol{u}_2\in\mathcal{S}^2$, $\forall f_1,f_2\in\mathbb{R}$, $\forall(\boldsymbol{x},\boldsymbol{y})\in\mathbb{R}^3\times\mathbb{R}^M$,

$$m_{\widehat{s},\overline{\widehat{s}}}(\boldsymbol{u}_1,f_1,\boldsymbol{u}_2,f_2)=\mathbb{E}[\widehat{s}(\Theta(\boldsymbol{x},\boldsymbol{y})\boldsymbol{u}_1,f_1)\overline{\widehat{s}(\Theta(\boldsymbol{x},\boldsymbol{y})\boldsymbol{u}_2,f_2)}].$$

Note that $\mathrm{cov}[\widehat{h}_i(f_1),\widehat{h}_j(f_2)]=\lambda J_\xi$ with J_ξ defined in (85) and

$$\begin{aligned}&\xi(\boldsymbol{r}_1,\boldsymbol{r}_2)=\beta(\boldsymbol{q}(\boldsymbol{r}_1)-\boldsymbol{q}(\boldsymbol{r}_2))\widehat{g}_i\left(\frac{\boldsymbol{r}_1}{\|\boldsymbol{r}_1\|_2},f_1\right)\overline{\widehat{g}_j\left(\frac{\boldsymbol{r}_2}{\|\boldsymbol{r}_2\|_2},f_2\right)}\\&m_{\widehat{s},\overline{\widehat{s}}}(\frac{\boldsymbol{r}_1}{\|\boldsymbol{r}_1\|_2},f_1,\frac{\boldsymbol{r}_2}{\|\boldsymbol{r}_2\|_2},f_2)e^{-\frac{\alpha(\boldsymbol{r}_1)+2\imath\pi f_1\|\boldsymbol{r}_1\|_2+\alpha(\boldsymbol{r}_2)-2\imath\pi f_2\|\boldsymbol{r}_2\|_2}{c}}\end{aligned}$$

is such that $\boldsymbol{x}\mapsto\xi\left(\boldsymbol{x}-\boldsymbol{x}_i,\boldsymbol{x}-\boldsymbol{x}_j\right)\in L^1(\mathbb{R}^3)\cap L^\infty(\mathbb{R}^3)$. Thus (91) yields

$$\begin{aligned}&\mathrm{cov}[\widehat{h}_i(f_1),\widehat{h}_j(f_2)]=\lambda\int_{\rho=\frac{D}{2}}^{+\infty}\int_{v=-1}^{1}\int_{\varphi=0}^{2\pi}\\&\beta\left(\boldsymbol{q}\left(\frac{2\rho v+D}{2\rho+vD},\varphi\right)(\rho+\tfrac{vD}{2})-\boldsymbol{q}\left(\frac{2\rho v-D}{2\rho-vD},\varphi\right)(\rho-\tfrac{vD}{2})\right)\\&e^{-\frac{\left(\alpha\left(\frac{2\rho v+D}{2\rho+vD},\varphi\right)+2\imath\pi f_1\right)(\rho+\frac{vD}{2})+\left(\alpha\left(\frac{2\rho v-D}{2\rho-vD},\varphi\right)-2\imath\pi f_2\right)(\rho-\frac{vD}{2})}{c}}\\&\widehat{g}_i\left(\frac{2\rho v+D}{2\rho+vD},\varphi,f_1\right)\overline{\widehat{g}_j\left(\frac{2\rho v-D}{2\rho-vD},\varphi,f_2\right)}\\&m_{\widehat{s},\overline{\widehat{s}}}\left(\frac{2\rho v+D}{2\rho+vD},\varphi,f_1,\frac{2\rho v-D}{2\rho-vD},\varphi,f_2\right)d\rho dv d\varphi.\end{aligned}$$

If the acoustic field is diffuse (*cf.* Definition 2) and if the microphones and the source are omnidirectional (*cf.* Definitions 3 and 4), we get the simplification

$$\begin{aligned}&\mathrm{cov}[\widehat{h}_i(f_1),\widehat{h}_j(f_2)]=2\pi\lambda\,\widehat{g}_i\left(f_1\right)\overline{\widehat{g}_j\left(f_2\right)}\widehat{s}(f_1)\overline{\widehat{s}(f_2)}\\&\int_{\rho=\frac{D}{2}}^{+\infty}e^{-\frac{(2\widehat{\alpha}^{\inf}+2\imath\pi(f_1-f_2))\rho}{c}}d\rho\int_{v=-1}^{1}\beta\left(\boldsymbol{q}vD\right)e^{-\frac{2\imath\pi\frac{f_1+f_2}{2}vD}{c}}dv.\end{aligned}\tag{115}$$

With the change of variable $\tau=\frac{vD}{c}$, which is such that $d\tau=\frac{D}{c}dv$, by substituting (19) into (115), we get (27). Moreover, function $(f_1,f_2)\mapsto\mathrm{cov}[\widehat{h}_i(f_1),\widehat{h}_j(f_2)]$ is smooth, as a product of smooth functions.

In particular, if $i=j$ and $f_1=f_2=f$, we get (28), hence the expression of the spectral correlation in (29).

Time-frequency domain: The Wigner distribution of (111) is

$$\begin{aligned}&\mathcal{W}_{\gamma_{i,j}}(t,f)=\lambda\int_{\boldsymbol{x}\in\mathbb{R}^3}\beta(\boldsymbol{q}(\boldsymbol{x}-\boldsymbol{x}_i)-\boldsymbol{q}(\boldsymbol{x}-\boldsymbol{x}_j))\\&\mathcal{W}_{g_i\otimes g_j}\left(\frac{\boldsymbol{x}-\boldsymbol{x}_i}{\|\boldsymbol{x}-\boldsymbol{x}_i\|_2},\frac{\boldsymbol{x}-\boldsymbol{x}_j}{\|\boldsymbol{x}-\boldsymbol{x}_j\|_2},.,f\right)\overset{t}{*}\\&\mathcal{W}_{m_{s,s}}(\frac{\boldsymbol{x}-\boldsymbol{x}_i}{\|\boldsymbol{x}-\boldsymbol{x}_i\|_2},\frac{\boldsymbol{x}-\boldsymbol{x}_j}{\|\boldsymbol{x}-\boldsymbol{x}_j\|_2},t-\frac{\|\boldsymbol{x}-\boldsymbol{x}_i\|_2+\|\boldsymbol{x}-\boldsymbol{x}_j\|_2}{2c},f)\\&\frac{e^{-\frac{\widehat{\alpha}(\boldsymbol{x}-\boldsymbol{x}_i)+\widehat{\alpha}(\boldsymbol{x}-\boldsymbol{x}_j)+2\imath\pi f\left(\|\boldsymbol{x}-\boldsymbol{x}_i\|_2-\|\boldsymbol{x}-\boldsymbol{x}_j\|_2\right)}{c}}}{\|\boldsymbol{x}-\boldsymbol{x}_i\|_2\|\boldsymbol{x}-\boldsymbol{x}_j\|_2}d\boldsymbol{x}\end{aligned}$$

where we have used the convolution property (4) of the Wigner distribution, and $m_{s,s}$ is defined in (112).

Note that $\mathcal{W}_{\gamma_{i,j}}(t,f)=\lambda\,J_\xi$ with J_ξ defined in (85), and

$$\begin{aligned}\xi(\boldsymbol{r}_1,\boldsymbol{r}_2)=\quad&\beta(\boldsymbol{q}(\boldsymbol{r}_1)-\boldsymbol{q}(\boldsymbol{r}_2))e^{-\frac{\widehat{\alpha}(\boldsymbol{r}_1)+\widehat{\alpha}(\boldsymbol{r}_2)+2\imath\pi f\left(\|\boldsymbol{r}_1\|_2-\|\boldsymbol{r}_2\|_2\right)}{c}}\\&\mathcal{W}_{g_i\otimes g_j}\left(\frac{\boldsymbol{r}_1}{\|\boldsymbol{r}_1\|_2},\frac{\boldsymbol{r}_2}{\|\boldsymbol{r}_2\|_2},.,f\right)\\&\overset{t}{*}\mathcal{W}_{m_{s,s}}(\frac{\boldsymbol{r}_1}{\|\boldsymbol{r}_1\|_2},\frac{\boldsymbol{r}_2}{\|\boldsymbol{r}_2\|_2},t-\frac{\|\boldsymbol{r}_1\|_2+\|\boldsymbol{r}_2\|_2}{2c},f)\end{aligned}$$

is such that $\boldsymbol{x}\mapsto\xi\left(\boldsymbol{x}-\boldsymbol{x}_i,\boldsymbol{x}-\boldsymbol{x}_j\right)\in L^1(\mathbb{R}^3)\cap L^\infty(\mathbb{R}^3)$. Thus (91) yields

$$\begin{array}{l}\mathcal{W}_{\gamma_{i,j}}(t,f)=\lambda\int_{\rho=\frac{D}{2}}^{+\infty}\int_{v=-1}^{1}\int_{\varphi=0}^{2\pi}\\ \beta\left(\boldsymbol{q}\left(\frac{2\rho v+D}{2\rho+vD},\varphi\right)(\rho+\frac{vD}{2})-\boldsymbol{q}\left(\frac{2\rho v-D}{2\rho-vD},\varphi\right)(\rho-\frac{vD}{2})\right)\\ e^{-\frac{\widehat{\alpha}\left(\frac{2\rho v+D}{2\rho+vD},\varphi\right)(\rho+\frac{vD}{2})+\widehat{\alpha}\left(\frac{2\rho v-D}{2\rho-vD},\varphi\right)(\rho-\frac{vD}{2})+2\imath\pi fvD}{c}}\\ \mathcal{W}_{g_i\otimes g_j}\left(\frac{2\rho v+D}{2\rho+vD},\varphi,\frac{2\rho v-D}{2\rho-vD},\varphi,.,f\right)\overset{t}{*}\\ \mathcal{W}_{m_{s,s}}(\frac{2\rho v+D}{2\rho+vD},\varphi,\frac{2\rho v-D}{2\rho-vD},\varphi,t-\frac{\rho}{c},f)d\rho dvd\varphi.\end{array}\tag{116}$$

If the acoustic field is diffuse (*cf.* Definition 2) and if the microphones and the source are omnidirectional (*cf.* Definitions 3 and 4), with the changes of variables $t'=t-\frac{\rho}{c}$ and $\tau=\frac{vD}{c}$, which are such that $dt'=\frac{d\rho}{c}$ and $d\tau=\frac{D}{c}dv$, (116) yields $\forall t\geq T+\frac{D}{2c}$,

$$\begin{array}{rl}\mathcal{W}_{\gamma_{i,j}}(t,f)= & \frac{2\pi\lambda c^2}{D}e^{-2\widehat{\alpha}^{\inf}t}\int_{\tau=-\frac{D}{c}}^{\frac{D}{c}}\beta\left(\boldsymbol{q}c\tau\right)e^{-2\imath\pi f\tau}d\tau\\ & \int_{t'\in\mathbb{R}}e^{2\widehat{\alpha}^{\inf}t'}\mathcal{W}_{g_i\otimes g_j}\left(.,f\right)\overset{t}{*}\mathcal{W}_{m_{s,s}}(t',f)dt'.\end{array}\tag{117}$$

Finally, by using the projection property (2) of the Wigner distribution and by substituting (19) into (117), we get (30). Moreover, function $f\mapsto B_{i,j}(f,D)$ defined in (31) is smooth, as a product of smooth functions.

In particular, if $i=j$, we get (32), hence the expression of the time-frequency correlation in (33). Then (34) is obtained as the inverse Fourier transform of the right member of (33) when $\forall f\in\mathbb{R}$, $\angle\widehat{g_i'}(f)=\angle\widehat{g_j'}(f)$.

Finally, function $\tau\mapsto\sigma_{i,j}(\tau,\boldsymbol{x}_j-\boldsymbol{x}_i)$ in (34) has the same support as function $\tau\mapsto b(\tau,D)$ defined in (19). It is continuous in the interior of this support, it reaches its maximum at $\tau=0$, and it is not differentiable at $\tau=0$, because so is function $\tau\mapsto b(\tau,D)$ as shown in Lemma 3. Moreover, (20) yields $\sigma_{i,j}(\tau,\boldsymbol{x}_j-\boldsymbol{x}_i)\in[0,\frac{c}{2D}]$. □

APPENDIX G
ASYMPTOTIC RESULTS

In this Appendix, we first prove Propositions 3 and 4 in Section III. Then Corollaries 1 and 2 will be proved in Appendix G.5.

G.1. General asymptotic results

First, we compute a few simple asymptotic forms, that will be used in Appendices G.2 and G.3.

Suppose that $\rho\to+\infty$. Then we get

$$\begin{array}{l}\frac{2\rho v+D}{2\rho+vD}=v+\frac{(1-v^2)D}{2\rho+vD}=v+O(\frac{D}{\rho}),\\ \frac{2\rho v-D}{2\rho-vD}=v-\frac{(1-v^2)D}{2\rho-vD}=v+O(\frac{D}{\rho}),\end{array}\tag{118}$$

and since function $\widehat{\alpha}(.)$ is twice continuously differentiable,

$$\begin{array}{rl}& \widehat{\alpha}\left(\frac{2\rho v+D}{2\rho+vD},\varphi\right)(\rho+\frac{vD}{2})+\widehat{\alpha}\left(\frac{2\rho v-D}{2\rho-vD},\varphi\right)(\rho-\frac{vD}{2})\\ = & 2\widehat{\alpha}\left(v,\varphi\right)\rho+O\left(\frac{D^2\sup_{\mathcal{S}^2}|\frac{\partial^2\widehat{\alpha}}{\partial v^2}|}{\rho}\right),\end{array}$$

therefore

$$\begin{array}{rl}& e^{-\frac{\widehat{\alpha}\left(\frac{2\rho v+D}{2\rho+vD},\varphi\right)(\rho+\frac{vD}{2})+\widehat{\alpha}\left(\frac{2\rho v-D}{2\rho-vD},\varphi\right)(\rho-\frac{vD}{2})}{c}}\\ = & e^{-\frac{2\widehat{\alpha}(v,\varphi)\rho}{c}}\left(1+O\left(\frac{D^2\sup_{\mathcal{S}^2}|\frac{\partial^2\widehat{\alpha}}{\partial v^2}|}{\rho c}\right)\right).\end{array}\tag{119}$$

In the same way, since function $\boldsymbol{q}(.)$ is twice continuously differentiable,

$$\begin{array}{rl}& \boldsymbol{q}\left(\frac{2\rho v+D}{2\rho+vD},\varphi\right)(\rho+\frac{vD}{2})-\boldsymbol{q}\left(\frac{2\rho v-D}{2\rho-vD},\varphi\right)(\rho-\frac{vD}{2})\\ = & \boldsymbol{q}\left(v,\varphi\right)vD+\frac{\partial\boldsymbol{q}(v,\varphi)}{\partial v}(1-v^2)D+O\left(\frac{D^2\sup_{\mathcal{S}^2}|\frac{\partial^2\boldsymbol{q}}{\partial v^2}|}{\rho}\right).\end{array}\tag{120}$$

Since function $\beta(.)$ is continuous and differentiable almost everywhere in $\mathbb{R}^M$, and all its partial derivatives belong to $L^\infty(\mathbb{R}^M)$ as shown in Lemma 2, then (120) yields

$$\begin{array}{rl}& \beta\left(\boldsymbol{q}\left(\frac{2\rho v+D}{2\rho+vD},\varphi\right)(\rho+\frac{vD}{2})-\boldsymbol{q}\left(\frac{2\rho v-D}{2\rho-vD},\varphi\right)(\rho-\frac{vD}{2})\right)\\ = & \beta\left(\boldsymbol{q}\left(v,\varphi\right)vD+\frac{\partial\boldsymbol{q}(v,\varphi)}{\partial v}(1-v^2)D\right)+O\left(\frac{D\sup_{\mathcal{S}^2}|\frac{\partial^2\boldsymbol{q}}{\partial v^2}|}{\rho}\right).\end{array}\tag{121}$$

G.2. Temporal domain

Since functions g_i, g_j and s have finite temporal support, when $t_1+t_2\to+\infty$ with t_1-t_2 fixed, (113) can be simplified by noting that $\rho\to+\infty$. Indeed, substituting the asymptotic forms (118), (119) and (121) into (113) yields:

$$\begin{array}{l}\gamma_{i,j}(t_1,t_2)=\lambda\int_{\rho=\frac{D}{2}}^{+\infty}\int_{v=-1}^{1}\int_{\varphi=0}^{2\pi}e^{-\frac{2\widehat{\alpha}(v,\varphi)\rho}{c}}\Big(\\ \beta\left(\boldsymbol{q}\left(v,\varphi\right)vD+\frac{\partial\boldsymbol{q}(v,\varphi)}{\partial v}(1-v^2)D\right)g_i\left(v,\varphi,t_1\right)\\ g_j\left(v,\varphi,t_2\right)\overset{t_1}{*}\overset{t_2}{*}m_{s,s}\left(v,\varphi,t_1-\frac{\rho+\frac{vD}{2}}{c},v,\varphi,t_2-\frac{\rho-\frac{vD}{2}}{c}\right)\\ +O\left(\frac{D}{\rho}\right)\Big)dvd\varphi d\rho,\end{array}\tag{122}$$

where $m_{s,s}$ is defined in (112).

By substituting (93) and (98) into (122), we get

$$\begin{array}{l}\gamma_{i,j}(t_1,t_2)=\lambda\int_{\rho=\frac{D}{2}}^{+\infty}\int_{\boldsymbol{u}\in\mathcal{S}^2}e^{-\frac{2\widehat{\alpha}(\boldsymbol{u})\rho}{c}}\Big(\\ \beta\left(\left(\boldsymbol{q}(\boldsymbol{u})\boldsymbol{u}^\top+\mathring{\mathbf{J}}_{\boldsymbol{q}}(\boldsymbol{u})\right)(\boldsymbol{x}_j-\boldsymbol{x}_i)\right)g_i\left(\boldsymbol{u},t_1\right)g_j\left(\boldsymbol{u},t_2\right)\\ \overset{t_1}{*}\overset{t_2}{*}m_{s,s}\left(\boldsymbol{u},t_1-\frac{\rho+\frac{\boldsymbol{u}^\top(\boldsymbol{x}_j-\boldsymbol{x}_i)}{2}}{c},\boldsymbol{u},t_2-\frac{\rho-\frac{\boldsymbol{u}^\top(\boldsymbol{x}_j-\boldsymbol{x}_i)}{2}}{c}\right)\\ +O\left(\frac{D}{\rho}\right)\Big)d\boldsymbol{u}d\rho.\end{array}\tag{123}$$

By applying the change of variable $\tau=\frac{t_1+t_2}{2}-\frac{\rho}{c}$, which is such that $d\tau=\frac{d\rho}{c}$, to (123), we get $\forall t_1+t_2\geq 2T+\frac{D}{c}$,

$$\begin{array}{l}\gamma_{i,j}(t_1,t_2)=\lambda c\int_{\boldsymbol{u}\in\mathcal{S}^2}e^{-\widehat{\alpha}(\boldsymbol{u})(t_1+t_2)}\Big(\\ \beta\left(\left(\boldsymbol{q}(\boldsymbol{u})\boldsymbol{u}^\top+\mathring{\mathbf{J}}_{\boldsymbol{q}}(\boldsymbol{u})\right)(\boldsymbol{x}_j-\boldsymbol{x}_i)\right)g_i'\left(\boldsymbol{u},.\right)*g_j'\left(\boldsymbol{u},.\right)\\ *m_{s'*\tilde{s'}}(\boldsymbol{u},t_1-t_2-\frac{\boldsymbol{u}^\top(\boldsymbol{x}_j-\boldsymbol{x}_i)}{c})+O\left(\frac{D}{c(t_1+t_2)}\right)\Big)d\boldsymbol{u},\end{array}\tag{124}$$

where $m_{s'*\tilde{s'}}$ is defined in (35).

Note that $\forall\Theta(\boldsymbol{x},\boldsymbol{y}) \in SO(3)$, $\forall t \in \mathbb{R}$, function $\boldsymbol{u} \mapsto s'(\Theta(\boldsymbol{x},\boldsymbol{y})\boldsymbol{u},.) \overset{t}{*} \widetilde{s'}(\Theta(\boldsymbol{x},\boldsymbol{y})\boldsymbol{u},.)$ is twice continuously differentiable, and all its second order derivatives are bounded on $\mathcal{S}^2$. Since $SO(3)$ is a compact set, the differentiability under the integral sign theorem proves that function $m_{s'*\widetilde{s'}}$ is twice continuously differentiable w.r.t. $\boldsymbol{u} \in \mathcal{S}^2$. In the same way, $\forall\Theta(\boldsymbol{x},\boldsymbol{y}) \in SO(3)$, $\forall\boldsymbol{u} \in \mathcal{S}^2$, function $t \mapsto s'(\Theta(\boldsymbol{x},\boldsymbol{y})\boldsymbol{u},.) \overset{t}{*} \widetilde{s'}(\Theta(\boldsymbol{x},\boldsymbol{y})\boldsymbol{u},.)$ is continuous and dominated by $T_s \sup_{\boldsymbol{u}\in\mathcal{S}^2} \|s'(\boldsymbol{u},.)\|_\infty^2$. Since $SO(3)$ is a compact set, the continuity under the integral sign theorem proves that function $m_{s'*\widetilde{s'}}$ is continuous w.r.t. $t \in \mathbb{R}$.

1) Early asymptotic state: Suppose that $\forall\boldsymbol{r} \in \mathbb{R}^3$, $\boldsymbol{q}(\boldsymbol{r}) = \boldsymbol{q}\|\boldsymbol{r}\|_2$ where $\boldsymbol{q} \in \mathbb{R}_+^M$ is a constant vector, therefore function $\widehat{\alpha}(.)$ defined in (7) is constant on $\mathcal{S}^2$: $\forall\boldsymbol{u} \in \mathcal{S}^2$, $\widehat{\alpha}(\boldsymbol{u}) = \widehat{\alpha}^{\inf}$, where $\widehat{\alpha}^{\inf} = \boldsymbol{q}^\top\widehat{\boldsymbol{\alpha}}$. Then (124) becomes $\forall t_1+t_2 \geq 2T + \frac{D}{c}$,

$$\gamma_{i,j}(t_1,t_2) = \lambda c\, e^{-\widehat{\alpha}^{\inf}(t_1+t_2)}\Big(\int_{\boldsymbol{u}\in\mathcal{S}^2} \beta\left(\boldsymbol{q}\boldsymbol{u}^\top(\boldsymbol{x}_j-\boldsymbol{x}_i)\right) g_i'(\boldsymbol{u},.) * \widetilde{g_j'}(\boldsymbol{u},.) * m_{s'*\widetilde{s'}}(\boldsymbol{u}, t_1\text{-}t_2 - \tfrac{\boldsymbol{u}^\top(\boldsymbol{x}_j-\boldsymbol{x}_i)}{c}) d\boldsymbol{u} + O(\tfrac{D}{c(t_1+t_2)})\Big).$$

In particular, if $i=j$ (thus D=0) and $t_1=t_2=t$, we get (36).

2) Late asymptotic state: Suppose that the attenuation function is regular (*cf.* Definition 7). If we let $x = t_1+t_2$, then (124) shows that $\gamma_{i,j}(t_1,t_2))$ can be decomposed as

$$\gamma_{i,j}(t_1,t_2)) = I_1(x) + I_2(x)\, O\left(\tfrac{D}{c(t_1+t_2)}\right) \tag{125}$$

where $I_2(x)$ is the integral defined in (99) with $\psi(\boldsymbol{u}) = \lambda c$, so that (102) proves that

$$I_2(x) = O\left(\tfrac{e^{-\widehat{\alpha}^{\inf}(t_1+t_2)}}{t_1+t_2}\right), \tag{126}$$

and $I_1(x)$ is the integral defined in (99) with

$$\begin{aligned}\psi(\boldsymbol{u}) = \quad & \lambda c\beta\left(\left(\boldsymbol{q}(\boldsymbol{u})\boldsymbol{u}^T + \mathring{\mathbf{J}}_{\boldsymbol{q}}(\boldsymbol{u})\right)\boldsymbol{r}\right) \\ & g_i'(\boldsymbol{u},.) * \widetilde{g_j'}(\boldsymbol{u},.) * m_{s'*\widetilde{s'}}(\boldsymbol{u}, t_1-t_2-\tfrac{\boldsymbol{u}^\top\boldsymbol{r}}{c})\end{aligned} \tag{127}$$

where $\boldsymbol{r} = \boldsymbol{x}_j - \boldsymbol{x}_i$. Since function $\beta(.)$ is continuous and differentiable almost everywhere in $\mathbb{R}^M$, and all its partial derivatives belong to L^∞, so is function ψ in (127). If in addition $i=j$, then $\boldsymbol{r}=0$ and function ψ is twice continuously differentiable.

Therefore if $\boldsymbol{r} \neq 0$, substituting (101), (126) and (127) into (125) shows that when $t_1+t_2 \to +\infty$,

$$\gamma_{i,j}(t_1,t_2) = \tfrac{2\pi\lambda c\, e^{-\widehat{\alpha}^{\inf}(t_1+t_2)}}{t_1+t_2}\Big(\sum_{k\in\mathcal{K}} \tfrac{\beta_k(\boldsymbol{r})}{\sqrt{\ddot{\widehat{\alpha}}_k}} g_i'(\boldsymbol{u}_k,.) * \widetilde{g_j'}(\boldsymbol{u}_k,.) * m_{s'*\widetilde{s'}}(\boldsymbol{u}_k, t_1-t_2-\tau_k) + O\left(\tfrac{1}{\sqrt{t_1+t_2}}\right)\Big)$$

where $\tau_k = \frac{\boldsymbol{u}_k^\top\boldsymbol{r}}{c}$ and $\beta_k(\boldsymbol{r})$ is defined in (51). If $i=j$ (thus $\boldsymbol{r}=0$ and $\tau_k=0$) and $t_1=t_2=t$, substituting (102) and (126) into (125) proves (49).

G.3. Time-frequency domain

Because of the temporal support property of the Wigner distribution, $\mathcal{W}_{g_i\otimes g_j}$ and $\mathcal{W}_{m_{s,s}}$ have finite temporal support. Therefore when $t \to +\infty$, (116) can be simplified by noting that $\rho \to +\infty$. Indeed, by substituting the asymptotic forms (118), (119) and (121) into (116), we get:

$$\begin{aligned}\mathcal{W}_{\gamma_{i,j}}(t,f) = \lambda \int_{\rho=\frac{D}{2}}^{+\infty}\int_{v=-1}^{1}\int_{\varphi=0}^{2\pi} e^{-\frac{2\widehat{\alpha}(v,\varphi)\rho}{c}}\Big(\\ \beta\left(\boldsymbol{q}(v,\varphi)\, vD + \tfrac{\partial\boldsymbol{q}(v,\varphi)}{\partial v}(1-v^2)D\right) e^{-2\imath\pi f\frac{vD}{c}} \\ \mathcal{W}_{g_i\otimes g_j}(v,\varphi,.,f) \overset{t}{*} \mathcal{W}_{m_{s,s}}(v,\varphi,t\text{-}\tfrac{\rho}{c},f) + O\left(\tfrac{D}{\rho}\right)\Big) dv d\varphi d\rho,\end{aligned} \tag{128}$$

where $m_{s,s}$ is defined in (112).

By substituting (93) and (98) into (128), we get

$$\begin{aligned}\mathcal{W}_{\gamma_{i,j}}(t,f) = \lambda \int_{\rho=\frac{D}{2}}^{+\infty}\int_{\boldsymbol{u}\in\mathcal{S}^2} e^{-\frac{2\widehat{\alpha}(\boldsymbol{u})\rho}{c}}\Big(\\ \beta\left(\left(\boldsymbol{q}(\boldsymbol{u})\boldsymbol{u}^\top + \mathring{\mathbf{J}}_{\boldsymbol{q}}(\boldsymbol{u})\right)(\boldsymbol{x}_j-\boldsymbol{x}_i)\right) e^{-2\imath\pi f\frac{\boldsymbol{u}^\top(\boldsymbol{x}_j-\boldsymbol{x}_i)}{c}} \\ \mathcal{W}_{g_i\otimes g_j}(\boldsymbol{u},.,f) \overset{t}{*} \mathcal{W}_{m_{s,s}}(\boldsymbol{u}, t-\tfrac{\rho}{c}, f) + O\left(\tfrac{D}{\rho}\right)\Big) d\boldsymbol{u} d\rho.\end{aligned} \tag{129}$$

By applying the change of variable $\tau = t - \frac{\rho}{c}$, which is such that $d\tau = \frac{d\rho}{c}$, to (129), we get $\forall t \geq T + \frac{D}{2c}$ with $T = T_g + T_s$,

$$\begin{aligned}\mathcal{W}_{\gamma_{i,j}}(t,f) = \lambda c \int_{\boldsymbol{u}\in\mathcal{S}^2} e^{-2\widehat{\alpha}(\boldsymbol{u})t}\Big(\\ \beta\left(\left(\boldsymbol{q}(\boldsymbol{u})\boldsymbol{u}^\top + \mathring{\mathbf{J}}_{\boldsymbol{q}}(\boldsymbol{u})\right)(\boldsymbol{x}_j-\boldsymbol{x}_i)\right) e^{-2\imath\pi f\frac{\boldsymbol{u}^\top(\boldsymbol{x}_j-\boldsymbol{x}_i)}{c}} \\ \widehat{g_i'}(\boldsymbol{u},f)\overline{\widehat{g_j'}(\boldsymbol{u},f)} m_{|\widehat{s'}|^2}(\boldsymbol{u},f) + O\left(\tfrac{D}{ct}\right)\Big) d\boldsymbol{u},\end{aligned} \tag{130}$$

where we have used the projection property (2) of the Wigner distribution, and the definition of $m_{|\widehat{s'}|^2}(\boldsymbol{u},f)$ in (37).

Finally, note that $\forall\Theta(\boldsymbol{x},\boldsymbol{y}) \in SO(3)$, $\forall f \in \mathbb{R}$, function $\boldsymbol{u} \mapsto \left|\widehat{s'}(\Theta(\boldsymbol{x},\boldsymbol{y})\boldsymbol{u},f)\right|^2$ is twice continuously differentiable, and all its second order derivatives are bounded on $\mathcal{S}^2$. Since $SO(3)$ is a compact set, the differentiability under the integral sign theorem proves that function $\boldsymbol{u} \mapsto \left|m_{\widehat{s'}}(\boldsymbol{u},f)\right|^2$ is twice continuously differentiable. Also note that $\forall\Theta(\boldsymbol{x},\boldsymbol{y}) \in SO(3)$, $\forall\boldsymbol{u} \in \mathcal{S}^2$, $\forall q \in \mathbb{N}$, function $f \mapsto \left|\widehat{s'}(\Theta(\boldsymbol{x},\boldsymbol{y})\boldsymbol{u},f)\right|^2$ is q times continuously differentiable and $\frac{\partial^q\left|\widehat{s'}(\Theta(\boldsymbol{x},\boldsymbol{y})\boldsymbol{u},f)\right|^2}{\partial f^q}$ is dominated by $\|t^q s'(\boldsymbol{u},t)\|_1^2$. Since $SO(3)$ is a compact set, the differentiability under the integral sign theorem proves that function $f \mapsto \left|m_{\widehat{s'}}(\boldsymbol{u},f)\right|^2$ is smooth.

1) Early asymptotic state: Suppose that $\forall\boldsymbol{r} \in \mathbb{R}^3$, $\boldsymbol{q}(\boldsymbol{r}) = \boldsymbol{q}\|\boldsymbol{r}\|_2$ where $\boldsymbol{q} \in \mathbb{R}_+^M$ is a constant vector, therefore function $\widehat{\alpha}(.)$ defined in (7) is constant on $\mathcal{S}^2$: $\forall\boldsymbol{u} \in \mathcal{S}^2$, $\widehat{\alpha}(\boldsymbol{u}) = \widehat{\alpha}^{\inf}$, where $\widehat{\alpha}^{\inf} = \boldsymbol{q}^\top\widehat{\boldsymbol{\alpha}}$; Then (130) yields (38) and (39). Moreover, $B_{i,j}(f,\boldsymbol{r})$ is obtained as the integral over the compact set $\mathcal{S}^2$ of a function of $(\boldsymbol{u},f)$ which is smooth w.r.t. f, and whose derivatives of all orders are bounded; therefore the differentiation under the integral sign theorem proves that function $f \mapsto B_{i,j}(f,\boldsymbol{r})$ is smooth. The proof of the even symmetry of $f \mapsto B_{i,j}(f,\boldsymbol{r})$ is straightforward. If $i=j$ (thus $D=0$), then (130) implies (40), and (38) leads to the expression of the time-frequency correlation in (41). This time-frequency correlation is asymptotically smooth and even symmetric w.r.t. f because so is function $f \mapsto B_{i,j}(f,\boldsymbol{x}_j-\boldsymbol{x}_i)$.

2) Late asymptotic state: Suppose that the attenuation function is regular (*cf.* Definition 7). If we let $x = 2t$, then (130) shows that $\mathcal{W}_{\gamma_{i,j}}(t,f)$ can be decomposed as

$$\mathcal{W}_{\gamma_{i,j}}(t,f) = I_1(x) + I_2(x)\, O\left(\tfrac{D}{ct}\right) \tag{131}$$

where $I_2(x)$ is the integral defined in (99) with $\psi(\boldsymbol{u}) = \lambda c$, so that (102) proves that

$$I_2(x) = O\left(\tfrac{e^{-2\widehat{\alpha}^{\inf} t}}{t}\right), \tag{132}$$

and $I_1(x)$ is the integral defined in (99) with

$$\begin{array}{rl} \psi(\boldsymbol{u}) = & \lambda c\beta\left(\left(\boldsymbol{q}\left(\boldsymbol{u}\right)\boldsymbol{u}^T + \mathring{\mathbf{J}}_{\boldsymbol{q}}(\boldsymbol{u})\right)\boldsymbol{r}\right) \\ & \overline{\widehat{g_i'}(\boldsymbol{u},f)}\widehat{g_j'}(\boldsymbol{u},f) m_{|\widehat{s'}|^2}(\boldsymbol{u},f) e^{-2\imath\pi f \frac{\boldsymbol{u}^\top \boldsymbol{r}}{c}} \end{array} \tag{133}$$

where $\boldsymbol{r} = \boldsymbol{x}_j - \boldsymbol{x}_i$. Since function $\beta(.)$ is continuous and differentiable almost everywhere in $\mathbb{R}^M$, and all its partial derivatives belong to L^∞, so is function ψ in (133). If in addition $i = j$, then $\boldsymbol{r} = 0$ and function ψ is twice continuously differentiable.

Therefore if $\boldsymbol{r} \neq 0$, substituting (101) and (132) into (131) proves (52). Moreover, function $f \mapsto B_{i,j}(f,\boldsymbol{r})$ in (50) is smooth, as a finite sum of smooth functions. The proof of its even symmetry is straightforward.

If $i = j$ (thus $\boldsymbol{r} = 0$), substituting (102), (132) and (133) into (131) proves (53), and (52) leads to the expression of the time-frequency correlation in (54). This time-frequency correlation is asymptotically smooth and even symmetric w.r.t. f because so is function $f \mapsto B_{i,j}(f, \boldsymbol{x}_j - \boldsymbol{x}_i)$.

G.4. Asymptotic normality

Substituting (60) into (80) applied to $\theta_1 = \theta$ and $\theta_2 = 0$ yields

$$\begin{array}{l} \ln \phi_{h_i(t)}(\theta) = \lambda \int_{\boldsymbol{x}\in\mathbb{R}^3} \int_{\boldsymbol{y}\in\mathbb{R}^M} p(1; \boldsymbol{y} - \boldsymbol{q}(\boldsymbol{x}-\boldsymbol{x}_i)) \\ \left(\phi_{g_i * s}\left(\frac{\theta e^{-\frac{\boldsymbol{y}^\top \widehat{\boldsymbol{\alpha}}}{c}}}{\|\boldsymbol{x}-\boldsymbol{x}_i\|_2}, \frac{\boldsymbol{x}-\boldsymbol{x}_i}{\|\boldsymbol{x}-\boldsymbol{x}_i\|_2}, t - \frac{\|\boldsymbol{x}-\boldsymbol{x}_i\|_2}{c}\right) - 1\right) d\boldsymbol{x} d\boldsymbol{y}. \end{array} \tag{134}$$

We consider the following series expansions:

$$\begin{array}{rcl} \ln \phi_{h_i(t)}(\theta) & = & \sum_{n=1}^{+\infty} \frac{\imath^n}{n!} \theta^n \kappa_n(t) \\ \phi_{g_i * s}(\theta, \boldsymbol{u}, t) & = & \sum_{n=0}^{+\infty} \frac{\imath^n}{n!} \theta^n \mu_n(\boldsymbol{u}, t) \end{array} \tag{135}$$

where $\forall t \in \mathbb{R}$, $\kappa_n(t)$ is the n-th order cumulant of $h_i(t)$, and

$$\forall \boldsymbol{u} \in \mathcal{S}^2, \quad \mu_n(\boldsymbol{u}, .) = \mathbb{E}\left[\left(g_i\left(\boldsymbol{u}, .\right) \overset{t}{*} s\left(\Theta(\boldsymbol{x}, \boldsymbol{y})\boldsymbol{u}, .\right)\right)^n\right]$$

is the n-th order moment of $g_i\left(\boldsymbol{u}, .\right) \overset{t}{*} s\left(\Theta(\boldsymbol{x}, \boldsymbol{y})\boldsymbol{u}, .\right)$.

Note that $\forall t \in \mathbb{R}$, $\forall \Theta(\boldsymbol{x}, \boldsymbol{y}) \in SO(3)$, function $\boldsymbol{u} \mapsto \left(g_i\left(\boldsymbol{u}, .\right) \overset{t}{*} s\left(\Theta(\boldsymbol{x}, \boldsymbol{y})\boldsymbol{u}, .\right)\right)^n$ is continuous, and it is dominated by C^n, with

$$C = \min(T_g, T_s) \sup_{\boldsymbol{u}\in\mathcal{S}^2, t\in[0,T_g]} |g_i(\boldsymbol{u}, t)| \sup_{\boldsymbol{u}\in\mathcal{S}^2, t\in[0,T_s]} |s(\boldsymbol{u}, t)|.$$

Since $SO(3)$ is a compact set, the theorem of continuity under the integral sign proves that function $\boldsymbol{u} \mapsto \mu_n(\boldsymbol{u}, t)$ is continuous on $\mathbb{R}^3$. Also note that

$$\sup_{\boldsymbol{u}\in\mathcal{S}^2, t\in\mathbb{R}} |\mu_n(\boldsymbol{u}, t)| \leq C^n. \tag{136}$$

By substituting (135) into (134) and by identifying the n-th order terms, we get $\forall n \in \mathbb{N}\backslash\{0\}$,

$$\begin{array}{l} \kappa_n(t) = \lambda \int_{\boldsymbol{x}\in\mathbb{R}^3} \int_{\boldsymbol{y}\in\mathbb{R}^M} p(1; \boldsymbol{y} - \boldsymbol{q}(\boldsymbol{x}-\boldsymbol{x}_i)) \\ \frac{e^{-n\frac{\boldsymbol{y}^\top \widehat{\boldsymbol{\alpha}}}{c}}}{\|\boldsymbol{x}-\boldsymbol{x}_i\|_2^n} \mu_n\left(\frac{\boldsymbol{x}-\boldsymbol{x}_i}{\|\boldsymbol{x}-\boldsymbol{x}_i\|_2}, t - \frac{\|\boldsymbol{x}-\boldsymbol{x}_i\|_2}{c}\right) d\boldsymbol{x} d\boldsymbol{y}. \end{array}$$

The changes of variables $\boldsymbol{r} = \boldsymbol{x} - \boldsymbol{x}_i$ and $\boldsymbol{z} = \boldsymbol{y} - \boldsymbol{q}(\boldsymbol{r})$, which are such that $d\boldsymbol{r} = d\boldsymbol{x}$ and $d\boldsymbol{z} = d\boldsymbol{y}$, yield

$$\kappa_n(t) = \lambda\beta_n \int_{\boldsymbol{r}\in\mathbb{R}^3} \frac{e^{-n\frac{\widehat{\alpha}(\boldsymbol{r})}{c}}}{\|\boldsymbol{r}\|_2^n} \mu_n\left(\frac{\boldsymbol{r}}{\|\boldsymbol{r}\|_2}, t - \frac{\|\boldsymbol{r}\|_2}{c}\right) d\boldsymbol{r} \tag{137}$$

where function $\widehat{\alpha}(.)$ is defined in (7) and $\forall n \in \mathbb{N}\backslash\{0\}$, β_n is defined in (13). Note that (137) is of the form J_ξ in (86) where

$$\xi(\boldsymbol{r}) = \lambda\beta_n \frac{e^{-n\frac{\widehat{\alpha}(\boldsymbol{r})}{c}}}{\|\boldsymbol{r}\|_2^{n-2}} \mu_n\left(\frac{\boldsymbol{r}}{\|\boldsymbol{r}\|_2}, t - \frac{\|\boldsymbol{r}\|_2}{c}\right)$$

belongs to $L^1(\mathbb{R}^3) \cap L^\infty(\mathbb{R}^3)$, because its support does not contain the point $\boldsymbol{r} = 0$, $|\mu_n|$ is upper bounded and $\widehat{\alpha}(\boldsymbol{r}) \geq \widehat{\alpha}^{\inf}\|\boldsymbol{r}\|_2$. Therefore (92) yields

$$\kappa_n(t) = \lambda\beta_n \int_{r=0}^{+\infty} \int_{v=-1}^{1} \int_{\varphi=0}^{2\pi} \frac{e^{-nr\frac{\widehat{\alpha}(v,\varphi)}{c}} \mu_n\left(v, \varphi, t - \frac{r}{c}\right)}{r^{n-2}} dr dv d\varphi.$$

The change of variable $\tau = t - \frac{r}{c}$, which is such that $d\tau = \frac{dr}{c}$, yields $\forall t \geq T = T_g + T_s$,

$$\begin{array}{rl} \kappa_n(t) = & \frac{\lambda\beta_n}{c^{n-3}} \int_{v=-1}^{1} \int_{\varphi=0}^{2\pi} e^{-n\widehat{\alpha}(v,\varphi)t} \\ & \int_{\tau=0}^{T} \frac{e^{n\widehat{\alpha}(v,\varphi)\tau} \mu_n(v,\varphi,\tau)}{(t-\tau)^{n-2}} d\tau dv d\varphi \end{array} \tag{138}$$

because the support of $\mu_n\left(v, \varphi, .\right)$ lies in $[0, T]$.

1) Early asymptotic state: Suppose that $\forall \boldsymbol{r} \in \mathbb{R}^3$, $\boldsymbol{q}(\boldsymbol{r}) = \boldsymbol{q}\|\boldsymbol{r}\|_2$ where $\boldsymbol{q} \in \mathbb{R}_+^M$ is a constant vector, therefore function $\widehat{\alpha}(.)$ defined in (7) is constant on $\mathcal{S}^2$: $\forall \boldsymbol{u} \in \mathcal{S}^2$, $\widehat{\alpha}(\boldsymbol{u}) = \widehat{\alpha}^{\inf}$, where $\widehat{\alpha}^{\inf} = \boldsymbol{q}^\top \widehat{\boldsymbol{\alpha}}$. Then (138) becomes

$$\kappa_n(t) = \frac{4\pi\lambda\beta_n}{c^{n-3}} e^{-n\widehat{\alpha}^{\inf} t} \int_{\tau=0}^{T} \frac{e^{n\widehat{\alpha}^{\inf}\tau} \mu_n(\tau)}{(t-\tau)^{n-2}} d\tau, \tag{139}$$

where

$$\mu_n(\tau) = \frac{1}{4\pi} \int_{v=-1}^{1} \int_{\varphi=0}^{2\pi} \mu_n\left(v, \varphi, \tau\right) dv d\varphi.$$

We note that (136) implies

$$\forall \tau \in \mathbb{R}, \, |\mu_n(\tau)| \leq C^n. \tag{140}$$

In particular, for $n = 2$, (139) implies

$$\kappa_2(t) = 4\pi\lambda c\beta_2 e^{-2\widehat{\alpha}^{\inf} t} \int_{\tau=0}^{T} e^{2\widehat{\alpha}^{\inf}\tau} \mu_2\left(\tau\right) d\tau.$$

Therefore, $\forall n \geq 3$, when $t \to +\infty$,

$$\frac{\kappa_n(t)}{\left(\kappa_2(t)\right)^{\frac{n}{2}}} = O\left(\frac{\beta_n \int_{\tau=0}^{T} e^{n\widehat{\alpha}^{\inf}\tau} |\mu_n(\tau)| d\tau}{c^{n-3} t^{n-2}}\right). \tag{141}$$

By substituting (14) and (140) into (141), we thus get $\forall n \geq 3$,

$$\frac{\kappa_n(t)}{\left(\kappa_2(t)\right)^{\frac{n}{2}}} = O\left(\frac{1}{t} \frac{C^n e^{n\left(\frac{|\boldsymbol{z}^{\inf}|^\top \widehat{\boldsymbol{\alpha}}}{c} + \widehat{\alpha}^{\inf} T\right)}}{n^{M+1} c^{n-3} t^{n-3}}\right).$$

If we consider the random variable $\frac{h_i(t)}{\sqrt{\mathrm{var}[h_i(t)]}}$, we obtain

$$\left|\ln\phi_{\frac{h_i(t)}{\sqrt{\mathrm{var}[h_i(t)]}}}(\theta)-\sum_{n=1}^{2}\frac{\imath^n}{n!}\theta^n\frac{\kappa_n(t)}{(\kappa_2(t))^{\frac{n}{2}}}\right|\leq\sum_{n=3}^{+\infty}\frac{1}{n!}|\theta|^n\frac{|\kappa_n(t)|}{(\kappa_2(t))^{\frac{n}{2}}}$$
$$=O\left(\frac{1}{t}e^{\frac{|\theta|Ce^{\frac{|\boldsymbol{z}^{\inf}|^\top\widehat{\boldsymbol{\alpha}}}{c}+\widehat{\alpha}^{\inf}T}}{ct}}\right)=O\left(\tfrac{1}{t}\right).$$

Therefore the characteristic function of $\frac{h_i(t)}{\sqrt{\mathrm{var}[h_i(t)]}}$ converges pointwise to that of the standard normal distribution when $t\to+\infty$, which proves that it is asymptotically normally distributed.

2) Late asymptotic state: Suppose that the acoustic field is non-diffuse and the attenuation function is regular (*cf.* Definition 7). Then (138) shows that $\kappa_n(t)$ can be written as the integral $I(x)$ in (99), if we let $x=nt$ and

$$\psi(\boldsymbol{u})=\frac{\lambda\beta_n}{c^{n-3}}\int_{\tau=0}^{T}\frac{e^{n\widehat{\alpha}(\boldsymbol{u})\tau}\mu_n(\boldsymbol{u},\tau)}{(t-\tau)^{n-2}}d\tau.$$

Note that $\forall t>T$, $\forall\tau\in[0,T]$, function $\boldsymbol{u}\mapsto\frac{e^{n\widehat{\alpha}(\boldsymbol{u})\tau}\mu_n(\boldsymbol{u},\tau)}{(t-\tau)^{n-2}}$ is continuous since we have proved that function $\boldsymbol{u}\mapsto\mu_n(\boldsymbol{u},\tau)$ is continuous, and it is dominated by $\frac{e^{n\left(\sup_{\mathcal{S}^2}\widehat{\alpha}(.)\right)T}C^n}{(t-T)^{n-2}}$. Since $[0,T]$ is a compact set, the theorem of continuity under the integral sign proves that function $\boldsymbol{u}\mapsto\psi(\boldsymbol{u})$ is continuous on $\mathbb{R}^3$. Since ψ is continuous, (100) proves that when $t\to+\infty$,

$$\kappa_n(t)\sim\quad\frac{2\pi\lambda\beta_n}{nc^{n-3}}\frac{e^{-n\widehat{\alpha}^{\inf}t}}{t^{n-1}}\sum_{k\in\mathcal{K}}\frac{\int_{\tau=0}^{T}e^{n\widehat{\alpha}(\boldsymbol{u}_k)\tau}\mu_n(\boldsymbol{u}_k,\tau)d\tau}{\sqrt{\ddot{\widehat{\alpha}}_k}}.$$

In particular, for $n=2$, we get

$$\kappa_2(t)\sim\quad\pi\lambda c\beta_2\frac{e^{-2\widehat{\alpha}^{\inf}t}}{t}\sum_{k\in\mathcal{K}}\frac{\int_{\tau=0}^{T}e^{2\widehat{\alpha}(\boldsymbol{u}_k)\tau}\mu_2(\boldsymbol{u}_k,\tau)d\tau}{\sqrt{\ddot{\widehat{\alpha}}_k}}.$$

Therefore, $\forall n\geq3$, when $t\to+\infty$,

$$\frac{\kappa_n(t)}{(\kappa_2(t))^{\frac{n}{2}}}=O\left(\frac{\beta_n\sum_{k\in\mathcal{K}}\frac{\int_{\tau=0}^{T}e^{n\widehat{\alpha}(\boldsymbol{u}_k)\tau}|\mu_n(\boldsymbol{u}_k,\tau)|d\tau}{\sqrt{\ddot{\widehat{\alpha}}_k}}}{nc^{n-3}t^{\frac{n}{2}-1}}\right).\quad(142)$$

By substituting (14) and (136) into (142), we thus get $\forall n\geq3$,

$$\frac{\kappa_n(t)}{(\kappa_2(t))^{\frac{n}{2}}}=O\left(\frac{1}{\sqrt{t}}\frac{C^ne^{n\left(\frac{|\boldsymbol{z}^{\inf}|^\top\widehat{\boldsymbol{\alpha}}}{c}+\left(\sup_{\mathcal{S}^2}\widehat{\alpha}(.)\right)T\right)}}{n^{M+2}c^{n-3}t^{\frac{n-3}{2}}}\right).$$

If we consider the random variable $\frac{h_i(t)}{\sqrt{\mathrm{var}[h_i(t)]}}$, we obtain

$$\left|\ln\phi_{\frac{h_i(t)}{\sqrt{\mathrm{var}[h_i(t)]}}}(\theta)-\sum_{n=1}^{2}\frac{\imath^n}{n!}\theta^n\frac{\kappa_n(t)}{(\kappa_2(t))^{\frac{n}{2}}}\right|\leq\sum_{n=3}^{+\infty}\frac{1}{n!}|\theta|^n\frac{|\kappa_n(t)|}{(\kappa_2(t))^{\frac{n}{2}}}$$
$$=O\left(\frac{1}{\sqrt{t}}e^{\frac{|\theta|Ce^{\frac{|\boldsymbol{z}^{\inf}|^\top\widehat{\boldsymbol{\alpha}}}{c}+\left(\sup_{\mathcal{S}^2}\widehat{\alpha}(.)\right)T}}{c\sqrt{t}}}\right)=O\left(\tfrac{1}{\sqrt{t}}\right).$$

Therefore the characteristic function of $\frac{h_i(t)}{\sqrt{\mathrm{var}[h_i(t)]}}$ converges pointwise to that of the standard normal distribution when $t\to+\infty$, which proves that it is asymptotically normally distributed.

G.5. Proofs of Corollaries 1 and 2 in Section III

Proof of Corollary 1. By substituting (42) into (40), we get (43). Then substituting (39) and (42) into (41) yields

$$\rho_{i,j}(t,f,\boldsymbol{r})=\frac{\int_{\boldsymbol{u}\in\mathcal{S}^2}\beta\left(\boldsymbol{q}\boldsymbol{u}^\top\boldsymbol{r}\right)\xi_{i,j}(\boldsymbol{u})e^{-2\imath\pi f\frac{\boldsymbol{u}^\top\boldsymbol{r}}{c}}d\boldsymbol{u}}{\beta_2\sqrt{\int_{\boldsymbol{u}\in\mathcal{S}^2}\xi_{i,i}(\boldsymbol{u})d\boldsymbol{u}}\sqrt{\int_{\boldsymbol{u}\in\mathcal{S}^2}\xi_{j,j}(\boldsymbol{u})d\boldsymbol{u}}}+O(\tfrac{1}{t}).\quad(143)$$

Applying the inverse Fourier transform to the limit when $t\to+\infty$ of the right member of (143) yields

$$\sigma_{i,j}(\tau,\boldsymbol{r})=\frac{\int_{\boldsymbol{u}\in\mathcal{S}^2}\beta\left(\boldsymbol{q}\boldsymbol{u}^\top\boldsymbol{r}\right)\xi_{i,j}(\boldsymbol{u})\delta\left(\tau-\frac{\boldsymbol{u}^\top\boldsymbol{r}}{c}\right)d\boldsymbol{u}}{\beta_2\sqrt{\int_{\boldsymbol{u}\in\mathcal{S}^2}\xi_{i,i}(\boldsymbol{u})d\boldsymbol{u}}\sqrt{\int_{\boldsymbol{u}\in\mathcal{S}^2}\xi_{j,j}(\boldsymbol{u})d\boldsymbol{u}}},\quad(144)$$

which proves that $\tau\mapsto\sigma_{i,j}(\tau,\boldsymbol{r})$ is nonnegative and that its support is $[-\frac{D}{c},\frac{D}{c}]$. Moreover, with the change of variables $\boldsymbol{u}=\left[\sqrt{1-v^2}\cos(\varphi),\sqrt{1-v^2}\sin(\varphi),v\right]$ with $v\in[-1,1]$ and $\varphi\in[0,2\pi]$, (144) can be rewritten as

$$\sigma_{i,j}(\tau,\boldsymbol{r})=\frac{\int_{v=-1}^{1}\int_{\varphi=0}^{2\pi}\beta(\boldsymbol{q}vD)\xi_{i,j}(v,\varphi)\delta\left(\tau-\frac{vD}{c}\right)dvd\varphi}{\beta_2\sqrt{\int_{\boldsymbol{u}\in\mathcal{S}^2}\xi_{i,i}(\boldsymbol{u})d\boldsymbol{u}}\sqrt{\int_{\boldsymbol{u}\in\mathcal{S}^2}\xi_{j,j}(\boldsymbol{u})d\boldsymbol{u}}}.$$

Therefore $\forall\tau\in[-\frac{D}{c},\frac{D}{c}]$,

$$\sigma_{i,j}(\tau,\boldsymbol{r})=\frac{c}{D}\frac{\beta(\boldsymbol{q}c\tau)}{\beta_2}\frac{\int_{\varphi=0}^{2\pi}\xi_{i,j}(\frac{\tau c}{D},\varphi)d\varphi}{\sqrt{\int_{\boldsymbol{u}\in\mathcal{S}^2}\xi_{i,i}(\boldsymbol{u})d\boldsymbol{u}}\sqrt{\int_{\boldsymbol{u}\in\mathcal{S}^2}\xi_{j,j}(\boldsymbol{u})d\boldsymbol{u}}},\quad(145)$$

which shows that function $\tau\mapsto\sigma_{i,j}(\tau,\boldsymbol{x}_j-\boldsymbol{x}_i)$ is obtained as the product of a continuous function of τ (as shown in Lemma 2) and of the integral on the compact set $[0,2\pi]$ of a function of (τ,φ) which is bounded by $\|\xi_{i,j}\|_\infty$ and continuous w.r.t. τ in $]-\frac{D}{c},\frac{D}{c}[$, therefore the continuity under the integral sign theorem proves that function $\tau\mapsto\sigma_{i,j}(\tau,\boldsymbol{x}_j-\boldsymbol{x}_i)$ is continuous in $]-\frac{D}{c},\frac{D}{c}[$.

If function $\xi_{i,j}(.)$ is even on $\mathcal{S}^2$ (*symmetric case*), then (145) shows that function $\tau\mapsto\sigma_{i,j}(\tau,\boldsymbol{x}_j-\boldsymbol{x}_i)$ is also even, thus its Fourier transform $\lim_{t\to+\infty}\rho_{i,j}(t,f,\boldsymbol{x}_j-\boldsymbol{x}_i)$ is real-valued.

If moreover function $\xi_{i,j}(.)$ is constant on $\mathcal{S}^2$ (*isotropic case*), the change of variables $\boldsymbol{u}=\left[\sqrt{1-v^2}\cos(\varphi),\sqrt{1-v^2}\sin(\varphi),v\right]$ with $v\in[-1,1]$ and $\varphi\in[0,2\pi]$ in (143) yields

$$\rho_{i,j}(t,f,\boldsymbol{r})=\frac{\int_{v=-1}^{1}\beta(\boldsymbol{q}vD)e^{-2\imath\pi f\frac{vD}{c}}dv}{2\beta_2}+O(\tfrac{1}{t}).\quad(146)$$

Finally, applying the change of variable $\tau=\frac{vD}{c}$, which is such that $d\tau=\frac{D}{c}dv$, and substituting (19) into (146) yields (44). Then (45) is obtained as the inverse Fourier transform of the limit when $t\to+\infty$ of the right member of (44). Moreover, (20) yields $\sigma_{i,j}(\tau,\boldsymbol{x}_j-\boldsymbol{x}_i)\in[0,\frac{c}{2D}]$. Besides, function $\tau\mapsto\sigma_{i,j}(\tau,\boldsymbol{x}_j-\boldsymbol{x}_i)$ reaches its maximum at $\tau=0$, and it is not differentiable at $\tau=0$, because so is function $\tau\mapsto b(\tau,D)$ as shown in Lemma 3. Finally, (46) is derived by substituting (23) into (44), and (47) is derived by substituting (22) into (45). □

Proof of Corollary 2. Substituting (42) into (53) yields (55). Then substituting (50) and (42) into (54) yields (56). Finally, (57) is obtained as the inverse Fourier transform of the limit when $t\to+\infty$ of the right member of (56). □

REFERENCES

[1] R. Badeau, "Unified stochastic reverberation modeling," in *Proc. of 26th European Signal Processing Conference (EUSIPCO)*, Rome, Italy, Sep. 2018.

[2] ——, "Common mathematical framework for stochastic reverberation models," *The Journal of the Acoustical Society of America*, vol. 145, no. 4, Apr. 2019, Special issue on room acoustics modeling and auralization.

[3] R. K. Cook, R. V. Waterhouse, R. D. Berendt, S. Edelman, and M. C. Thompson Jr., "Measurement of correlation coefficients in reverberant sound fields," *The Journal of the Acoustical Society of America*, vol. 27, no. 6, pp. 1072–1077, 1955.

[4] M. R. Schroeder, "Frequency-correlation functions of frequency responses in rooms," *The Journal of the Acoustical Society of America*, vol. 34, no. 12, pp. 1819–1823, 1962.

[5] M. R. Schroeder and K. H. Kuttruff, "On frequency response curves in rooms. Comparison of experimental, theoretical, and Monte Carlo results for the average frequency spacing between maxima," *The Journal of the Acoustical Society of America*, vol. 34, no. 1, pp. 76–80, 1962.

[6] J. A. Moorer, "About this reverberation business," *Computer Music Journal*, vol. 3, no. 2, pp. 13–28, 1979.

[7] M. R. Schroeder, "Statistical parameters of the frequency response curves of large rooms," *The Journal of the Audio Engineering Society*, vol. 35, no. 5, pp. 299–306, 1987.

[8] J. D. Polack, "La transmission de l'énergie sonore dans les salles (*The transmission of sound energy in rooms*)," Ph.D. dissertation, Université du Maine, Le Mans, France, 1988.

[9] J.-D. Polack, "Modifying chambers to play billiards: the foundations of reverberation theory," *Acta Acustica united with Acustica*, vol. 76, no. 6, pp. 256–272(17), Jul. 1992.

[10] ——, "Playing billiards in the concert hall: The mathematical foundations of geometrical room acoustics," *Applied Acoustics*, vol. 38, no. 2, pp. 235–244, 1993.

[11] J. B. Allen and D. A. Berkley, "Image method for efficiently simulating small-room acoustics," *Journal of the Acoustical Society of America*, vol. 65, no. 4, pp. 943–950, 1 1979.

[12] H. Kuttruff, *Room Acoustics, Fifth Edition*. Boca Raton, FL, USA: CRC Press, 2014.

[13] R. Badeau, "General stochastic reverberation model," Télécom ParisTech, Paris, France, Tech. Rep. 2019D002, Feb. 2019.

[14] L. Cohen, "Time-frequency distributions-a review," *Proc. IEEE*, vol. 77, no. 7, pp. 941–981, Jul. 1989.

[15] E. Vincent and D. R. Campbell, "Roomsimove," GNU Public License, 2008, http://homepages.loria.fr/evincent/software/Roomsimove_1.4.zip.

[16] R. Stewart and M. Sandler, "Database of omnidirectional and B-format impulse responses," in *Proc. of IEEE Int. Conf. on Acoustics, Speech, and Signal Processing (ICASSP)*, Dallas, Texas, Mar. 2010.

[17] A. Farina, "Simultaneous measurement of impulse response and distortion with a swept sine technique," in *108th AES Convention*, Paris, France, Feb. 2000.

Dépôt légal : 2019 – 2e trimestre
Imprimé à Télécom ParisTech – Paris
ISSN 0751-1345 ENST D (Paris) (France 1983-9999)

Télécom ParisTech

Institut Mines-Télécom - membre de l'Université Paris Saclay

46, rue Barrault - 75634 Paris Cedex 13 - Tél. + 33 (0)1 45 81 77 77 - www.telecom-paristech.fr

Département IDS